

**TIDAL ENERGY POTENTIAL ESTIMATION
AND IMPACTS ON HYDRODYNAMICS
AROUND TIDAL POWER SYSTEMS ALONG
THE INDIAN COAST**

Thesis

Submitted in partial fulfillment of the requirements for the degree of

DOCTOR OF PHILOSOPHY

by

Vikas Mendi



DEPARTMENT OF WATER RESOURCES AND OCEAN
ENGINEERING
NATIONAL INSTITUTE OF TECHNOLOGY KARNATAKA,
SURATHKAL, MANGALURU – 575025
NOVEMBER 2020

*This thesis is dedicated to my parents, my
loving wife Jyothi Lingala and my beloved
friend Thripti*

ACKNOWLEDGEMENTS

Completing the Ph.D. thesis has been probably the most challenging activity of my life. During the journey, I worked and acquainted with many people who contributed in different ways to the success of this study and made it an unforgettable experience for me. It is a pleasure to convey my gratitude to them.

First and foremost, I wish to acknowledge the love and support by my ever loving parents Mr. M. K. Thyagaraj and Mrs. C. H. Jayashree, my shadow and light. Special thanks to my wife Jyothi Lingala who stood by me, encouraged, helped me in all aspects of life. All these years have not been an easy ride for us; their sacrifice and patience are beyond words. I truly thank them for being my side during the difficult times. I doubt if I will ever be able to convey my appreciation fully, but I owe everything for being so patient, understanding and self-sacrificing.

I would like to express my deep gratitude to my research supervisors **Dr. Jaya Kumar Seelam**, Senior Principal Scientist, CSIR-NIO, Goa and **Prof. Subba Rao**, Professor, Department of Water Resources and Ocean Engineering, National Institute of Technology Karnataka (NITK), Surathkal, for their patient guidance, stimulating suggestions and invaluable advices they have been provided throughout my doctoral research endeavor. Their insightful observations and constructive criticism helped me to establish the overall direction of the research and move forward with investigation in depth.

I take this opportunity to thank Prof. G. S. Dwarakish, Prof. Amai Mahesha, Prof. Amba Shetty (Formerly Heads, AMD), Prof. B M Doddamani, Professor and Head, all faculty of Water Resources and Ocean Engineering Department, NITK Surathkal for their continuous and timely suggestions.

I wish to thank the members of the Research Program Assessment Committee, Dr. Arkal Vittal Hegde, Professor (Rtd.), Department of Water Resources and Ocean Engineering, Dr. Vadivuchezhian Kaliveeran, Assistant Professor, Department of Water Resources and

Ocean Engineering and Dr. M. C. Narasimhan, Professor, Department of Civil Engineering for their appreciation and constructive criticism all through my research work.

I am thankful to the Director, CSIR-National Institute of Oceanography, Goa for granting me the permission to carry out and utilize the facilities of the Institute to accomplish my research work.

I would like to express my gratitude to Mrs. Jyoti, CSIR-NIO for her willingness to patiently answer my queries on MIKE21 anytime and for all her help and support during my stay at CSIR-NIO.

Mike21 Software has been used extensively in this study. I acknowledge the support extended by DHI team by providing me student license that helped to carry out the simulations in this work.

I wish to thank the President of RSST Dr. M. K. Panduranga Shetty; Principal, Prof. K. N. Subramanya, RV College of Engineering[®]; Former Head of the Department Prof. M. V. Renuka Devi and all my colleagues of Department of Civil Engineering, RV College of Engineering[®], Bengaluru, for their enough support and encouragement given during my research.

I also express my gratitude and deep apparition to my dearest friends Dr, N. Amarnatha Reddy (HoD, KSRMCE), Dr. V Venkateshwarlu (NITK), I Srinivasa Reddy (NITK), Palani Kumar (NITK), Lavanya (Project staff, CSIR-NIO), V Kumaran (NITK), N Murugan (NITK).

I personally thank Er. T. N. Manjunath, Assistant Engineer, KUWSDB, Govt. of Karnataka, whose support and caring have enlightened and entertained me over the many years of friendship. Finally, I would like to thank everybody who helped me directly or indirectly to the successful realization of this thesis.

Vikas Mendi

DECLARATION

I hereby *declare* that the Research Thesis entitled “**TIDAL ENERGY POTENTIAL ESTIMATION AND IMPACTS ON HYDRODYNAMICS AROUND TIDAL POWER SYSTEMS ALONG THE INDIAN COAST**” which is being submitted to the **National Institute of Technology Karnataka, Surathkal** in partial fulfillment of the requirements for the award of the Degree of **Doctor of Philosophy in Department of Water Resources and Ocean Engineering** is a *bonafide report of the research work carried out by me*. The material contained in this Research Thesis has not been submitted to any University or Institution for the award of any degree.

Register Number : **165133AM16P04**

Name of the Research Scholar : **Vikas Mendi**

Signature of the Research Scholar :



Department of Water Resources and Ocean Engineering

Place : **NITK, Surathkal**

Date : **22-05-2021**

C E R T I F I C A T E

This is to *certify* that the Research Thesis entitled “**TIDAL ENERGY POTENTIAL ESTIMATION AND IMPACTS ON HYDRODYNAMICS AROUND TIDAL POWER SYSTEMS ALONG THE INDIAN COAST**” submitted by **Mr. Vikas Mendi (Register Number: 165133AM16P04)** as the record of the research work carried out by him, is *accepted as the Research Thesis submission* in partial fulfillment of the requirements for the award of the degree of **Doctor of Philosophy**.



Prof. Subba Rao

Research Supervisor & Professor
Department of Applied Mechanics
NITK, Surathkal



Dr. Jaya Kumar Seelam

Research Supervisor & Senior Principal Scientist
CSIR-National Institute of Oceanography
Dona Paula, Goa



Chairman - DRPC

Chairman (DRPC)
Dept. of Water Resources & Ocean Engineering



DEPARTMENT OF WATER RESOURCES AND OCEAN
ENGINEERING
NATIONAL INSTITUTE OF TECHNOLOGY KARNATAKA,
SURATHKAL, MANGALURU – 575025

ABSTRACT

Tidal energy is the energy derived using the tides. Most of the tidal energy feasibility studies are conducted for barrage method of tidal energy extraction. In Indian scenario, the observed conditions and the methods proposed are mostly for the barrage method mainly in the states of Gujarat in the west and West Bengal in the east where the tidal range is maximum. Assessment of energy extraction from barrage method has not been carried out in the southern parts of India due to low to medium tidal range. The first objective mainly focuses on tidal energy resource availability and the energy that can be harnessed from tides along the coast of India. Two methods are considered viz. tidal barrage and tidal stream energy. Out of 471 tidal inlets identified in 9 maritime states along the Indian coast, 130 inlets are shortlisted considering a threshold of 2.53 Mm³ tidal prism and potential energy was estimated. Total potential energy estimate considering 130 inlets is 2254.906 MW. Further 107 inlets are shortlisted considering both tidal prism greater than 2.53Mm³ and inlet throat width greater than 63m and the corresponding potential energy is estimated as 2127.281 MW. The Kinetic energy estimated was 11.68kW, 5.60kW and 25.64kW at Chapora, Mandovi and Zuari respectively. The second objective intends to study the impact of tidal energy of local hydrodynamics. The turbines are placed at the locations where highest tidal currents were observed as presented in objective 1. Five cases were considered where the simulations were carried for different locations of the tidal turbine. Total energy generated by 0.5m diameter turbine was estimated to be 118kW. Whereas the 1m diameter turbine increased the energy to 409.35kN. The total energy estimates for the turbines in parallel and turbines in tandem considering 0.4 m/s threshold for current speeds was approximated to 417.5kW and 409.35kW respectively. The morphodynamics were simulated and the sea bed morphology of Zuari creek was studied. The results of the coupled model proved that the location chosen for tidal energy extraction does not exhibit sediment transport and longer durations of simulations are required. In the third objective, tidal lagoons are established and the morphodynamics due the energy extraction are studied. A tidal lagoon can be constructed either on an existing natural rock/headland or completely by artificial means. It can either be constructed nearshore adjacent to the coast of in the tidal reservoir where conditions are feasible. Locations for the construction of tidal lagoons are identified along in Maharashtra (Jaigad 1 and Jaigad 2). The potential energy that can be extracted from the established tidal pools is estimated to be 3.69MW and 1.3MW respectively. Results of morphodynamic study for 20 days are analyzed. The bed level changes observed at Jaigad 1 and Jaigad 2 prove less sensitive to hydrodynamics. Bed level changes observed are of the order 0.04m (in 20 days) due to the construction of tidal barrage.

Keywords: Tides, energy, hydrodynamics, morphology.

CONTENTS

Page
No.

Declaration	
Certificate	
Acknowledgements	
Abstract	i
List of Contents	ii
List of Figures	v
List of Tables	x
1. INTRODUCTION	1
1.1. General	1
1.2. Spring & Neap tides	2
1.3. The current state of knowledge	3
1.3.1 Demonstration Project at Sundarbans	3
1.3.2 Tidal Power Projects in the Gulf of Kutch	4
1.4 Tidal energy around the world	4
1.5 Methods of tidal energy extraction	5
1.5.1 Tidal barrage	5
1.5.2 Tidal Stream Energy	7
1.6 Tidal Stream projects	8
1.7 Tidal stream energy devices	9
1.8 Tidal energy in India	11
1.9 Numerical models for coastal environment	11
1.10 Organization of the thesis	12
1.11 Necessity and relevance of the present study	13
2. HISTORY –LITERARURE	15
2.1. General	15
2.2. Tidal stream energy estimates and studies	20
2.3. Formulation of research objectives	24
2.3.1 Research Objectives	25

3.	IDENTIFICATION OF POTENTIAL LOCATIONS FOR TIDAL ENERGY EXTRACTION	27
3.1.	Introduction	27
3.2.	Methodology	28
3.3.	Calculation of tidal energy	30
3.3.1	Potential energy	30
3.3.2	Kinetic energy	33
3.4	Comparison of measured and modelled (simulated) data	42
3.5	Statistical maxima of current speeds	43
3.6	Results and discussion	47
3.6.1	Tidal energy (Potential energy)	47
3.6.2	Tidal Stream energy (Kinetic energy)	49
3.7	Conclusions	70
4.	IMPACT OF TIDAL ENERGY FARM ON LOCAL HYDRODYNAMICS AND ON ENERGY ESTIMATES	71
4.1.	Introduction	71
4.2	Methodology	72
4.3	Numerical model	73
4.3.1	Mud Transport (MT) model	73
4.3.2	Sediment transport model	74
4.4	Description of the model domain	74
4.5	Validation of modelled currents	76
4.6	Results and discussion	77
4.7	Conclusions	91
5.	TO ESTABLISH POTENTIAL SITES FOR TIDAL LAGOONS ALONG THE INDIAN COAST AND ITS INFLUENCE ON HYDRODYNAMICS	93
5.1.	Introduction	93
5.2.	Tides along the Indian coastline	94
5.3.	Construction of tidal lagoons	94
5.4	Site selection	94
5.5	Identification of locations for tidal pools	95

5.6	Description of the model domain	97
5.7	Morphodynamic study at the tidal pool	101
5.8	Summary and conclusions	102
6	SUMMARY AND CONCLUSIONS	105
6.1	Summary	105
6.2	Conclusions	106
6.3	Scope for future work	107
6.4	Limitations of the study	107
6.5	Contributions from the present study	108
	REFERENCES	109
	PUBLICATIONS BASED ON PRESENT WORK	116
	APPENDIX	117

LIST OF FIGURES

Figure No.	Description	Page No.
1.1	Relative distance of the earth to sun and moon	2
1.2	Moon-Earth System	2
1.3	Types of tides: diurnal, semidiurnal and mixed	3
1.4	La Rance tidal station setup	6
1.5	World Tidal Potential Locations	7
1.6	SeaGen tidal stream generator	8
3.1	Locations of Inlets considered in Study area	29
3.2a	Mesh generated in MIKE21 for Mandovi and Zuari inlets, Goa, India	31
3.2b	Bathymetry interpolated in MIKE21 used for simulation.	32
3.2c	Tides extracted in MIKE21 at the throat of Mandovi and Zuari inlets, Goa, India	32
3.3	Instrument locations at Goa, India	35
3.4a	Measured currents at Chapora 1 between 09 Feb 2017 and 10 Mar 2017	35
3.4b	Measured currents at Chapora 2 between 16 Feb 2017 and 18 Mar 2017	35
3.4c	Instrument locations at Chapora 1 and Chapora 2	36
3.5a	Measured currents at Mandovi 1321 between 05 Sep 2015 and 11 Sep 2015	37
3.5b	Measured currents at Mandovi 1420 between 05 Sep 2015 and 11 Sep 2015	37
3.5c	Instrument locations at Mandovi 1321, Mandovi 1420	38
3.6a	Measured currents at Zuari 1418 between 08 Aug 2017 and 23 Aug 2017	39
3.6b	Measured currents at Zuari 1420 between 08 Aug 2017 and 23 Aug 2017	39
3.6c	Measured currents at Zuari 1421 between 07 Aug 2017 and 24 Aug 2017	40

3.6d	Measured currents at Zuari 1422 between 07 Aug 2017 and 24 Aug 2017	40
3.6e	Instrument locations at Zuari 1418, Zuari 1421, Zuari 1422, Zuari 1420	41
3.7a	Validation of modelled current speed with measured current speed for Mandovi	42
3.7b	Validation of modelled current speed with measured current speed for Zuari	42
3.7c	Validation of modelled current speed with measured current speed for Chapora	42
3.7d	Validation of modelled tide with measured tide for Mandovi	43
3.7e	Validation of modelled tide with measured tide for Zuari	43
3.7f	Validation of modelled tide with measured tide for Chapora	43
3.8a	Locating maximum currents at Chapora River (Statistical maxima)	44
3.8b	Locating maximum currents at Mandovi River (Statistical maxima)	45
3.8c	Locating maximum currents at Zuari River (Statistical maxima)	46
3.9a	Variation of tidal prism along the coast of India	48
3.9b	Inlet throat width for 130 inlets	49
3.10a	Tidal stream energy (measured) at Chapora 2 having current speed greater than 0.4m/s	50
3.10b	Tidal stream energy (measured) at Mandovi 1321 having current speed greater than 0.4m/s	52
3.10c	Tidal stream energy (measured) at Mandovi 1420 having current speed greater than 0.4m/s	53
3.10d	Tidal stream energy (measured) at Zuari 1418 having current speed greater than 0.4 m/s	53
3.10e	Tidal stream energy (measured) at Zuari 1420 having current speed greater than 0.4 m/s	54
3.10f	Tidal stream energy (measured) at Zuari 1421 having current speed greater than 0.4 m/s	55
3.10g	Tidal stream energy (measured) at Zuari 1422 having current speed greater than 0.4 m/s	55

311a	Modelled currents at Point 1 in Chapora river	55
3.11b	Modelled currents at Point 2 in Chapora river	56
3.11c	Modelled currents at Point 3 in Chapora river	56
3.11d	Modelled currents at Point 4 in Chapora river	57
3.11e	Modelled currents at Point 1 in Mandovi river	57
3.11f	Modelled currents at Point 2 in Mandovi river	58
3.11g	Modelled currents at Point 3 in Mandovi river	58
3.11h	Modelled currents at Point 4 in Mandovi river	59
3.11i	Modelled currents at Point 5 in Mandovi river	59
3.11j	Modelled currents at Point 6 in Mandovi river	60
3.11k	Modelled currents at Point 1 in Zuari river	60
3.11l	Modelled currents at Point 2 in Zuari river	61
3.11m	Modelled currents at Point 3 in Zuari river	61
3.11n	Modelled currents at Point 4 in Zuari river	62
3.12a	Tidal stream energy (modelled) at Point 1 in Chapora River having current speed greater than 0.4 m /s	62
3.12b	Tidal stream energy (modelled) at Point 2 in Chapora River having current speed greater than 0.4 m /s	63
3.12c	Tidal stream energy (modelled) at Point 3 in Chapora River having current speed greater than 0.4 m /s	63
3.12d	Tidal stream energy (modelled) at Point 4 in Chapora River having current speed greater than 0.4 m /s	64
3.12e	Tidal stream energy (modelled) at Point 1 in Mandovi River having current speed greater than 0.4 m /s	64
3.12f	Tidal stream energy (modelled) at Point 2 in Mandovi River having current speed greater than 0.4 m /s	65
3.12g	Tidal stream energy (modelled) at Point 3 in Mandovi River having current speed greater than 0.4 m /s	65
3.12h	Tidal stream energy (modelled) at Point 4 in Mandovi River having current speed greater than 0.4 m /s	66

3.12i	Tidal stream energy (modelled) at Point 5 in Mandovi River having current speed greater than 0.4 m /s	66
3.12j	Tidal stream energy (modelled) at Point 6 in Mandovi River having current speed greater than 0.4 m /s	67
3.12k	Tidal stream energy (modelled) at Point 1 in Zuari River having current speed greater than 0.4 m /s	67
3.12l	Tidal stream energy (modelled) at Point 2 in Zuari River having current speed greater than 0.4 m /s	68
3.12m	Tidal stream energy (modelled) at Point 3 in Zuari River having current speed greater than 0.4 m /s	68
3.12n	Tidal stream energy (modelled) at Point 4 in Zuari River having current speed greater than 0.4 m /s	69
4.1	Model domain considered for simulation	75
4.2	Validation of modelled currents with measured currents (scatter plot)	76
4.3	Modelled currents at Zuari 3 (Base case)	77
4.4	Bed level change for the base case	78
4.5	Turbine location in case ii	79
4.6	Comparison of current speeds for the base case with one turbine of 0.5m dia	79
4.7	Bed level change when one turbine of 0.5m dia is deployed	79
4.8	Comparison of current speeds for the base case with one turbine of 1m dia	80
4.9	Bed level change when one turbine of 1m dia is deployed	80
4.10	Comparison of current speeds for the base case with one turbine of 0.5m and 1m	80
4.11	Turbines placed parallel to the flow	81
4.12	Variation of current speeds (a) and bed level changes (b) around T1	82
4.13	Variation of current speeds (a) and bed level changes (b) around T2	83
4.14	Variation of current speeds (a) and bed level changes (b) around T3	84
4.15	Turbines placed perpendicular to the flow	85
4.16	Variation of current speeds (a) and bed level changes (b) around T1	87

4.17	Variation of current speeds (a) and bed level changes (b) around T2	88
4.18	Variation of current speeds (a) and bed level changes (b) around T3	89
4.19	Comparison of current speeds for the base case and with a decrease in water depth by 10 percent	90
5.1	Tidal range along the Indian coast	94
5.2	Tidal pools at Jaigad 1	96
5.3	Tidal pools at Jaigad 2	96
5.4	Model domain considered for the study	97
5.5	Simulation for base case – without tidal pool at Jaigad1 and Jaigad 2	98
5.6	Simulation by considering tidal pool at Jaigad 1 and Jaigad 2	98
5.7	Locations of current speed extraction (Points 1 to 11)	99
5.8	Current speeds comparison before and after construction of the tidal pool at Jaigad 1	100
5.9	Current speeds comparison before and after construction of the tidal pool at Jaigad 2	101
5.10	Percentage change in current speeds	102
5.11	Bed level changes at Jaigad 1 and Jaigad 2 after construction at the tidal pool	103
A1	Current speeds (mean) at Chapora	132
A2	Current speeds (mean) at Mandovi	132
A3	Current speeds (mean) at Zuari	133

LIST OF TABLES

Table No.	Descriptions	Page No
1.1	Highest tides of the global Ocean	6
1.2	Existing large tidal power plants	6
1.3	Tidal stream energy extraction devices	10
2.1	Tidal Energy Potential in India	17
3.1	Details of existing tidal power plants around the world	28
3.2	Identified number of tidal inlets and ICOLLs along the Indian coast	29
3.3	Instrument details, locations and measured currents in Goa	34
3.4	State-wise potential energy extraction based on the tidal prism and throat width.	49
3.5	Kinetic energy calculated/day for different threshold velocities	51
4.0	r^2 values for the current speed and tide	77
4.1	Data extraction locations for case i (no turbines) and case iv (decreased depth)	77
4.2	Data extraction locations for T1 73.8965, 15.414	82
4.3	Data extraction locations for T2 at 73.8970, 15.414	83
4.4	Data extraction locations for T3 at 73.8975, 15.414	84
4.5	Bed level changes observed at T1, T2 and T3	85
4.6	Data extraction locations for T1 at 73.8965, 15.41385	86
4.7	Data extraction locations for T2 at 73.8965, 15.41395	88
4.8	Data extraction locations for T3 at 73.8965, 15.41405	89
4.9	Bed level changes observed at T1, T2 and T3	90
5.1	Locations of tidal pools chosen for assessment and potential energy estimation	94
A1	Tidal inlets along Gujarat coast	119
A2	Tidal inlets along Maharashtra coast	120
A3	Tidal inlets along Goa coast	122
A4	Tidal inlets along Karnataka coast	122
A5	Tidal inlets along Kerala coast	123

A6	Tidal inlets along Tamil Nadu coast	125
A7	Tidal inlets along Amdhra Pradesh coast	128
A8	Tidal inlets along Odisha coast	130
A9	Tidal inlets along West Bengal coast	131

CHAPTER 1

INTRODUCTION

1.1 General

The periodic rising and lowering of ocean waters are responsible for the phenomenon called 'tides'. Tides are the periodic motion of the waters of the sea due to the inter-attractive forces between the celestial bodies. Tides are very long-period waves that move through the oceans in response to the forces exerted by the Moon and the Sun. Tide and current are not the same. Tide is the vertical rise and fall of the water and tidal current is the horizontal flow. In simple words, the tide rises and falls, the tidal current floods and ebbs. The tidal forces are generated by the gravitational effect of the Moon and the Sun. By the mid-seventeenth century, three different theories for the origin of tides were being seriously considered:

1. Kepler was one of the originators of the idea that the Moon exerted a gravitational attraction on the water of the ocean, drawing it towards the place where it was overhead. This attraction was balanced by the Earth's attraction on the waters, for 'If the Earth should cease to attract its waters, all marine waters would be elevated and would flow into the body of the Moon'.
2. Galileo proposed that the rotations of the Earth produced motions of the sea, which were modified by the shape of the seabed to give the tides.
3. The French mathematician, philosopher, and scientist Rene Descartes introduced the third theory in the early part of the seventeenth century. Descartes argued that space was full of invisible matter. As the Moon travelled around the Earth, it compressed the matter in a way that transmitted pressure to the sea, hence forming the tides.

Although there was merit in each of these approaches, it was Sir Isaac Newton's introduction of the concept of force in a heliocentric solar system that was finally to resolve the differences between them. However, the first, accurate, global maps of deep-sea tides were only published in 1994 (Le Provost C. 1994) as presented in figure 1.1 and figure 1.2.

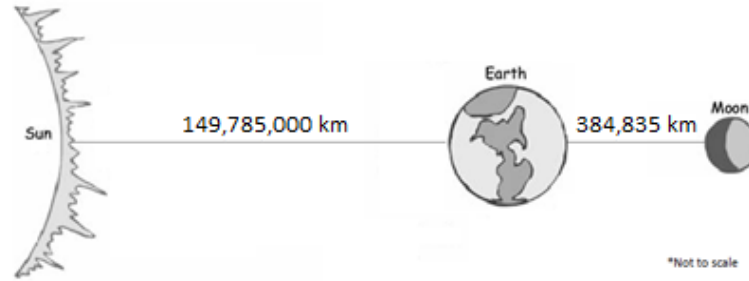


Figure 1.1: Relative distance of the earth to sun and moon (www.universetoday.com)

Newton's Law of gravitation

$$F_g = G \frac{m_1 m_2}{r^2} \quad (1.1)$$

Where,

F_g is the gravitational force (m/s^2)

m_1 and m_2 are masses of two objects (kg)

r is the separation between the objects (km)

G is the universal gravitational constant

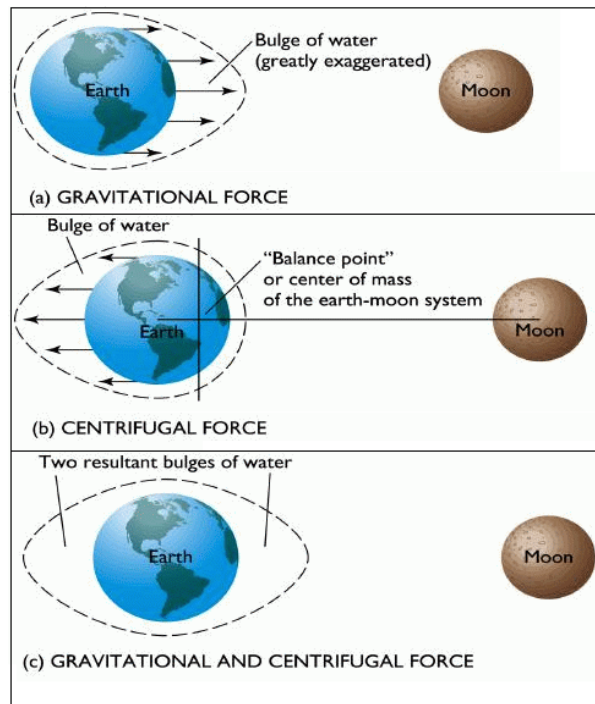


Figure 1.2: Moon-Earth System (www.usna.edu)

1.2 Spring & Neap tides

The range of tide, defined as the vertical difference in height between consecutive high and low tides, varies from place to place and also varies over time. The combination of the solar and lunar

envelopes during the synodic month (period of the moon's phases) causes spring tides and neap tides. The lunar tide is 2.16 times more influential than the solar tide, as the moon is closer to earth than the sun (although the mass of the sun is huge). When the moon is new or full, the tide-generating forces of the sun and moon are aligned. The high tides of the solar envelope occur at the same time as the high tides of the lunar. This increases the height of the composite high tides, called **Spring tides**.

When the moon is in its first/third quarter, the tide generating forces of the sun are at right angles to those of the moon. The envelope of the tide-generating forces of the sun is shown to conflict with the force envelope of the moon. The low tides of the solar envelope occur at the times of the high tides of the lunar. This reduces the height of the composite high tides, called **Neap tides**. Figure 1.3 shows different phases of a tidal cycle.

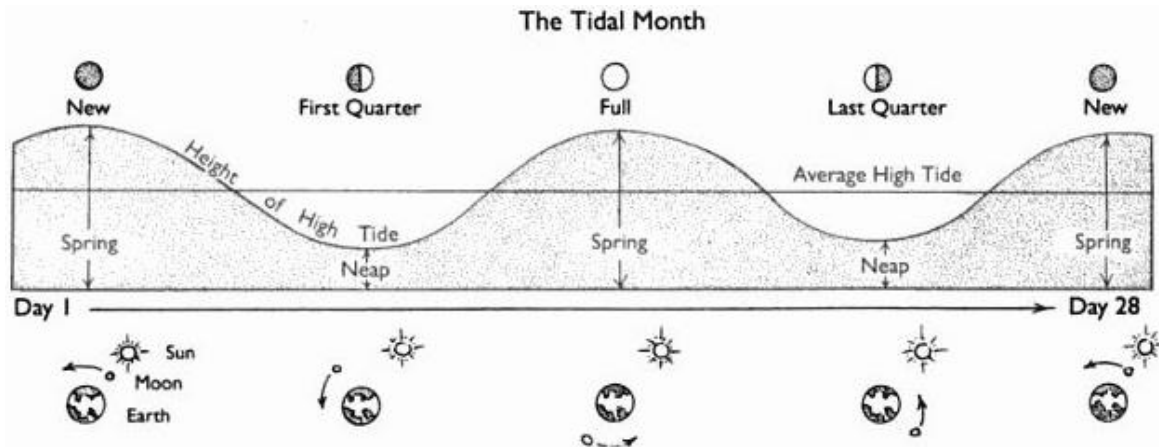


Figure 1.3: Types of tides: diurnal, semidiurnal and mixed. (Hagerman and Polagye 2006)

1.3 The current state of knowledge

1.3.1 Demonstration Project at Sundarbans

A report was submitted to MNRE by West Bengal Renewable Energy Development Agency (WBREDA) in 2001 for setting up a 3.65 MW capacity tidal power station at Durgaduani Creek in Sundarbans Island of West Bengal. These details were submitted to the Ministry in June 2006. Also, WBREDA entered into an MoU with the National Hydroelectric Power Corporation Limited (NHPC), Faridabad for updating the Project Report and its execution. The updated Report prepared by NHPC was received by the Ministry in November 2007. NHPC Limited was given the

responsibility to complete the project. However, the project has been discontinued due to very high tender cost.

1.3.2 Tidal Power Projects in the Gulf of Kutch

A committee was established under the Central Electricity Authority (CEA) on the 900MW Kutch Tidal Power Project for estimating the cost of the project. The project was not found to be commercially viable due to the high capital cost as well as the high cost of generation of electricity.

In January 2011, Gujarat signed an MoU with Gujarat Power Corporation Ltd. (GPCL) for establishing a 250 MW tidal power project at Mandvi district in the Gulf of Kutch. GPCL has initially started a 50MW tidal power project in Kutch. GPCL has requested a grant for the tidal power plant to the Ministry of New and Renewable Energy (MNRE). The experience gained in the above project will decide the future course of action for the advancement of tidal energy in India.

1.4 Tidal energy around the world

The necessity to reduce CO₂ emissions and a gradual increase in the cost of fossil fuel has resulted in a significantly increased use of tidal energy (Nicholls-Lee and Turnock 2008). Today, tidal energy around the world is increasingly being considered as a potential source of renewable energy (Bryden and Couch 2007). Extreme tides are found in many locations across the globe. Some of them are the Pentland Firth, Scotland; the Severn estuary; the Aleutians; the fjords of Norway; the Philippines; the Straits of Messina, Italy; the Bosphorus, Turkey; the English Channel; Indonesia, and the straits of Alaska and British Columbia.

The first major hydroelectric plant was put to operation in 1967 that used the energy of the tides to generate electricity. It produced about 540,000 kW of electricity (Charlier R. H. and Finkl C. W. 2009). Studies have shown that the European territorial waters have 106 locations for extracting tidal energy that would provide electricity of 48 TW per year. It is estimated around 50,000 MW of installed capacity being achievable along the coasts of British Columbia alone. There are greater predictions of extracting an energy of about 90,000 MW off the North West coast of Russia and about 20,000 MW at the inlet of Mezen River and White Sea of Russia.

Table 1.1 gives the highest available tidal levels in some of the regions that have the potential to establish tidal power stations. Tidal power plants have already been set up at some of these locations and some are still in the planning phase. The main characteristics of four large-scale tidal power plants that were constructed after World War II and currently exist are given in Table 1.2.

1.5 Methods of tidal energy extraction

Different methods have been suggested by authors for the extraction of tidal energy. However, the basic principle behind the methods remains the same. However, there are two primary methods to extract energy from the tides.

- a. Estuaries into which large amounts of ocean water flows in due to high tidal range are captured behind barrages and the turbines are rotated by utilizing the potential energy of the stored water.
- b. The kinetic energy of moving water can be used to extract energy similar to the principle of extraction of wind energy.

Both methods that are mentioned above have been suggested and followed and each has its advantages and disadvantages (Bryden and Melville 2004). It may also be possible to employ pumping strategies for barrages to obtain better efficiency and to match electricity demand better (MacKay 2007).

The devices that are used in the energy generation vary in size, shape and specifications. (Discusser et al. 2006) has classified the devices into two types:

- a. Tidal barrages that store tidal flow and generate power through discharge.
- b. Tidal current devices which are fixed or moored within a tidal stream.

1.5.1 Tidal barrage

A tidal barrage is a structure generally built across the mouth of the estuary through which the water flows in and out of the basin. The tidal barrage has sluice gates that allow the flow of water in and out of the basin. The water flows into the bay during high tide and the water is retained by closing the sluice gates at the beginning of low tide. The barrage gates are controlled by knowing the tidal range of the location and operating it at right times of the tidal cycle. There are turbines located at the sluice gates which produce electricity when the gates are opened during the low tide. Using this principle, different methods have been proposed for the extraction of energy like ebb

generation, flood generation, ebb and flood generation, pumping, two basin schemes, etc. Figure 1.4 shows the plan view of a hypothetical tidal barrage. Even though the barrage method has high theoretical efficiency, only one large scale tidal barrage has been constructed at La Rance, France (Blunden and Bahaj 2006).

The advantage of using the barrage method to generate electricity in comparison with fossil fuels is that it reduces the greenhouse effects, to provide a better environment. La Rance tidal power plant, France is an example of the barrage method. On the top of the barrage, there is a four-lane highway that cuts 35 km of distance between the towns of Saint-Malo and Dinard.

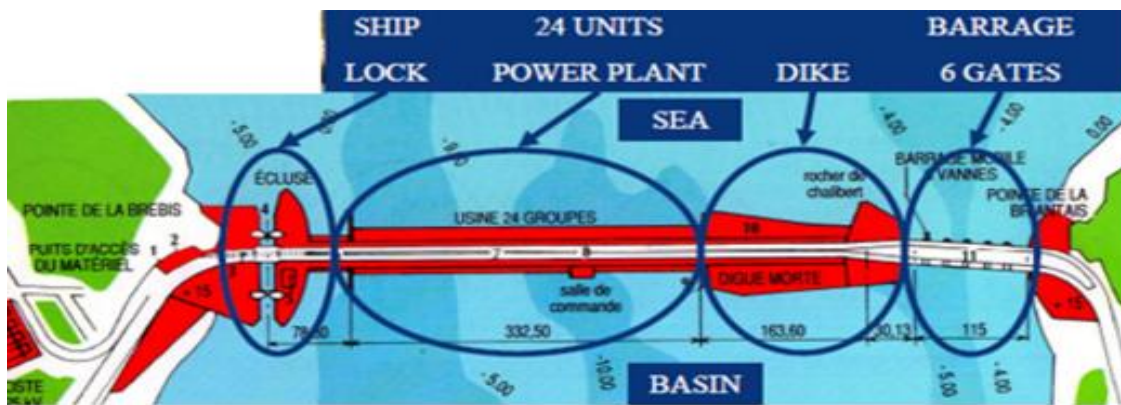


Figure 1.4: La Rance tidal station setup (Charlier R.H., 2007)

Table 1.1. Highest tides of the global Ocean (Gorlov 2003)

Site	Country	Tidal elevation (m)
Bay of Fundy	Canada	16.2
Severn Estuary	England	14.5
Port of Granville	France	14.7
La Rance	France	13.5
Puerto Rio Gallegos	Argentina	13.3
Bay of Mezen (White Sea)	Russia	10
Penzhinskaya Guba (Sea of Okhotsk)	Russia	13.4
Gujarat	India	11

Table 1.2. Existing large tidal power plants (Gorlov 2003)

Site	Country	Bay area (km ²)	Avg. tide (m)	Installed Power (MW)
La Rance	France	22	8.55	240
Sihwa	South Korea	30	5.6	254
Annapolis	Canada	15	6.4	18
Jiangxia	China	1.4	5.08	3.9
Kislaya Guba	Russia	1.1	2.3	0.4

1.5.2 Tidal Stream Energy

In the early 1990s, tidal power was mainly focused on harnessing the tidal flow and generating energy using potential storage rather than through tidal stream. Tidal stream technologies have made massive progress towards commercialisation in the last decade. Extensive research is being carried out in UK waters related to tidal stream energy. The UK has a target to achieve 20% of its electricity requirement through ocean resources by 2020. About 40 energy converting machines are being developed and prototypes are being tested in the labs and waters of UK (O'Doherty et al. 2017). Since the tidal stream energy is still an emerging technology, it has no standardizations, but varieties of devices are being developed to make use of the water flow to extract electricity. However, the efficiency of each of the devices has to be flawlessly examined by extensive testing to choose the appropriate device for a particular location.

The map in Figure 1.5 represents the global locations where it would be beneficial to implement tidal power. The scale on the bottom represents the overall change in ocean height from high tide to low tide, with the greater difference representing the greater possibility for tidal energy production. Although this specifically correlates with the barrage type tidal power plant, the other forms of energy extraction are most beneficial in these locations as well due to the presence of shallower waters as well as strong currents.

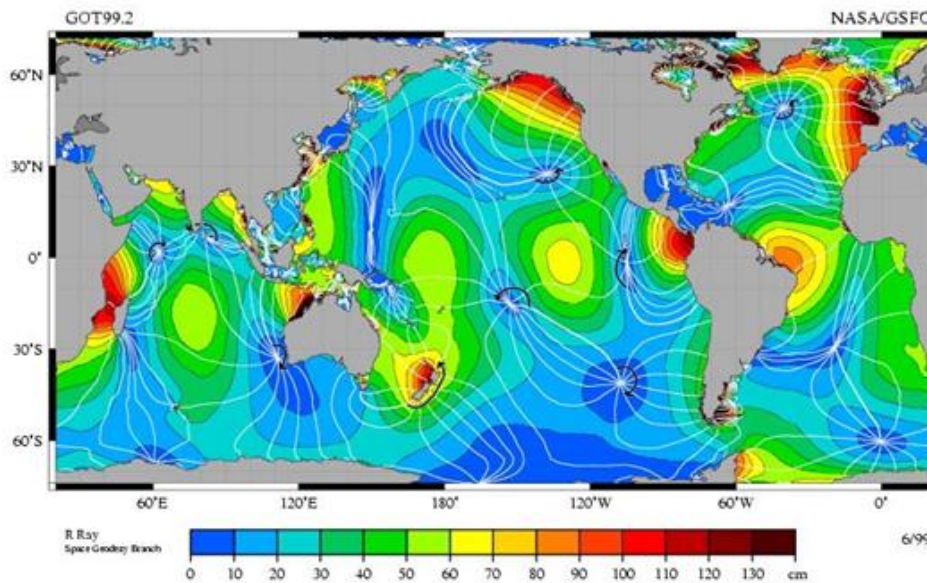


Figure 1.5: World Tidal Potential Locations (https://en.wikipedia.org/wiki/File:M2_tidal_constituent.jpg)

1.6 Tidal Stream projects

a. SeaGen

SeaGen is the world's first large scale commercial tidal stream generator (Douglas et al. 2008). The first SeaGen generator was installed in Strangford Narrows between Strangford and Portaferry in Northern Ireland, the UK in April 2008 and was connected to the grid in July 2008. It was four times more powerful than any other tidal stream generator in the world at the time of installation. It generates 1.2 MW for between 18 and 20 hours a day while the tides are forced in and out of Strangford Lough through the Narrows.

Each wing drives a generator through a gearbox like a hydro-electric or wind turbine. These turbines have a patented feature by which the rotor blades can be pitched through 180 degrees allowing them to operate in both flow directions – on ebb and flood tides. The power units of each system are mounted on arm-like extensions either side of a tubular steel monopile about 3 metres in diameter and the arms with the power units can be raised above the surface for safe and easy maintenance access. The SeaGen was built at Belfast's Harland and Wolff's shipyards.

The project can supply power to 1,500 homes. Irish energy company ESB Independent Energy buys the power generated by the turbines for its customers in Northern Ireland and the Republic of Ireland. The grid connection work was undertaken in partnership with Northern Ireland Electricity.

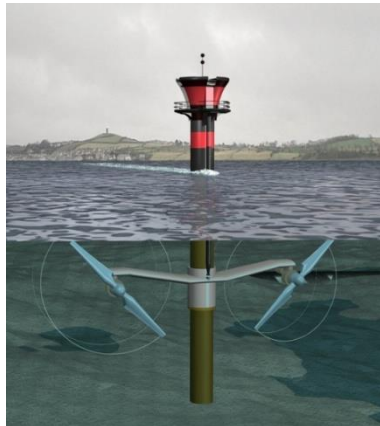


Figure 1.6: SeaGen tidal stream generator (www.power-technology.com)

b. The RITE Project, New York, NY (East River - East Channel):

Verdant Power's Roosevelt Island Tidal Energy (RITE) Project is located in the East Channel of the East River, which is a tidal strait connecting the Long Island Sound with the Atlantic Ocean in the New York Harbour. Since 2002, Verdant Power has conducted prototype and pre-commercial

testing of its Kinetic Hydropower System (KHPS) technology at the RITE Project, as well as ground-breaking environmental analysis of the system. The East River is a tidal strait, with strong water currents that change direction between -flood and ebb tides approximately four times each day. When the water velocity exceeds approximately 1.0 m/s, the turbine blades begin to rotate and the units generate electricity for about 4 hours. As the tide shifts direction, the yaw of the turbines (turn approx. 170 degrees) to generate power from the current flowing in the opposite direction. This cycle repeats in a very predictable manner approximately every 6 hours. The regular nature of tidal currents provides a significant advantage for tidal power as compared to other energy systems.

Located off of Roosevelt Island in Manhattan, Verdant power has been conducting a location-specific experiment of tidal stream potential in the East River since 2002. This location is ideal due to the fast-flowing current of the East River in addition to the distance between the possible farm location and the area of electrical generation use. The first phase of the project was to explore the potential and efficiency of a tidal stream turbine. These turbines were the world's first turbines to be bidirectional and the first to be implemented into a tidal farm, allow for the East River tidal turbines to achieve anywhere between 80-90% capacity factor. This allows for electrical production regardless of tidal direction.

Through the effort, Verdant Power successfully demonstrated the KHPS as an efficient source of renewable energy with the following outcomes:

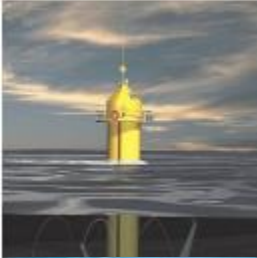
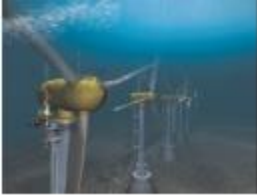

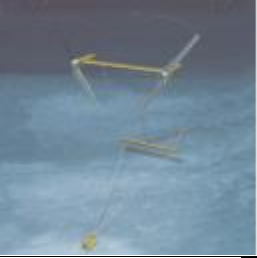


- Grid-connected power with no power quality problems.
- Excellent hydrodynamic, mechanical and electrical performance.
- Fully bidirectional operation – passive yawing with high efficiency on both ebb and flood tides.
- Automatic control and continuous, unattended operation.
- No fouling or damage from debris.
- 70-megawatt hours of energy delivered to commercial end-users.
- 9,000 turbine-hours of operation.

1.7 Tidal stream energy devices

There is a wide range of tidal energy devices used for energy extraction based on site conditions. The details of some of them are given in Table 1.3. Recent developments in low head and low flow

turbines have driven studies even in locations where there is a moderate tidal range of about 2m and tidal stream velocity as low as 1 m/s.

Table 1.3. Tidal stream energy extraction devices (Nicholls-Lee and Turnock 2008)

Turbine	Power Output	Description	Image	Operating/ Conceptual
Seagen, Marine Current Turbines Ltd. UK	1 MW	Twin two-bladed rotor, sheath mounted, horizontal axis tidal turbine		Operating
The Blue Concept, Hammerfest Strom, Norway	1 MW	Three bladed pile mounted horizontal axis tidal turbine		Conceptual
THG, Hydraulic Generator	3 MW	An array of four-bladed horizontal axis turbines attached to a gravity mounted frame		Conceptual
TidEL SMD Hydrovision, UK	1 MW	Twin two-bladed tethered rotor, able to yaw into the current		Conceptual
Stingray, Engineering Business Ltd., UK	500 kW	Oscillating Hydroplane		Conceptual
Blue energy, Blue energy Canada	500 kW	Four bladed, moored, surface piercing, vertical axis turbine		Conceptual

1.8 Tidal energy in India

The Ministry of New and Renewable Energy (MNRE), Government of India, estimates that the total identified potential of Tidal Energy is about 12455 MW, with potential locations identified at Khambhat & Kutch regions, and large backwaters. These estimates were provided considering barrage technology for tidal energy extraction. The Gulf of Khambhat, Gulf of Kutchh in Gujarat state and delta of Ganga in Sunderbans, West Bengal state have been identified as potential sites for generating tidal power. The maximum available power densities, from the tidal stream, are estimated to be about 3 kW/m² and 0.7 kW/m² during spring and neap, respectively, in the Gulf of Khambhat (Satheesh Kumar and Balaji 2017). The tidal stream energy estimates provided by (Murali and Sundar 2017) along the Indian coast where the available average kinetic energy was 2604.3, 4500.2, 1333.4, 562.5, 562.5, 562.5, 85.3, 166.7, 562.5 and 2604.3 in Khambhat, Kutch, South Gujarat, Maharashtra, Karnataka, Kerala, Tamil Nadu, Andhra Pradesh, Odisha and Sunderbans respectively. However, no estimates are available at Goa. Numerical modelling studies are carried out in India in the recent past to study the sediment, hydrodynamic and morphodynamic characters due to the effects of various oceanic processes and construction activities and these are proving reliable to replicate the ocean environment (Sheela Nair and Sundar 2010; Muni Reddy et al. 2007; Pradhan et al. 2020; Rose and Bhaskaran 2017).

1.9 Numerical models for coastal environment

Delft3D, TELEMAC and MIKE by DHI are well known software packages that deal with the simulation of flows in rivers, estuaries, and coastal ocean regions. MIKE is more advanced than other models being used for simulation of flow dynamics coupled with waves and bed morphology. All these numerical flow models solve the Navier-Stokes (NS) equations. The major differences between the models are mainly in the schemes used to solve the NS equations and in the way the coupling takes place between different modules of waves, flow and morphology.

In Delft3D, a cell-centered finite difference method is used for spatial discretization of the equations and implicit scheme is used for time integration. Whereas, in MIKE21 FM (model used in the thesis), a cell-centered finite volume method is used for spatial discretization of the equations and explicit scheme is used for time integration. The open source version of Delft3D uses rectangular grids whereas the commercial MIKE has choice of both rectangular and triangular grids. Delft3D does not include a dedicated provision for studies on tidal turbines and the code

needs to be modified to incorporate the tidal turbine studies. MIKE has a built-in structure type called "turbines", the hydrodynamic module can be coupled with mud/sand transport, MIKE does not need modification of the code provided by the developers. The effect of tidal turbines is modelled as sub-grid structures using a simple drag-law to capture the increasing resistance imposed by the turbine blades as the flow speed increases. Turbines are assumed always to have their axis aligned with the flow direction. While adding a new turbine, the location of the turbine and the turbine data is specified. The diameter of the turbine and the z-coordinate of the centroid of the turbine should be specified. The resistance imposed by the turbine blades can be specified in one of two ways:

- Fixed drag coefficient.
- Tabulated drag and lift coefficient.

When "Fixed drag coefficient" is selected, the turbine is assumed to have the axis aligned with the flow direction. Hence no lift force is calculated. When "Fixed drag coefficient" is selected, the turbine is assumed to have the axis aligned with the flow direction. Hence no lift force is calculated.

Many authors including Symonds et.al, 2016, Waldman et.al, 2017, have compared MIKE and Delft and found that there is no change in the flow characteristics from both the models. However, based on other factors like hands on experience in MIKE, availability of commercial license, MIKE21 is chosen for the present study as the emphasis is on tidal energy.

1.10 ORGANIZATION OF THE THESIS

Chapter 1 presents a general introduction to the formation of tides, types of tides and the research work carried out on tidal energy in the Indian and global context is highlighted. The importance of extraction of energy from renewable energy sources without having negative impacts on the ecosystem is brought out. The organisation of the thesis is presented.

Chapter 2 briefs the literature review where current state of knowledge of tidal energy extraction, adverse impacts of non-renewable sources of tidal energy extraction, has been highlighted. Some of the available methods for tidal energy extraction, highest tides across the globe and a review on the existing tidal power plants are presented. The need for switching to renewable energy sources

and the advantages of tidal energy extraction has been brought out. Necessity and relevance of the present study along with research objectives are presented.

Chapter 3 deals with the identification of potential locations for tidal energy extraction and provides an estimate of the overall energy that could be extracted from the tidal energy sources along the Indian coastline. This chapter describes the two methods of tidal energy extraction viz. barrage method and tidal stream energy method. Numerical simulations are carried out and validated with the measured tides. The overall potential energy that could be extracted is estimated by establishing a few criteria and the tidal stream energy assessment is carried out.

Chapter 4 deals with the numerical modelling of the hydrodynamics and corresponding morphology changes and the impact of tidal energy farm on local hydrodynamics and energy estimates. Five typical cases are considered in the Zuari inlet for the estimation of tidal stream energy and assessment of the impact on morphodynamics. The hydrodynamic module of MIKE21 coupled with sand transport is used for the simulation. The energy extracted in each of these cases is compared with the base case. A detailed comparison of the tidal stream energy estimates and the effect on morphodynamics is discussed.

Chapter 5 presents a detailed study on the introduction, concept and establishment of tidal pools at select locations along the west coast of India. Basic criteria to establish a tidal pool is discussed. Few locations along the west coast of India are identified to establish tidal pools. Numerical simulation is carried out to assess the energy that can be extracted and the effect on the local hydrodynamics is studied.

Chapter 6 summarizes salient aspects of the present research along with the conclusions derived from the present study. The scope for future research in this area is put forth at the end.

References and the relevant Tables and Figures are presented Chapter-wise in the Appendices at the end.

1.11 NECESSITY AND RELEVANCE OF THE PRESENT STUDY

Tidal energy is inexhaustible and can be considered as a renewable energy source. Tidal power in particular is receiving a great deal of attention at present, driven by issues, including the security

of supply and the availability of hydrocarbon energy sources. Tidal Energy is one of the new and evolving technologies. Energy is being extracted from tides in some parts of the world, while most of them use tidal barrage. However, there are other methods of energy extraction like tidal stream energy, tidal lagoons, or tidal pools which are still at the proposal stage. We hardly find “one” tidal power plant that is so far installed which uses the tidal stream to generate electricity. In many locations, tidal stream energy extraction is commercially not viable and still in Research & Development (R&D) stage. It is an advantage to extract energy from tides because it is less vulnerable to climate change; while the other sources are all vulnerable to the random changes in climate. Few locations like Gulf of Kutch, Gulf of Khambhat, Sundarbans have been suggested for tidal energy extraction. Also, very limited studies are carried out in other parts of India. However, all these suggested sites prove good for the energy by barrage method. There is a need to assess the tidal stream energy potential to extract energy from the tides to deviate from the conventional tidal barrage method. The energy extraction from the tidal stream is similar to that of wind energy extraction. The tidal stream devices or turbines are immersed inside the ocean where tidal stream energy is higher. On the other hand, there is a need to develop devices that are capable of operating in low head and low flow conditions; called low flow turbines. This study, however, moves the focus forward to assess the tidal energy potential (both potential and kinetic energies) to generate power directly from the ebbing and flooding of the tidal currents.

CHAPTER 2

HISTORY –LITERARURE

2.1 General

Tidal energy is inexhaustible and can be considered as a renewable energy source (Tousif and Taslim 2011). It is an advantage because it is less vulnerable to climate change; while the other sources are all vulnerable to the random changes in climate (Nicholls-Lee and Turnock 2008). The review is given by the Energy Technology Support Unit (ETSU) on the Tidal Stream Energy was the initial attempt to estimate the energy from tidal stream resources in the UK (Tidal stream energy review (ETSU) 1993). The points marked by the ETSU were later studied and modified in 2001 in a document submitted to the UK Department of Trade and Industry (DTI) by Binnie, Black and Veatch (www.bv.com).

Most of the existing technology used for tidal energy conversion is from the wind power industry (Bahaj et al. 2007; Batten et al. 2007; Fraenkel 2002). Researchers have predicted that the UK is capable to produce over 20% of its electrical needs from its tidal resources (Callaghan 2006). It is also a fact that the studies carried out so far in predicting the energy that can be extracted from tides, has only focused on the past and the present availability of the energy. But it is also important to consider and address the effects of exploiting renewable energy sources for energy extraction. There has to be an understanding among the developers as to when and where to stop the energy extraction so that there is minimum or no disturbance caused to the regular natural phenomenon.

The tides that are generated along some parts of the Indian coastline have the potential to extract energy from the turbines. The tidal elevation in India is as high as 8.5 m at Bhavnagar, Gujarat and as low as 0.5 m at the Southern part of India. Survey of India predicts tide levels at some locations along the Indian coastline and Tide Tables are published for every year (Kumar et al. 2011).

As per the studies carried out by Central Water and Power Commission (CWPC) in 1975, the Gulf of Kutch and Gulf of Khambhat in Gujarat and Sundarbans area in West Bengal are the only suitable sites in India for the production of Tidal Energy. In the 1980s, the Central Electricity Authority (CEA) took up a study for the assessment of tidal energy potential in India. CEA listed a few places of Potential Tidal Energy extraction in India as shown in Table 2.1.

No tidal power generation plant has been installed in India due to its high cost of generation of electricity and lack of techno-economic viability. However, there are proposals for setting up of tidal power stations at Gujarat.

Table 2.1 Tidal Energy Potential in India (Kumar et al. 2011)

Site	State	Tidal Range (m)	Tidal Potential (MW)
Gulf of Khambhat	Gujarat	12	7000
Gulf of Kutch	Gujarat	8.5	1200
Gangetic Delta, Sundarbans	West Bengal	7	100

It is in recent times that the finite element based numerical/mathematical models are being extensively used for ocean modelling. Various authors, including (Cornett et al. 2011; Cousineau et al. 2012; Greenberg 1979; Karsten et al. 2008) have developed numerical models to simulate tidal hydrodynamics at various locations across the globe over the years. In the late 90s, (Ranasinghe et al. 1999) used a morphodynamic model that could simulate both cross-shore and longshore transport processes which were further used for simulating the seasonal dynamics of tidal inlets.

Chiou et al., 2010 used a numerical model to simulate the tides on the Taiwan Banks (Formosa Shoals) in the Taiwan Strait region. The numerical model was validated against sea-level observations from 34 tidal stations located on the coast of Mainland China and Taiwan. Trajectory records from two SVP drifters were used to compare with the simulations using wavelet-based rotary spectral analysis.

Chatzirodou and Karunarathna (2014) studied the impacts of tidal energy extraction on sea bed morphology covering the area of Pentland Firth channel (Scotland, UK) by application of a 3D numerical model (Delft 3D) to examine the hydrodynamics due to the energy extraction by tides. Initial results indicated that the current morphodynamics of the detected sandbank zones inside Inner Sound Channel was notably dynamic. The results obtained strongly suggested there is possible increase/decrease in tidal flows due to which energy extraction may have significant effects on the existing morphodynamic regime.

Masters et al. (2015) conducted a comprehensive contrast of various methods of Numerical Modelling for the assessment of currents Tidal Streams. Several models considering different configurations of turbines that were built on the horizontal axis principle at different spatial scales were equated. Many numerical schemes were presented to demonstrate the exploitation of tidal energy from the moving streams of water. They concluded that the foremost applicable alternative of arrangement depends on the physical scale where answers are required and the computational resources available.

Fairley et al. (2015) conducted a study on the cumulative impact of tidal stream turbine arrays on sediment transport in the Pentland Firth, Scotland. A 3D hydrodynamic model that is coupled to provide inputs to the sand transport module was used to examine the influence on sediment transport and bed level changes due to tidal stream turbines. Two typical cases were considered here, the first one predicted the dynamics of the sea bed parameters instigated by multiple tidal stream turbine farms in the Pentland Firth and secondly as a case study to determine the connection between effects of single tidal arrays and collective influences of multiple tidal turbine arrays. It was found that there were no significant bed level changes due to an individual tidal farm whereas a notable change in bed level was observed when multiple tidal farms were used for energy extraction.

Fairley et al. (2017) modelled the Effects of Marine Energy Extraction on Non-Cohesive Sediment Transport and Morphological Change in the Pentland Firth and Orkney Waters. MIKE3 and Delft3D models were used for the assessment. It was observed that both the 3-dimensional models produced comparable results and it was observed that the implementation of tidal turbines had a significant effect on the bed level change.

Karunarithna et al. (2017) modelled the hydrodynamics of a Tidal Stream Energy extraction site using a depth-averaged numerical model that was proposed in the Inner Sound channel of Pentland Firth that is located between mainland Scotland and the Orkney Islands. The simulation results recommended the appropriate suitability of the selected site for tidal stream energy harvesting. However, some predictions on the morphological changes were expected in sedimentary deposits located close to the proposed tidal turbine farm, which may have effects on benthic environmental conditions of the area.

McPherson et al. (2013) investigated the penetration of tides and tidal anomalies in New South Wales Estuaries. Several different techniques were employed in the analysis of the penetration of tides and anomalies in estuaries. It was concluded that the Tides appeared to attenuate faster than anomalies within all estuary types. Within rivers and bays, the difference between tidal attenuation and anomaly attenuation was found smaller. In lakes and ICOLLs attenuation of the tide was much greater than the anomaly.

Haverson et al. (2017) conducted the impact assessment of tidal stream energy extraction in the Irish Sea. A high resolution depth-averaged hydrodynamic model, Telemac2D was utilized for this study. Eight locations were examined, where the tidal energy farms were being proposed during the time of this study. The locations were: West of Islay, Ramsey Sound, Mull of Kintyre, Strangford Loch, Anglesey, Sound of Islay, Fair Head and Torr Head. Only three projects showed array-array interaction: Mull of Kintyre, Torr Head and Fair Head. Results disclosed Mull of Kintyre had slight influence. The energy production at Torr Head was decreased by 17% due to Fair Head, whereas, Fair Head only reduced by 2%. This was caused by the tidal asymmetry whereby the flood was stronger. When worked alongside, the peak power-output at Torr Head was 64.5 MW, measuring a 31% decrease.

Waldman et al. (2017) compared the MIKE 3 and Delft3D software, intending to examine the appropriateness for forecasting the impacts of tidal stream energy development. Representative conditions for energy extraction by tides were executed in each of the models, and the forecasts of the models with and without turbines were compared. Similar estimates were done for the current speeds, but the bed stress in one model reflected more than twice that in the other due to the use of different values for bed resistance. The impacts of energy extraction were comparable among both the models at a regional scale but showed considerable local differences. It was concluded that these model codes are suitable for the broad-scale assessment of the effects of energy extraction but that caution, and more detailed survey data, is required at fine scales.

Draycott et al. (2017) made Model-scale testing of tidal turbines in the wave-current environment. Different combinations of realistic current-wave scenarios were considered at the basin, where the main intention was to analyze the characteristics of testing in a joint wave-current atmosphere and evaluate if the wave effects on the flow field can be foretold. The methodology and results offered

increased learning about the wave-current testing atmosphere and provided a better understanding of analysis tools able to improve test outputs and conclusions from scale model testing.

Haverson et al. (2018) modelled the hydrodynamic and morphological impacts of a tidal stream development in Ramsey Sound. A high-resolution two-dimensional depth-averaged numerical model, Telemac2D, was used to examine variations to hydrodynamics and morphodynamics. Outcomes presented that the planned group of nine tidal energy turbines caused changes to eddy propagation that led to modifications in the velocity field up to 24 km from the tidal farm. The morphodynamic changes were predicted by altering the bed shear stress parameter. Altering the mean and maximum bed shear stress, over 30 days, were found to be more localized and extend 12 km from the array. These alterations showed that the planned tidal energy farm cause changes to localised sediment accretion and will act as a barrier to sediment transport.

Bonar et al. (2018) highlighted the suggestion put forth by the study of theoretical models to make the most of the collective power output, tidal turbines should be arranged in a single cross-stream row and optimally spaced to exploit local blockage effects. Depth-averaged open-source hydrodynamic numerical model, ADCIRC, was utilised to further examine whether the energy extraction capacity of a tidal turbine array can be improved by fluctuating solely the local blockage, solely the local resistance, or both local blockage and resistance together, across the width of the tidal energy farm. The results that were obtained recommended that if both the flow pattern and tidal turbine arrays were maintained uniform in terms of diameter, spacing and resistance, the results were encouraging as it proved cheaper and easier to design and operate the tidal energy farm. Also, the performance of the tidal energy form is the best, when they are specifically designed to match the site conditions case by case.

An experimental investigation into non-linear wave loading on horizontal axis tidal turbines was conducted by Draycott et al. (2019b; 2019a) where a 1:15 scale tidal turbine was subjected to severe wave action to examine its response to the action of waves. Continuous, high intense currents and waves were imposed on the turbine to check if they had an impact on the fatigue, extreme loading and power flow requirements of the turbine. Results substantiated that wave action had a greater impact on the turbine power and thrust compared to current only conditions. These wave-induced fluctuations were shown to increase with wave amplitude and decrease with wave frequency.

Bonar et al. (2019) used numerical methods to explore how optimal turbine arrangements change as the flow transitions from frictionless and steady to rough and oscillatory. Results showed that the performance of a tidal turbine array can be enhanced by varying the lateral spacing between the turbines to exploit local blockage effects.

A study on the tidal propagation characteristics of Hooghly estuary was carried out by Jena et al. (2018), using a two-dimensional depth-averaged numerical model, ADCIRC, and analytical models along with observations. From the results, it was interpreted that the estuary is yet to attain a steady-state and reach its equilibrium morphology. It could be close to its equilibrium as minute intensification (0.1 m) was observed in the predominant semi-diurnal constituent M2 over 78 km (barely 7%) in the estuary. The parameters of width difference and the ratio amongst friction and inertia have been used to define the marginal condition for intensification. The relative position of Hooghly in terms of marginal condition was consistent with a similar set of estuaries elsewhere that were grouped using the above parameters.

Rose et al. (2015) had carried out Tidal analysis and prediction for the Gangra location, Hooghly estuary in the Bay of Bengal. The study performed location-specific tidal analysis and prediction utilizing one-hourly tide data with SLPR2 harmonic tidal analysis tool for Gangra situated upstream of the Hooghly River. This study also performed a comprehensive validation between the computed monthly tidal prediction from SLPR2 and measured water level at Gangra. The skill level of prediction exhibited a good match. This study also investigated the influence of atmospheric effects on sea-level pressure variations and the resultant water-level elevation from extreme weather events such as depressions and severe cyclonic storms that occurred during 2013. The study signified the importance of tidal analysis and prediction for operational needs.

2.2 Tidal stream energy estimates and studies

The first and most important step in energy extraction is to evaluate the available energy present in a tidally driven stream. There has to be a good understanding of the geography of the area and the tidal conditions at the site. Many published reports/technical papers have made estimates of exploitable resources, as follows.

Early estimations of tidal stream energy were provided by the Energy Technology Support Unit (ETSU) in 1993 (Tidal stream energy review (ETSU) 1993). The report focused on estimating the tidal stream energy in 33 sites of the UK. The basic criterion considered was the tidal stream speed

of 2 m/s and a water depth of about 20m. The total surface area was divided into grids with water depth as a criterion. Based on this criterion, the total energy output (annually) of all the sites under study was estimated to be 57639 GWh.

A technical report on the exploitation of tidal and marine currents (European Commission 1996) estimated the tidal power in Europe that also included some locations in the UK, using a similar approach as ETSU mentioned above. It was calculated that the European resources have potential sites of about 12500 MW and the locations in the UK including 8900 MW amongst the total. The criterion considered was currents greater than 1.5 m/s.

In 2005, the tidal stream energy at Portland Bill, South UK was evaluated (Blunden and Bahaj 2006) using a 2D model TELEMAC that used finite element mesh. The location had tidal current speeds up to 3.6 m/s. The obtained results were validated with tidal diamonds (30 numbers) from Admiralty charts that considered the effects of all the tidal constituents. The peak power output from the turbines located in the study area was found to be 730 kW.

Bryden and Couch (2005) addressed some issues that needed to be considered when assessing tidal energy. They strongly recommended that the influence of the tidal energy extraction on the local hydrodynamics and the environment have to be majorly considered. Four types of tidal current technologies were discussed; Horizontal axis systems, Vertical axis systems, Variable foil systems and Venturi based systems. It was explained that the cost consideration for effective device fixing of any of the above-mentioned systems had a major role in the economics of any project. Tidal current energy was estimated by considering a channel of 1000m wide and 40m deep and peak spring tide of 3 m/s. They concluded that only 10% of the raw energy flux can be extracted without disturbing the natural environmental conditions.

The most important variables to be considered for suitability of any site for tidal stream energy extraction was recommended by Couch and Bryden (2006). The parameters they considered were; local water depth of at least 25 meters, the proximity of the location to the city, reliable current speeds of about 3 m/s. Five simple generic cases were considered and numerical modelling based on shallow water equations (MIKE21, DIVSAT) were used. Of the five regimes, the first two were found most prevalent, but least suitable for exploration.

Bryden and Couch (2007) addressed the tidal energy that was extracted from a simplified channel in which the flow occurred because of the potential energy i.e. difference in water levels between the input and output. The kinetic energy was extracted using a channel of known dimensions but

with a multiplying factor. They also realized that the multiplying factor had a strong correlation to the physical properties of the channel and it exceeded unity at times. The simple channel that was considered had some resemblances to tidal channels but it was presented as an abstraction to allow appreciation of the relationships between energy extractions, flow speed and channel properties. The channel length considered was 400m, width 500m and depth 40m. Manning's coefficient was assumed to be 0.025 and an undisturbed current speed of 3 m/s. The kinetic energy potential in this channel was found to be 276 MW.

The commercialization of tidal turbines had begun and large scale testing of the prototypes was being carried out in Norway, Italy, and the United Kingdom (Sun et al. 2008). In the two-dimension simulation model, an absorption zone was created in the middle of the channel which was treated as the coordinate origin. The height assumed was 0.5 m, which was half of the water depth. The free surface of the water was 0.5 m from the midpoint of the absorption zone. An unsteady flow condition was assumed and time stepped at 0.01 seconds intervals until a stable state was attained. It was absorbed that an approximate of 38% energy was absorbed when the water was made to pass through the absorption zone.

A three-dimensional model DELFT3D, developed by Delft Hydraulics was used for the evaluation of flow velocities in Ria de Muris, NW Spain (Carballo et al. 2009), simulations were carried out to compute the tidal currents in the study area. Greater flow speeds were observed in the inner area, with a maximum of 2.3 m/s at mid-flood of a spring tide. The velocity was observed comparatively larger during the flood tidal condition than during the ebb tide. At mid-flood of a mean springtide, the power density of the turbine aperture reached a maximum of 5 kW/m² and exceeded 2 kW/m² over. Two points were chosen for further detailed study.

Tousif and Taslim (2011) demonstrated the theoretical calculation of potential and kinetic components of tidal energy from using the equations and $E = \frac{\rho Agh^2}{2}$ and $P = \frac{\xi \rho AV^3}{2}$ respectively. They also discussed on the different energy generating methods based on the ebb and flood condition of tides.

TELEMAC-2D numerical simulation was carried out and the tidal velocities were validated with Acoustic Doppler Current Profiler (ADCP) measurements in the tidal channel Skarpsundet in Norway (Lalander et al. 2013). The current speeds generated from the two-dimensional numerical model showed good correspondence with the average cross-sectional velocities measured across

the channel cross-section but showed poor comparison in the middle of the channel. Velocity details from the model output were used to compute the kinetic energy at various locations in the channel. It was concluded that the model generated values were not accurate enough for evaluating the tidal energy resource.

Tidal stream energy was theoretically estimated in the Singapore Strait to aid the effort to reduce the carbon footprints in Southeast Asia (Behera and Tkalich 2014). The tidal hydrodynamics were modelled using a Semi-Implicit Eulerian-Lagrangian Finite Element (SELFE) model that solves the three-dimensional shallow water equations with Boussinesq approximations. Few points that have tidal currents up to 2.5 m/s in the Singapore Strait were identified from this study. Also, various operational factors that influence the installation of tidal energy devices were taken into account while assessing the theoretical power output for the tidal energy farm. This theoretical estimate showed a contribution of up to 4.36% of the total energy demand of the country in 2011. Thus, the study suggested a thorough examination of the location to calculate the total tidal stream energy available in the Singapore Strait.

Previous investigations on hydrodynamic studies

Several authors have developed numerical models to study the hydrodynamic impacts due to the tidal energy extraction. Some of them developed numerical models to simulate tidal hydrodynamics in the Gulf of Mexico (GoM) and Bay of Fundy (BoF) over the years. Greenberg (1979) estimated changes in the tidal range throughout the BoF and GoM associated with various proposals to construct large tidal barrages in the upper part of the BoF. Because of the near-resonant state of the existing system, it has been shown that small changes in the geometry of the Bay, associated with the construction of a tidal barrage, could produce significant changes in tidal amplitudes as far away as Boston. Karsten et al. (2008) applied a three-dimensional model to investigate the energy that could, in theory, be extracted from the tidal flows at Minas Passage, a 5.5 km wide channel located at the entrance to Minas Basin in the upper part of the BoF. They showed that the energy that could (in theory) be recovered exceeds the kinetic energy associated with the undisturbed flow through the Passage by a factor of three or more. They also developed relationships between the amount of energy dissipated at the Passage and the change in the tidal range at various locations throughout the BoF and the GoM. Cornett et al. (2010) developed detailed two- and three-dimensional models of the tidal flows in the BoF and applied these models

to delineate and assess the considerable kinetic energy resources around the Bay associated with the energetic tidal currents.

The potential hydrodynamic impacts on the Severn Estuary due to several different proposed renewable-energy projects, including a large coastal lagoon were examined (Falconer et al. 2009; Xia et al. 2010a). The Severn Estuary is another ideal site for tidal renewable-energy projects, since it has the third-highest tidal range in the world, with a spring tide amplitude approaching 7 m. They used a two-dimensional finite volume numerical model and applied it to forecast the hydrodynamic impacts due to several different power projects. They modelled a large coastal lagoon with an area of approximately 86 km² and an installed capacity of 1,500 MW and concluded that the lagoon would have little influence on the hydrodynamic processes in the Severn Estuary.

Xia et al. (2010b) examined the impact of constructing a very large tidal barrage across the Severn Estuary. They refined a two-dimensional hydrodynamic model and used the model to simulate the tidal hydrodynamics with and without the barrage. They concluded that discharges, water levels, and tidal currents would all decrease significantly above the barrage. Xia et al. (2010c) also discussed the influence of alternative operating modes on the hydrodynamic impacts of a large tidal barrage across the Severn Estuary. After considering various factors, they conclude that, for efficient electricity generation and reduced flood risk, ebb-generation or bi-directional generation are preferred over flood-generation.

2.3 FORMULATION OF RESEARCH OBJECTIVES

From the literature, it is evident that the feasibility studies are mostly made for the barrage method. In the Indian scenario, the observed conditions and the methods proposed are for the barrage method in Gujarat and West Bengal. Energy extraction from barrage method has not been carried out in the southern parts of India. Tidal stream potential estimation is also an immature concept globally. So, the studies on estimation of potential and kinetic energy from the tides have to be studied to meet the future electricity needs and to extract energy without burning coal or fossil fuels or without emitting CO₂.

471 tidal inlets were identified and were classified along the Indian coast (Seelam et al. 2015; Vikas M 2015; Reddy et al. 2015; Vikas et al. 2015). The Intermittently Closed and Open Lakes and Lagoons (ICOLLs) and wave-dominated inlets are excluded. This is because the ICOLLs are

seasonally opening and closing and the wave-dominated inlets that have the formation of shoals which reduce the tidal streamflow. However, if the inlet is ICOLL or wave-dominated, the possibility of energy extraction is still open with required maintenance. But the inlets identified along the Indian coast is not just sufficient for this study as the tidal barrages and tidal stream devices can also be installed inside the tidal reservoir because of the decrease of cross-sections towards the land.

2.3.1 RESEARCH OBJECTIVES

Based on the research gaps, the following objectives are framed:

- i. To identify potential locations for tidal energy extraction and to estimate tidal energy potential (Potential energy and kinetic energy) along the Indian coast.
- ii. To study the impact of tidal energy farm on local hydrodynamics and energy estimates.
- iii. To establish potential sites for tidal lagoons at select locations along the west coast of India and its influence on hydrodynamics.

CHAPTER 3

IDENTIFICATION OF POTENTIAL LOCATIONS FOR TIDAL ENERGY EXTRACTION

3.1 Introduction

From the literature review, it is evident that the majority of the feasibility studies are mostly made for the barrage method of tidal energy extraction. In the Indian scenario, the observed conditions and the methods proposed are mostly for the barrage method mainly in the states of Gujarat and West Bengal where the tidal ranges are maximum. The assessment of energy extraction from the barrage method has not been carried out in the southern parts of India due to the low to medium tidal range.

Tidal stream potential estimation is also an upcoming concept globally. Researchers are working to develop the tidal stream energy devices to be able to extract the energy from tide induced currents. In the Indian context, a very less number of studies have been carried out in assessing the tidal stream energy. Therefore, studies related to kinetic energy from the tides are essential to supplement the future electricity needs and to extract energy thereby reducing or eliminating the use of depleting fossil fuels.

Previously, 471 tidal inlets were identified and were classified along the Indian coast. The Intermittently Closed and Open Lakes and Lagoons (ICOLLS) are excluded from the estimation of tidal energy in this study. This is because the ICOLLS are seasonally opening and closing which reduce the tidal streamflow. However, if the inlet is ICOLL, the possibility of energy extraction is still open with required maintenance. But mere identification of tidal inlets does not aid for tidal energy extraction. The energy extraction can be done either at the entrance of the tidal inlet or inside the tidal reservoir. Energy extraction inside the tidal reservoir is beneficial as the chances of increasing tidal elevation/speeds become more because of the decrease of cross-sections towards the land. The first objective is to identify such locations and estimate the potential and kinetic energy due to tides along the Indian coast.

However, certain parameters are depending on which the feasibility of extraction of potential energy can be based. Important among them considered in this study are tidal range, basin area and inlet throat width. There have been discussions in the literature about the minimum height of the tide that can be considered suitable for energy extraction by the construction of barrage. The

inlet throat width should be such that it facilitates the maximum amount of water to enter the tidal basin during the spring tide and also accommodates enough number of turbines for energy extraction. Basin area has to be large enough to store the incoming waters during the high tide. In the process of defining the thresholds to the above-mentioned parameters, some of the existing tidal power plant data that operate on the barrage concept have been referred and are listed in Table 3.1. The oldest, existing and operating tidal power plant is the La Rance tidal power plant in France. Its capacity is 240 MW supported by 24 bulb turbines working in both flow directions extracting tidal stream energy. The basin area is 22 km². SeaGen is the first commercial tidal energy system installed in Northern Ireland's Strangford Lough. At 1.2MW capacity, SeaGen is presently the world's largest-ever tidal current device by a significant margin and it can generate clean and sustainable electricity for approximately 1000 homes. Also, it is the only commercially operating turbine in the world that is producing energy on a large scale.

Table 3.1: Details of existing tidal power plants around the world (www.power-technology.com)

Site	Country	Bay area (km²)	Avg. tide (m)	Installed Power (MW)	Barrage width (m)
La Rance	France	22	8.55	240	750
Sihwa	South Korea	30	5.6	254	350
Annapolis	Canada	15	6.4	18	75
Jiangxia	China	1.4	5.08	3.9	81
Kislaya Guba	Russia	1.1	2.3	0.4	63

3.2 Methodology

The first objective mainly focuses on tidal energy resource availability and the energy that can be harnessed from tides along the coast of India. Two methods are considered viz. tidal Barrage and tidal stream energy. For potential energy calculation, all 471 inlets are considered and for kinetic energy (stream energy) 3 inlets along the Goa coast are considered which showed maximum potential energy generation. Amongst the 471 tidal inlets that are identified in 9 maritime states along the Indian coast, 252 are on the east coast and 219 are on the west coast (Figure 3.1). Based on Geomorphologic classification (de Vriend et al. 2002) as tabulated in Table A1 to Table A9, the ICOLLs are exempted from this study as the tidal plant needs stable inlet conditions. Table 3.2 gives information about ICOLLs along the Indian coast. As tabulated in Table 3.2, around 15% of inlets act as ICOLLs in India.

Table 3.2: Identified number of tidal inlets and ICOLLs along the Indian coast (Vikas M, 2015)

State	Number of Inlets	ICOLLs
Gujarat	42	06
Maharashtra	65	01
Goa	11	00
Karnataka	27	00
Kerala	68	24
Tamil Nadu	121	17
Andhra Pradesh	106	23
Odisha	23	01
West Bengal	08	00
Total	471	72

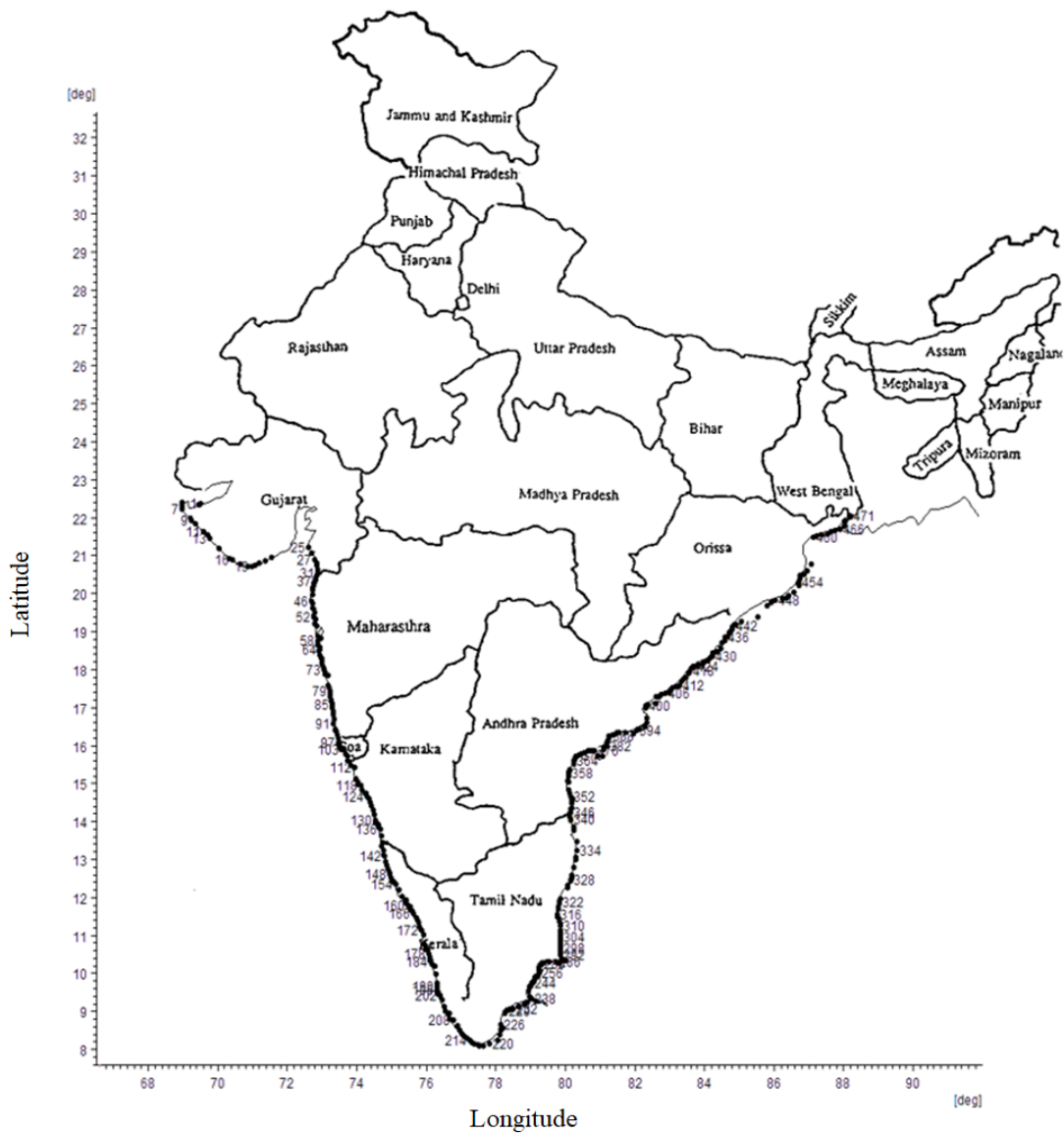


Figure 3.1: Locations of Inlets considered in Study area

3.3 Calculation of tidal energy

The total tidal energy is the energy due to release of the stored water in the basin (potential energy) and due to the tidal stream (kinetic energy). It is also a fact that the increase in tidal variation or the tidal stream energy results in an increase of energy extraction to a large extent (Bryden and Melville 2004). The potential energy is estimated based on the tidal range, the area of the basin and inlet throat width. The inlets that are between islands having large basin area are considered to have a greater amplification effect because of the reduction in the throat area and the water depth relative to the surroundings, producing a Venturi effect. This accelerates the water flow as it is forced through a channel with a smaller cross-sectional area.

3.3.1 Potential energy

The potential tidal energy is the energy due to the release of the stored water in the basin. The potential energy mainly depends on the tidal prism of the basin. Potential energy obtained due to the stored water can be calculated as shown Eq. (2.1) (Tousif and Taslim 2011).

$$E = \frac{1}{2}A\rho gh^2 \quad (2.1)$$

where h is the mean tidal range, A is the area of the tidal basin, ρ is the density of sea water = 1025 kg/m³, and g is the acceleration due to gravity = 9.81 m/s².

From the above equation, it can be seen that the potential energy varies with the square of the tidal range. So, a barrage should be placed in such a location to achieve maximum head.

Lagoon area or basin area shown in Table A1 to Table A9 for the identified basins is calculated from high-resolution data obtained from Landsat 8 OLI (Operational Land Imager) and TIRS (Thermal Infrared Sensor) from U.S. Geological Survey Department. This data consists of various high definition images of different bands and these are overlaid and the final image is obtained using ArcMap[®] 10.1. From such a composed image, the lagoon or bay area is calculated by creating new shapefile in ArcMap[®] and further verifying the same using the online area calculation tool from Draftlogic[®] software.

The tidal elevation measurements presented in Table A1 to Table A9 are obtained by simulating the tidal variations along the coast using MIKE21 flow model (FM). MIKE21 is a numerical model that provides a quick and better understanding of the behaviour of ocean waves, currents,

and sediment transport. The flow model is a comprehensive modelling system for two- and three-dimensional water modelling developed by DHI. The modelling system has been developed for complex applications within oceanographic, coastal and estuarine environments. MIKE21 is a general hydrodynamic flow modelling system based on finite volume method on an unstructured mesh. The flow model houses the Hydrodynamic Module which is based on the numerical solution of the two-dimensional shallow water equations - the depth-integrated incompressible Reynolds averaged Navier-Stokes equations. The boundaries for the MIKE21 FM tidal model are taken from the global tidal constituents available through the MIKE21 tidal prediction toolbox. The first step is the generation of mesh i.e., defining the model domain and grid size (Figure 3.2a). Once the domain is formed (after defining the open and closed boundaries) thereafter mesh is generated. Mesh can be made smooth by increasing the number of iterations. Scatter data of depth or the bathymetry values are imported on the mesh and are interpolated (Figure 3.2b). The model is simulated with open boundary tides and after the simulation, the tides are extracted at the throat of the inlet which is shown in Figure 3.2c. Some of the tidal elevation values are given in Sanil Kumar et al. (2010). The results obtained are cross-checked with the tidal stream flow in hydrographic charts, published by the National Hydrographic Office, Dehra Dun, India.

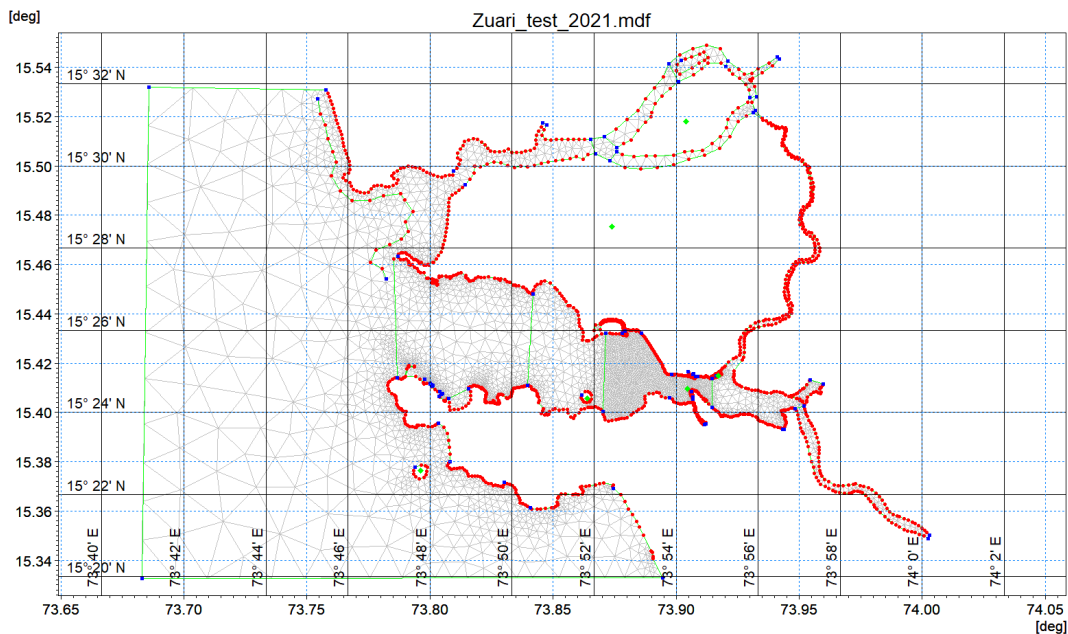


Figure 3.2a: Mesh generated in MIKE21 for Mandovi and Zuari inlets, Goa, India.

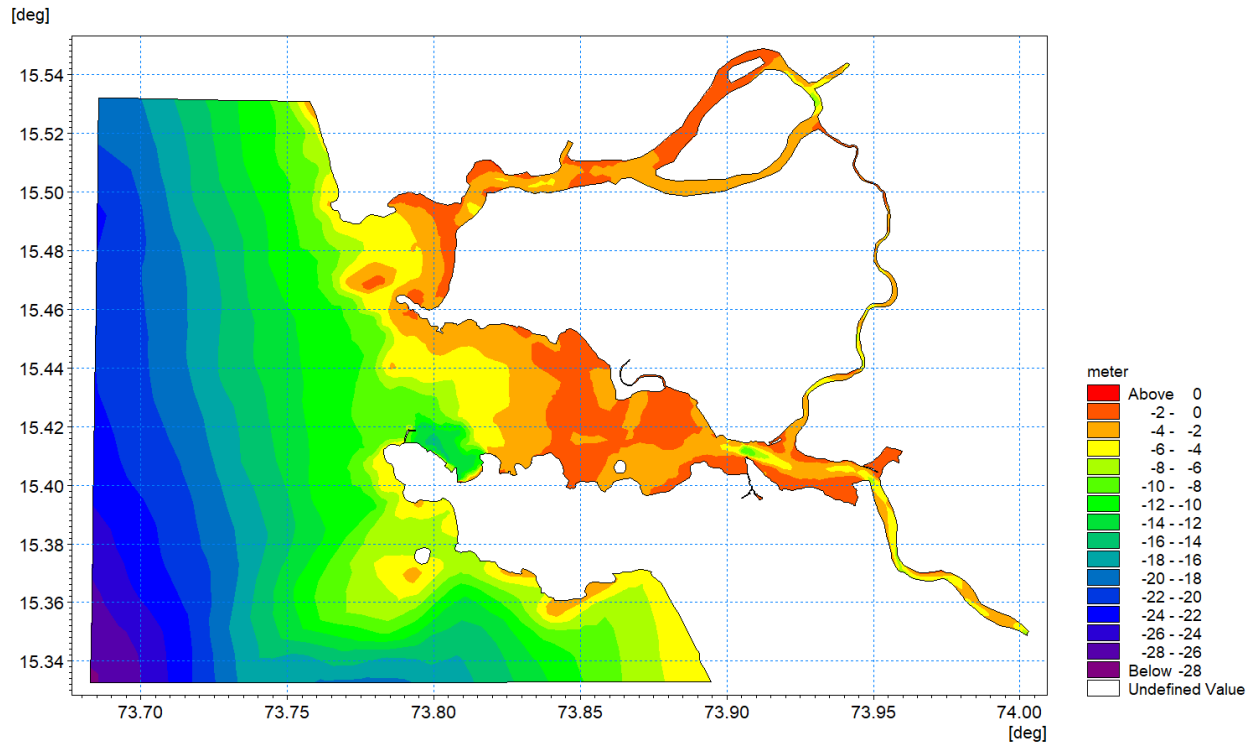


Figure 3.2b: Bathymetry interpolated in MIKE21 used for simulation.

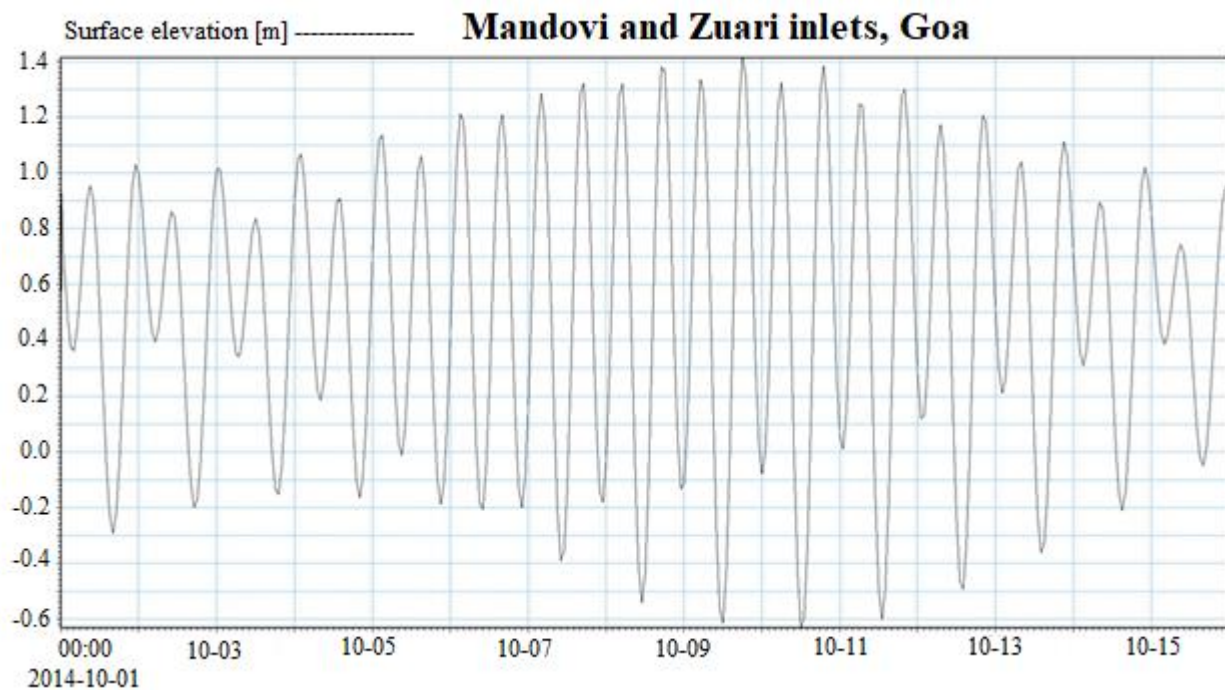


Figure 3.2c: Tides extracted in MIKE21 at the throat of Mandovi and Zuari inlets, Goa, India.

Potential energy estimation

Sample calculation of potential tidal energy at Kawai creek, Gujarat (20°48'16.88" N 72°50'02.88" E; inlet number 28 in Table A1) is briefly described below:

The mean tidal range of tide at Kawai creek, Gujarat = 6.11m

The surface area of the tidal energy harnessing plant = 744537.83 m²

Density of sea water = 1025 kg/m³

The potential energy content of the water in the basin at high tide = $E = \frac{1}{2}A\rho gh^2$
= $\frac{1}{2} \times 744537.83 \text{ m}^2 \times 1025 \text{ kg/m}^3 \times 9.81 \text{ m/s}^2 \times (6.11 \text{ m})^2 = 13.97 \times 10^{10} \text{ J}$ (approx.)

Now we have 2 high tides and 2 low tides every day. At low tide, the potential energy is zero.

Therefore, the total energy potential per day = Energy for a single high tide $\times 2$

= $13.97 \times 10^{10} \text{ J} \times 2 = 27.94 \times 10^{10} \text{ J}$

Therefore, the mean power generation potential = Energy generation potential / time in 1 day = $27.94 \times 10^{10} \text{ J} / 86400 \text{ s} = 3.235 \text{ MW}$

From the above procedure, potential energy/day is calculated for all the inlets as shown in Table A1 to Table A9. This is the theoretical potential energy obtained and it can be exactly quantified by knowing the type of turbine used i.e by considering suitable turbine efficiency.

3.3.2 Kinetic energy

The power output or the efficiency of the turbine " ξ " depends on the design of the turbine. The power output for a turbine from these kinetic systems can be obtained by the following equation (Tousif and Taslim 2011).

$$P = \frac{\xi \rho A_t V^3}{2} \quad (2.2)$$

ξ is turbine efficiency

P is power generated (in watts)

ρ is the density of the water (seawater is 1025 kg/m³)

A_t is sweep area of the turbine (in m²)

V is the velocity of the flow

Hydrodynamic module in MIKE21 flow model (FM) is used to simulate for tide induced currents at certain locations in Goa, India. 11 inlets are present in Goa. Three inlets that can produce the largest potential energy are selected to measure tidal stream energy and assess kinetic energy. The domain was forced with the predicted tides and simulated waves using MIKE21, measured winds available at CSIR-National Institute of Oceanography, Goa and also from the global wind model data from MIKE21 toolbox from three boundaries (North, West and South) for selected periods as presented in Table 3.3 and figure 3.3.

Table 3.3: Instrument details, locations and measured currents in Goa

Name	Instrument used	Instrument location	Avg. Current speed (m/s)	Max. Current speed. (m/s)	Duration
Chapora 1 (Figure 3.4a)	RCM 9	Off Chapora (Figure 3.4c)	0.104	0.305	09 Feb 2017 to 10 Mar 2017
Chapora 2 (Figure 3.4b)	RCM 9	River (Figure 3.4c)	0.294	1.123	16 Feb 2017 to 18 Mar 2017
Mandovi 1321 (Figure 3.5a)	RCM 9	River (Figure 3.5c)	0.419	0.847	05 Sep 2015 to 11 Sep 2015
Mandovi 1420 (Figure 3.5b)	RCM 9	River (Figure 3.5c)	0.302	0.809	05 Sep 2015 to 11 Sep 2015
Zuari 1418 (Figure 3.6a)	RCM 9	River (Figure 3.6e)	0.476	0.833	08 Aug 2017 to 23 Aug 2017
Zuari 1420 (Figure 3.6b)	RCM 9	River (Figure 3.6e)	0.483	1.184	08 Aug 2017 to 23 Aug 2017
Zuari 1421 (Figure 3.6c)	RCM 9	River (Figure 3.6e)	0.424	1.31	08 Aug 2017 to 23 Aug 2017
Zuari 1422 (Figure 3.6d)	RCM 9	River (Figure 3.6e)	0.532	1.188	08 Aug 2017 to 23 Aug 2017



Figure 3.3: Instrument locations at Goa, India. (Source: Google Earth®)

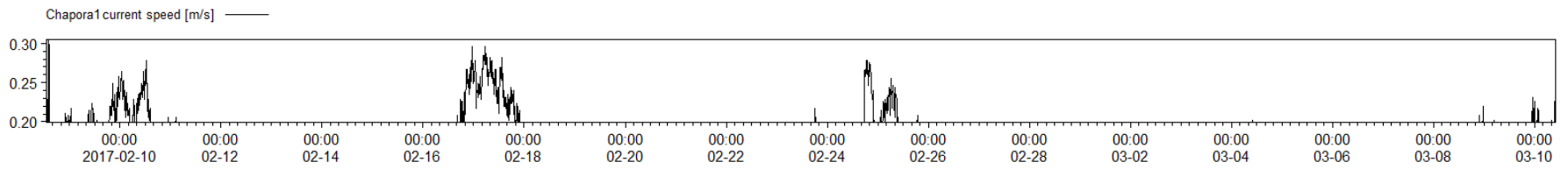


Figure 3.4a: Measured currents at Chapora 1 between 09 Feb 2017 and 10 Mar 2017

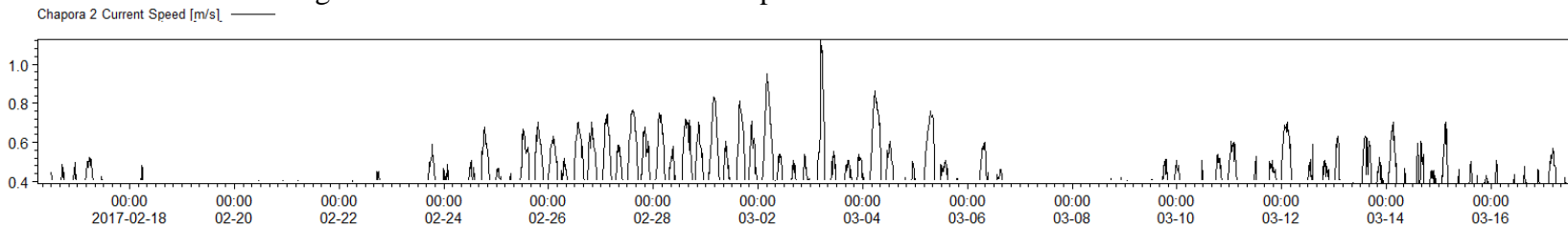


Figure 3.4b: Measured currents at Chapora 2 between 16 Feb 2017 and 18 Mar 2017

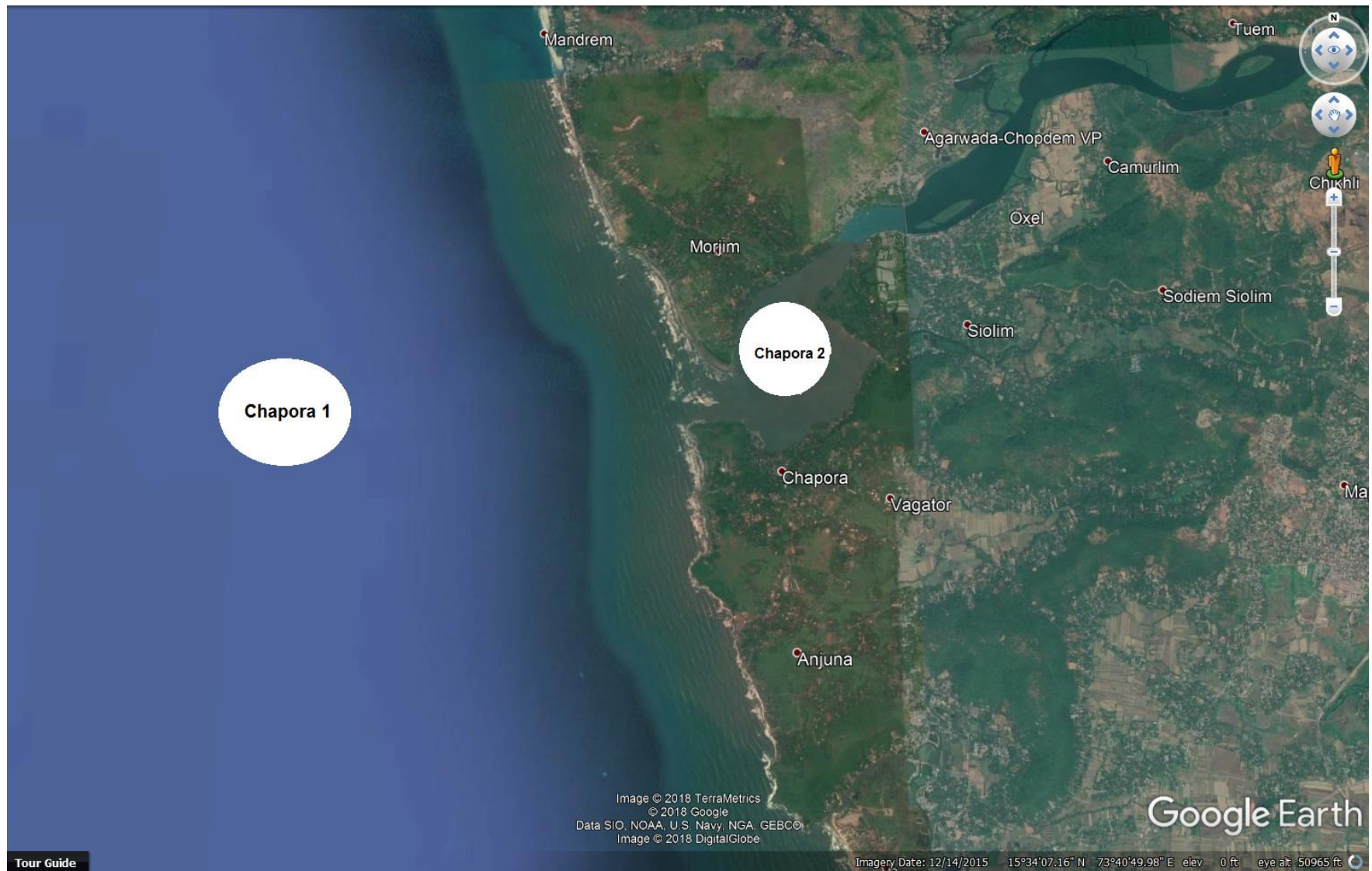


Figure 3.4c: Instrument locations at Chapora 1 and Chapora 2 (Source: Google Earth®)

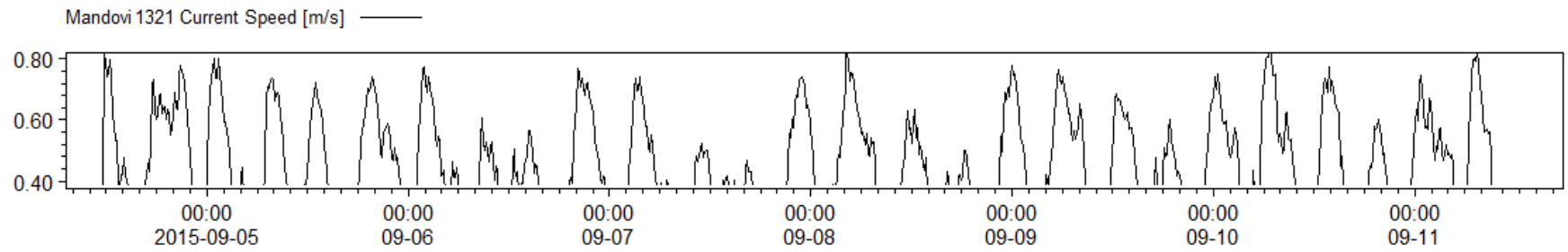


Figure 3.5a: Measured currents at Mandovi 1321 between 05 Sep 2015 and 11 Sep 2015

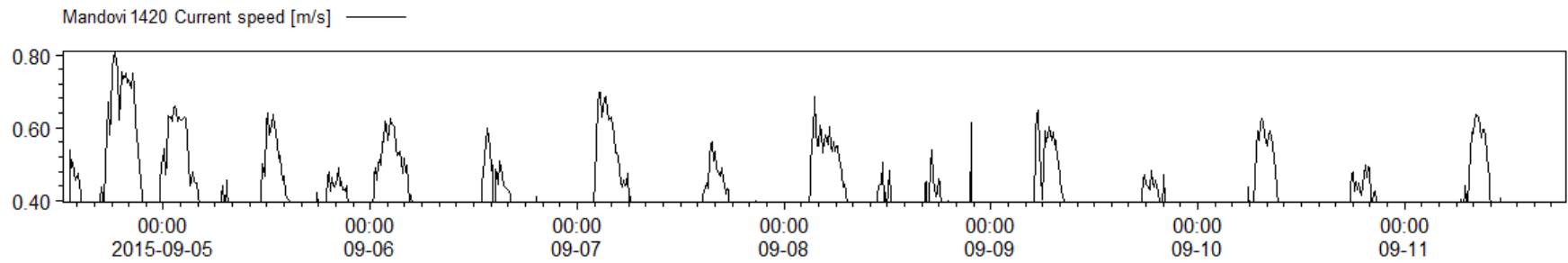


Figure 3.5b: Measured currents at Mandovi 1420 between 05 Sep 2015 and 11 Sep 2015



Figure 3.5c: Instrument locations at Mandovi 1321, Mandovi 1420 (Source: Google Earth®)

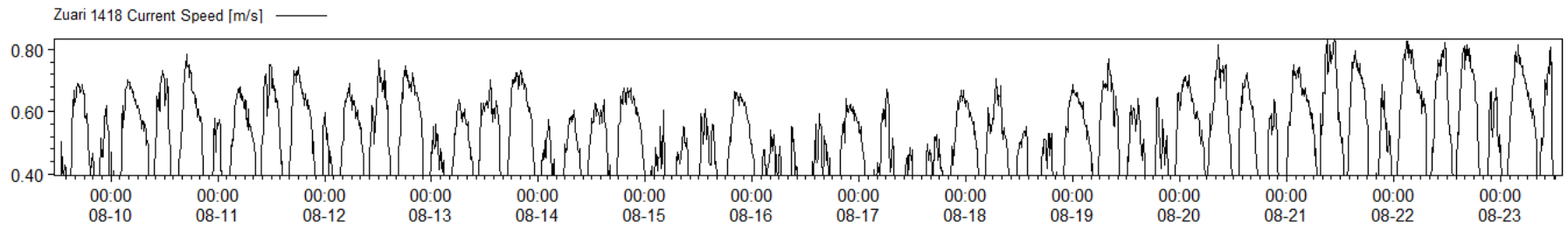


Figure 3.6a: Measured currents at Zuari 1418 between 08 Aug 2017 and 23 Aug 2017

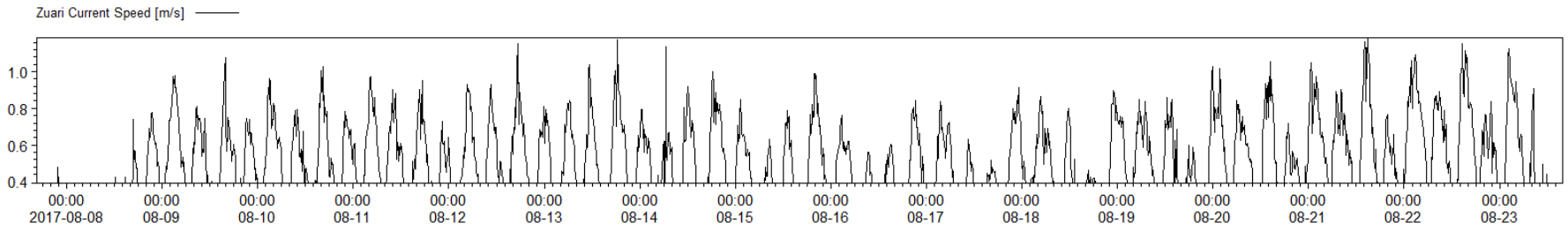


Figure 3.6b: Measured currents at Zuari 1420 between 08 Aug 2017 and 23 Aug 2017

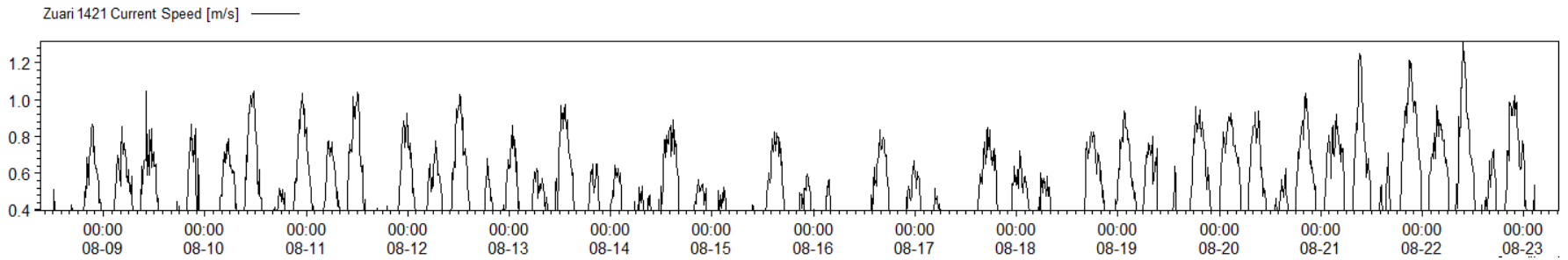


Figure 3.6c: Measured currents at Zuari 1421 between 07 Aug 2017 and 24 Aug 2017

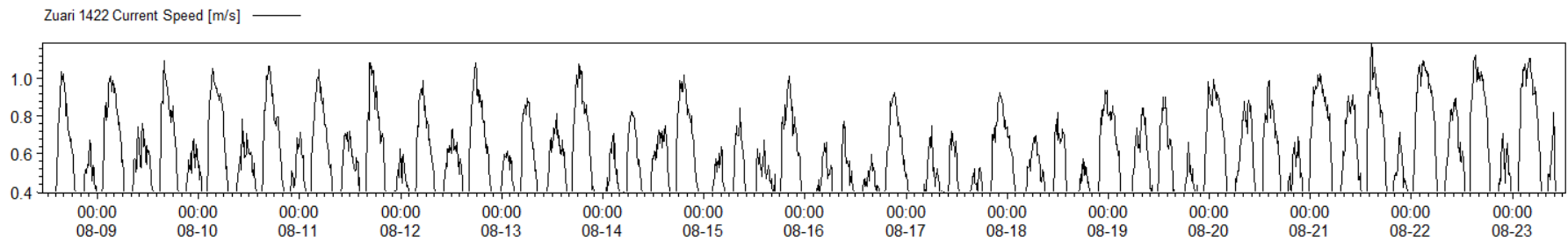


Figure 3.6d: Measured currents at Zuari 1422 between 07 Aug 2017 and 24 Aug 2017



Figure 3.6e: Instrument locations at Zuari 1418, Zuari 1421, Zuari 1422, Zuari 1420 (Source: Google Earth®)

3.4 Comparison of measured and modelled (simulated) data

The hydrodynamic flow model (FM) values are validated with the measured current speeds to authenticate the modelled currents at Mandovi 1321 and Mandovi 1420. Measured tides, simulated waves and wind speeds are provided as input at Mandovi 1321 and Mandovi 1420 North, West and South boundaries by defining the closed and open boundaries in the mesh file.

The comparison of total flow speeds with the model results at Mandovi 1321 and Mandovi 1420 is presented in Figure 3.7. It can be seen that the currents at Mandovi 1321 and Mandovi 1420 as predicted by the model are in good agreement as observed from the measurements.

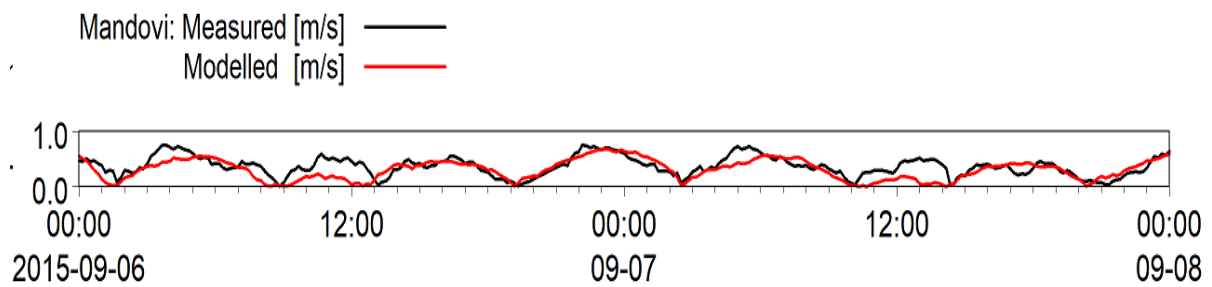


Figure 3.7a: Validation of modelled current speed with measured current speed for Mandovi

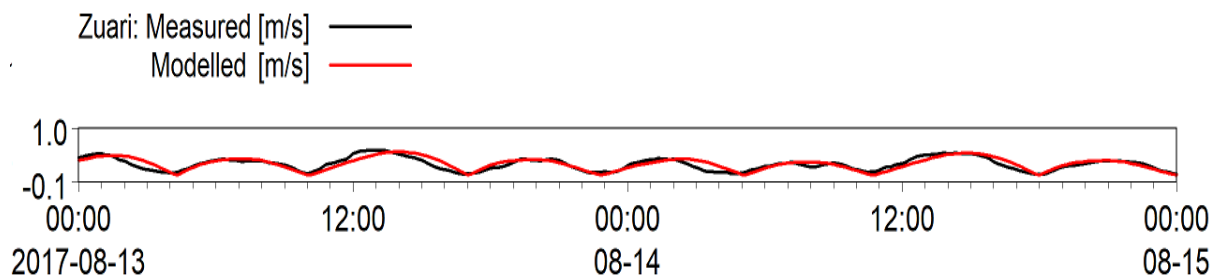


Figure 3.7b: Validation of modelled current speed with measured current speed for Zuari

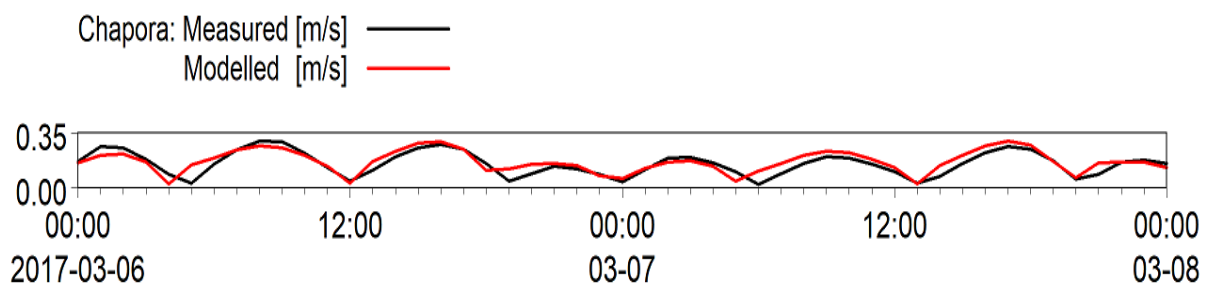


Figure 3.7c: Validation of modelled current speed with measured current speed for Chapora

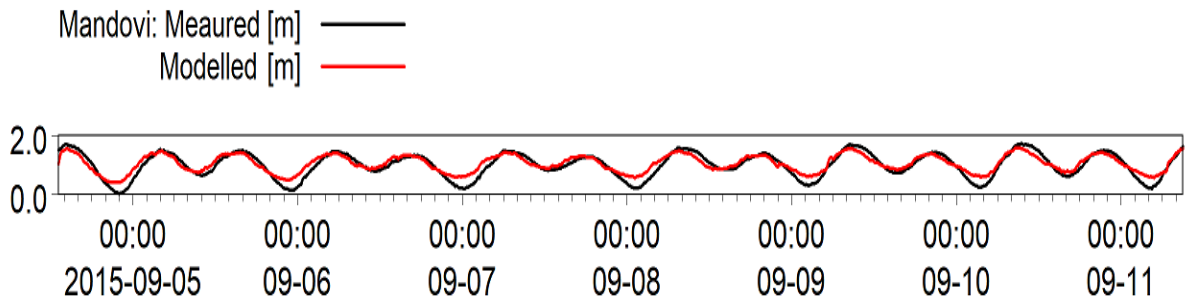


Figure 3.7d: Validation of modelled tide with measured tide for Mandovi

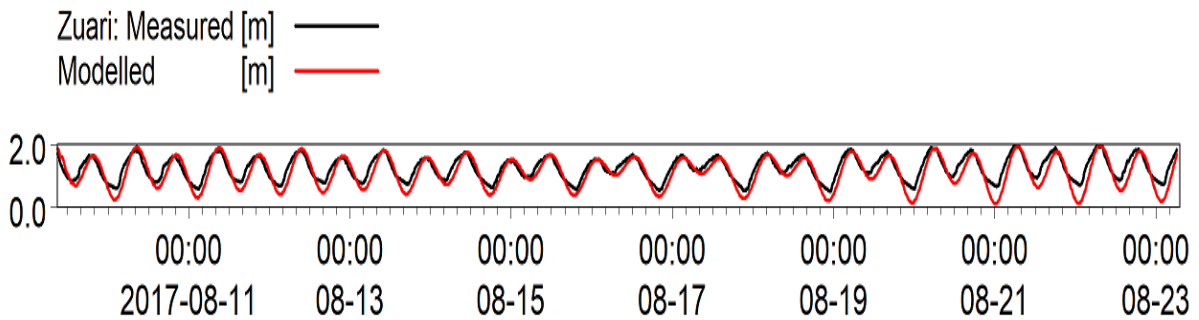


Figure 3.7e: Validation of modelled tide with measured tide for Zuari

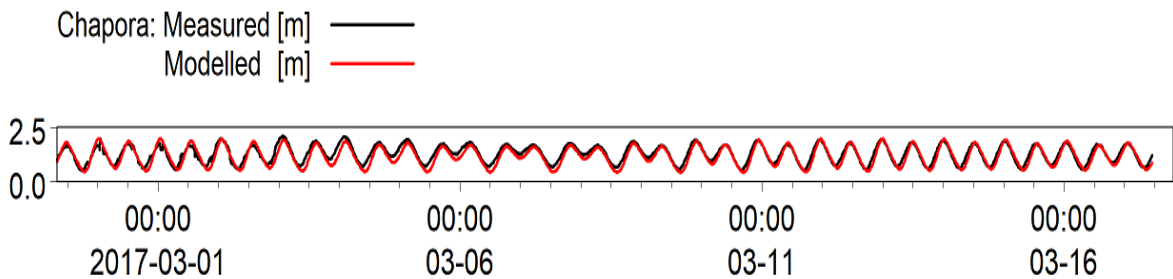


Figure 3.7f: Validation of modelled tide with measured tide for Chapora

3.5 Statistical maxima of current speeds

The currents are measured at the locations shown in Figure 3.6e. At the locations of measurement, the maximum currents are analyzed. However, the maximum currents in a particular domain need not be present at the measured locations. To assess the maximum currents in the entire domain, modelled data is used and the statistics are looked in, to identify the maximum current locations within the domain. Figure 3.8a to Figure 3.8c shows the identified locations having maximum currents in the domains Chapora, Mandovi, and Zuari. 4 locations each are identified at Chapora and Zuari and 6 locations are identified in Mandovi.

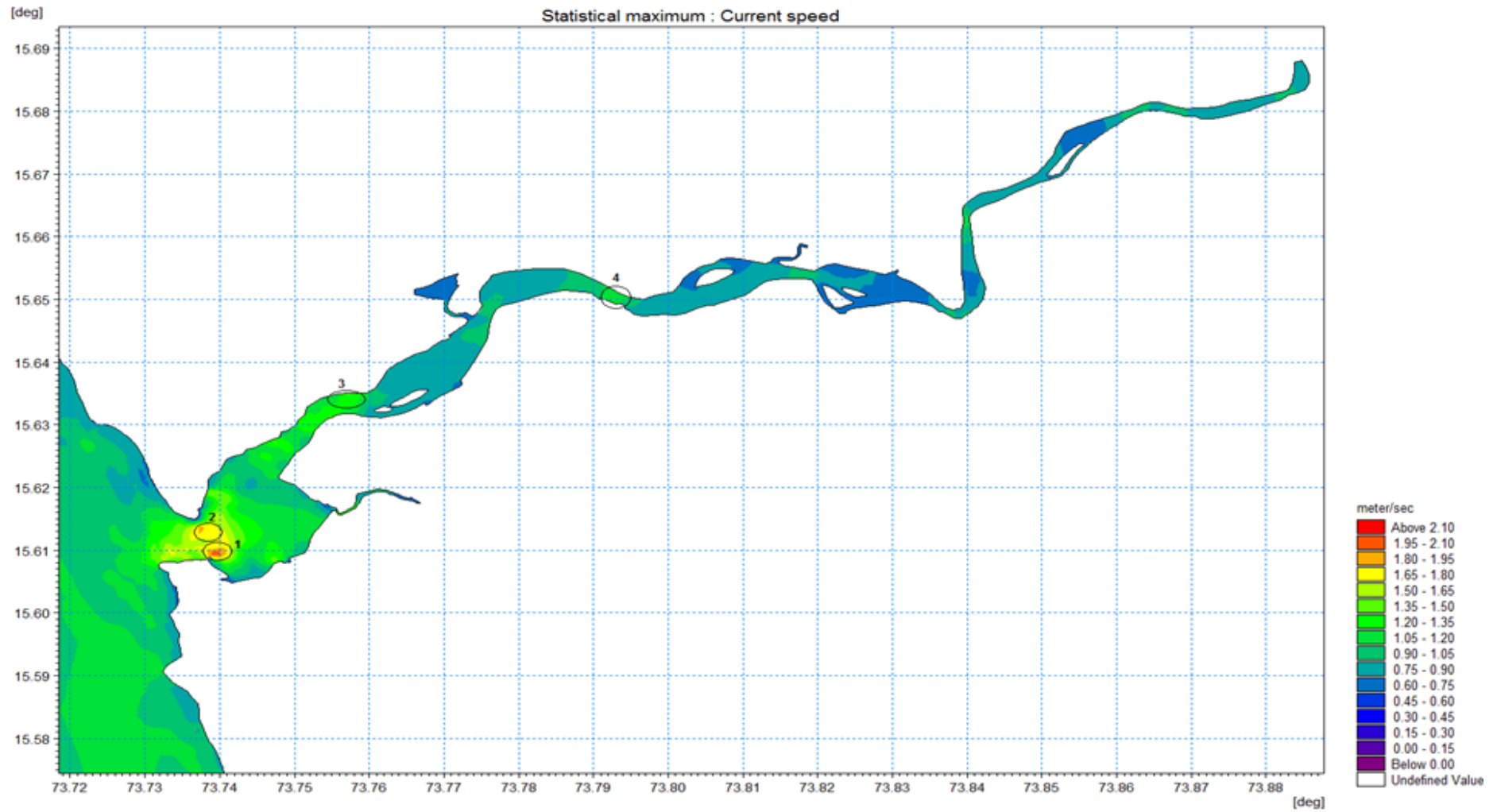


Figure 3.8a: Locating maximum currents at Chapora River (Statistical maxima)

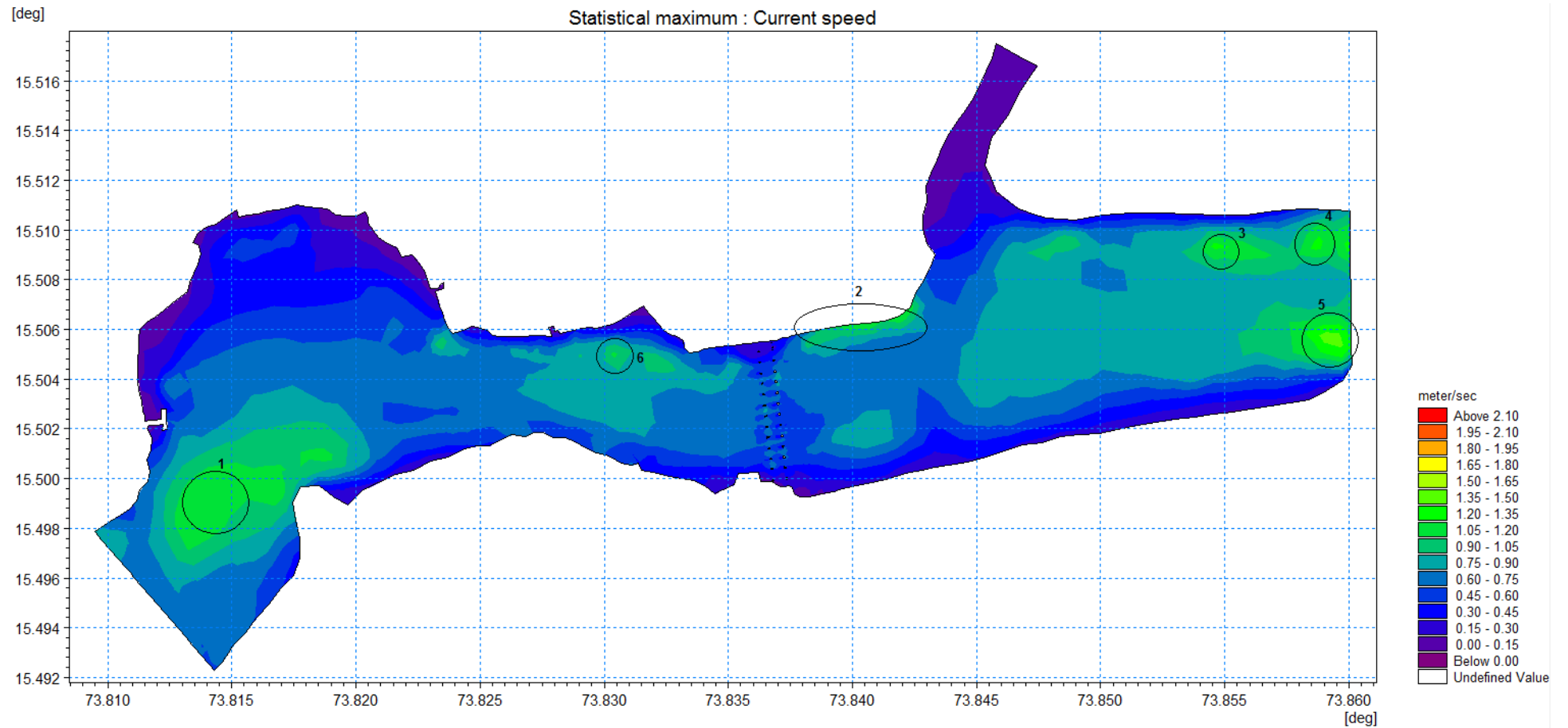


Figure 3.8b: Locating maximum currents at Mandovi River (Statistical maxima)

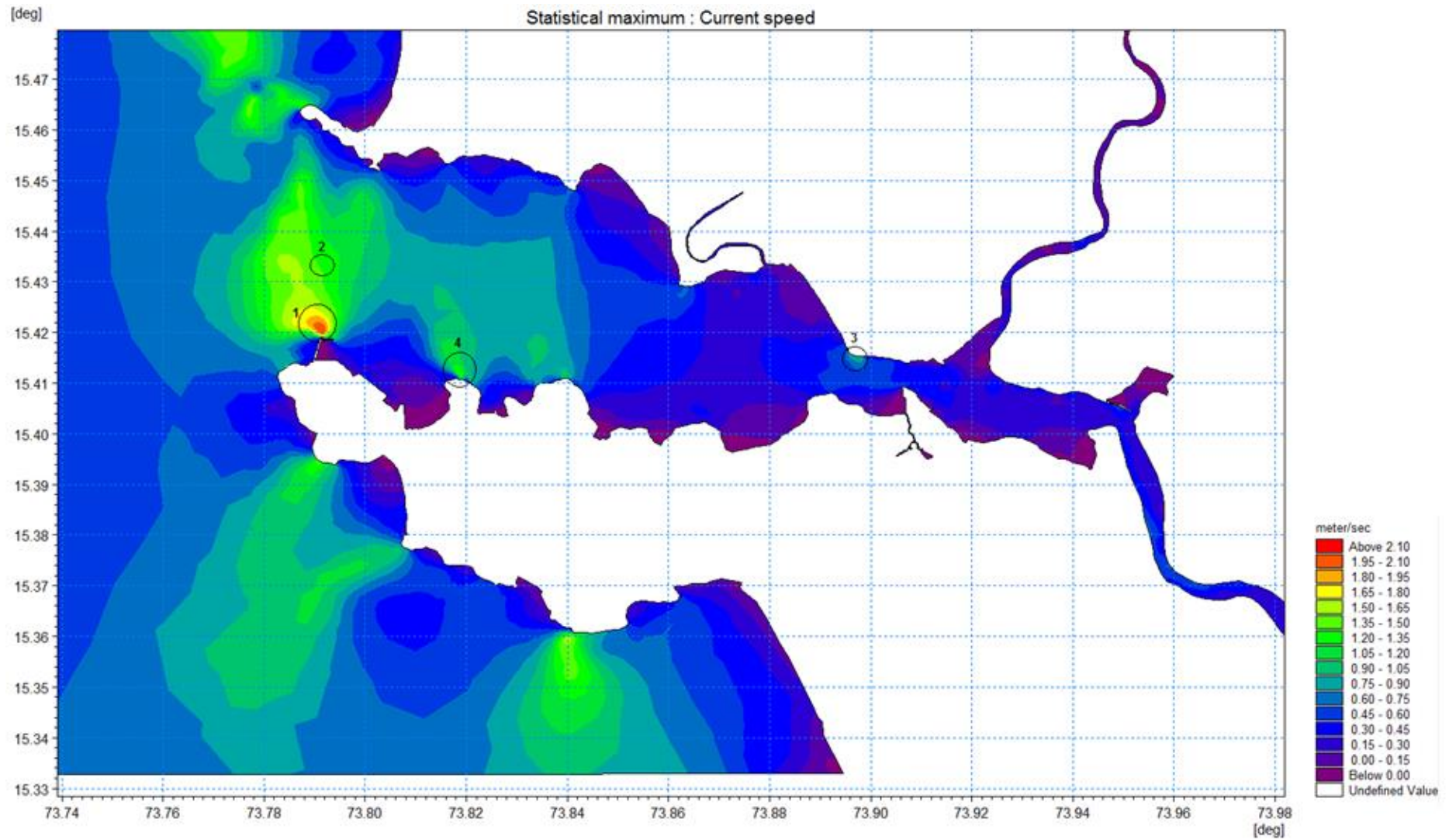


Figure 3.8c: Locating maximum currents at Zuari River (Statistical maxima)

3.6 Results and discussion

3.6.1 Tidal energy (Potential energy)

As shown in Table A1 to Table A9, the potential tidal energy is calculated for 471 inlets. The total energy that can be extracted of all these 471 inlets without considering any factors is approximately 2310 MW. If ICOLLs are not considered (72 inlets), then the total energy that can be extracted from the remaining inlets (399 inlets) is approximately 2254 MW. The above two numbers show a variation of about 56 MW which is less and it is evident that ICOLLs do not majorly contribute to the total extraction of energy.

The tidal prism varies proportionally with the basin area and those inlets which have large basin area and greater tidal prism values in common are favourable for energy extraction. If the tidal range and basin area are larger, the tidal prism is higher. In other words, it can be said that the consideration of tidal inlets for energy extraction based on tidal prism is dependent on the tidal range and basin area. From Table 3.1, it can be observed that, in existing tidal power plants, energy is being extracted from basins having areas of 1.1 km² and average tide as low as 2.3m. This means that the energy has been extracted for the tidal prism of 2.53Mm³. This is considered as the threshold for energy extraction. From Figure 3.9a, it is evident that there are quite a few inlets that have favourable conditions for energy extraction in terms of the tidal prism. Details of the number of inlets favourable for tidal energy extraction considering the threshold tidal prism values are presented in Table 3.4. It can be observed that 13 inlets in Gujarat, 29 in Maharashtra, 5 in Goa, 10 in Karnataka, 16 in Kerala, 14 in Tamil Nadu, 23 in Andhra Pradesh, 16 in Odisha and 4 in West Bengal (130 inlets in total) whose tidal prism exceeds 2.53 Mm³.

By definition, the tidal prism is the volume of water filled in the tidal basin. This volume of water filled in the tidal basin also depends on the width of the inlet. The width of the tidal inlet should be such that it allows enough water to fill the basin during the high tide condition so that the required head is obtained to extract energy. Also, the inlet has to be wide enough to accommodate the barrage that houses the turbines for energy extraction. Table 3.1 gives the barrage widths of the existing tidal power plants. It can be observed that the barrage width ranges from 63-750 meters depending on the tidal prism. If the tidal prism is less, then the number of turbines required will be less as a result of which the barrage width can be reduced. A threshold of 63m can be considered for the inlet throat width for the identified 130 inlets by

considering tidal prism criteria of 2.53 Mm^3 to extract power. Details of inlets favourable for tidal energy extraction considering the inlet throat width are presented in Table 3.4 and Figure 3.9b. It can be observed that 11 inlets in Gujarat, 29 in Maharashtra, 5 in Goa, 9 in Karnataka, 14 in Kerala, 4 in Tamil Nadu, 15 in Andhra Pradesh, 16 in Odisha and 4 in West Bengal (107 inlets in total) whose throat width exceeds 63 m.

The above threshold values are set by considering the operating/proposed tidal power generating stations around the globe. Initially, when ICOLLs are not considered, the 72 inlets are not considered for energy extraction out of 471. When considered tidal prism condition, there is a decrease in the number of inlets suitable for energy extraction from 399 to 130. And when the inlet throat width condition is considered, it is found that 23 inlets do not have a minimum throat width of 63m and hence the number of inlets decreased to 107. The total estimated energy that can be extracted considering 107 inlets is 2127.281 MW and of course, this depends on the efficiency of the turbine. These approximations can be exactly quantified by knowing the type of turbine used for energy extraction based on the onsite conditions. Once the type of turbine is determined, the efficiency can be known and the energy generated can be calculated precisely.

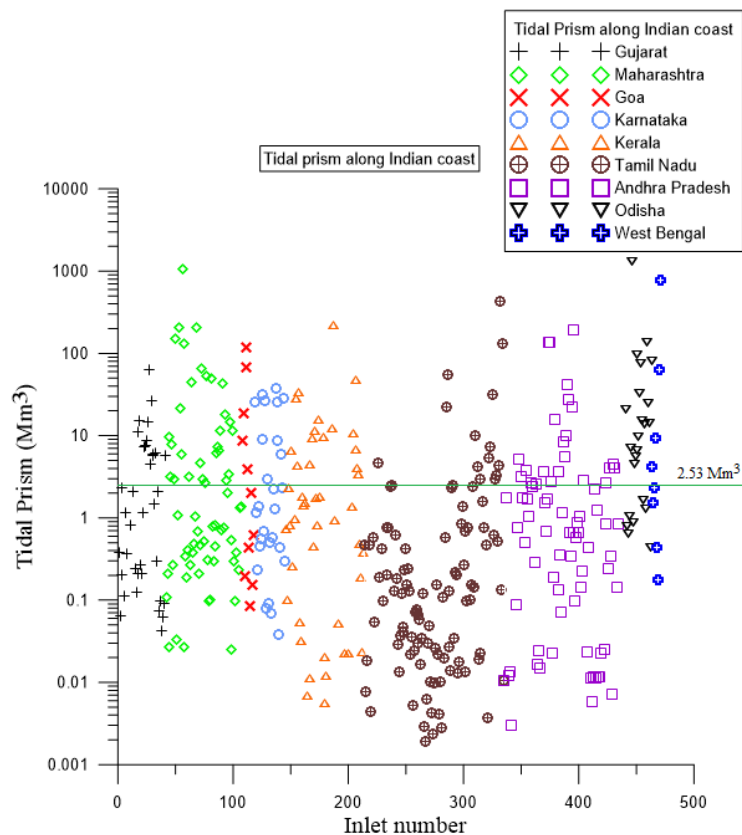


Figure 3.9a: Variation of tidal prism along the coast of India

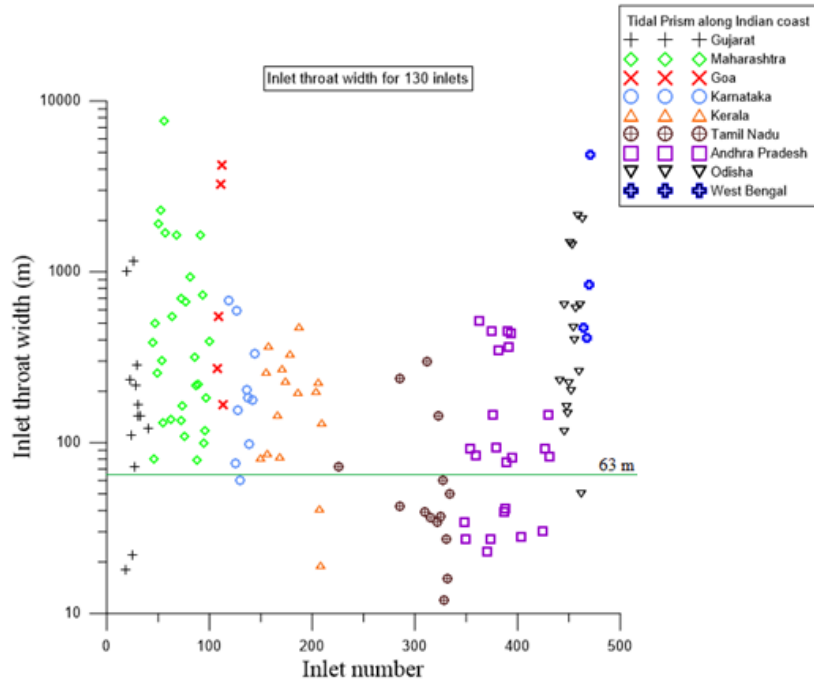


Figure 3.9b: Inlet throat width for 130 inlets

Table 3.4. State-wise potential energy extraction based on the tidal prism and throat width.

	Estimated potential energy neglecting ICOLLs and considering Tidal prism greater than 2.53 Mm ³		Estimated potential energy neglecting ICOLLs, considering Tidal prism greater than 2.53 Mm ³ and inlet throat width greater than 63m	
	No. of inlets	Energy generated (MW)	No. of inlets	Energy generated (MW)
Gujarat	13	107.858	11	98.626
Maharashtra	29	1009.319	29	1009.319
Goa	5	51.726	5	51.726
Karnataka	10	42.521	9	41.856
Kerala	16	56.933	14	55.773
Tamil Nadu	14	96.062	4	4.554
Andhra Pradesh	23	97.416	15	72.335
Odisha	16	472.925	16	472.925
West Bengal	4	320.147	4	320.147
Total gross energy	130	2254.906	107	2127.281

3.6.2 Tidal Stream energy (Kinetic energy)

The least value of the current speed to extract energy mainly depends on the technology available. Tidal stream energy turbines are being developed around the world to harness energy from the horizontal flow of water which operates at speeds of 1 m/s to 2 m/s. However, there is a need for the development of low flow turbines which operate at lower speeds to produce

energy on a small scale. Keeping the low flow turbines into consideration, a minimum of 0.4 m/s has been considered to assess the tidal stream energy. Tidal stream energy is calculated at the locations having current speed (measured) greater than 0.4 m/s are shown in Figure 3.10a to Figure 3.10g. The tidal stream energy is calculated for water density 1025 m/s and considering the efficiency of the turbine as 40%. If current speed is less than 0.4 m/s, the kinetic energy at those points is not calculated because the currents below 0.4 m/s do not contribute to producing energy.

From Figure 3.10a it can be seen that there is no energy generated for about 3 days in a 30-day tidal cycle. The turbines remain static during those days. The total energy generated during this period is 44.74kW. In Figure 3.10b it can be seen that at Mandovi 1321 there is continuous energy generation for only about the first 10 days of the assessment period which keeps the turbine at a halt in the remaining days. The total energy generated during this period is 27.61kW. At location Mandovi 1420 (in Figure 3.10c) also does not show continuous energy generation. The total energy generated during this period is 10.52kW. The above-mentioned locations may not be preferred for energy generation because of the intermittent power supply but at the same time, they may also be preferred because of the amount of energy generated.

Whereas in Figures 3.10d to 3.10g, the tidal stream energy potential at Zuari 1418, 1420, 1421, and 1422 respectively are observed to produce comparatively continuous energy during the entire period. This aids the continuous production of energy which is much more preferred over the other locations mentioned above, which do not produce continuous energy. The total energy produced at Zuari 1418, 1420, 1421 and 1422 was observed to be 63.32kW, 89.07kW, 75.95kW, 117.43kW respectively which is higher than the locations shown in Figures 3.10a to 3.10c.

These are the estimated tidal stream energy values by considering the measured current speeds. But, the currents need not be maximum at measured locations only. To assess this, MIKE21 Flow Model (FM) is used to simulate for current speeds. Statistical analysis is done to analyze the points of maximum currents within the domain as indicated in Figures 3.8a, 3.8b and 3.8c. Four locations in Chapora, six in Mandovi and four in Zuari Rivers are identified to have maximum currents. Currents at these identified locations that have maximum currents are extracted as shown in Figures 3.10a to 3.10n.

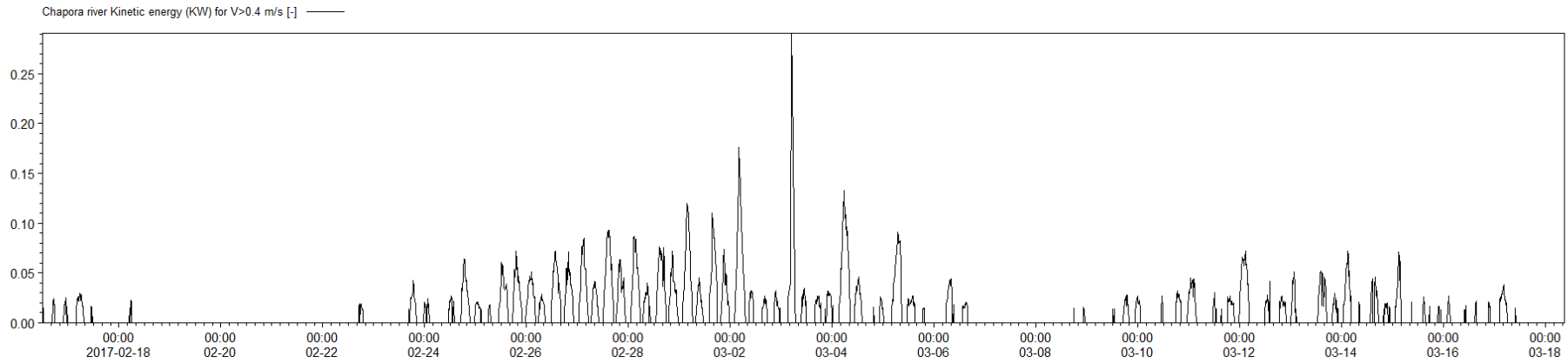
The energies generated for the maximum simulated current speeds are presented in Figures 3.11a to 3.11n. The currents less than 0.4 m/s are not considered. Out of four points considered in Chapora, the total tidal stream energy generated was found to be 11.68kW, 10.11kW, 5.17kW and 4.72kW. Figures 3.12a to 3.12d show that the energy generation is relatively continuous at point 1 in Chapora and the total energy generated was found to be 11.68kW.

Out of the six locations identified in Mandovi, the total tidal stream energy was found to be 31.37kW, 1.77kW, 1.77kW, 25.25kW, 39.66kW and 19.12kW at point 1 to point 6 respectively. The maximum total tidal stream energy is found at point 5 i.e from Figure 3.11i.

The four identified locations in Zuari produce energy of 0.00kW, 25.64kW, 24.72kW and 0.01kW at point 1 to point 4 respectively. The maximum observed here is 25.64kW i.e at point 2 which is shown in Figure 3.11l.

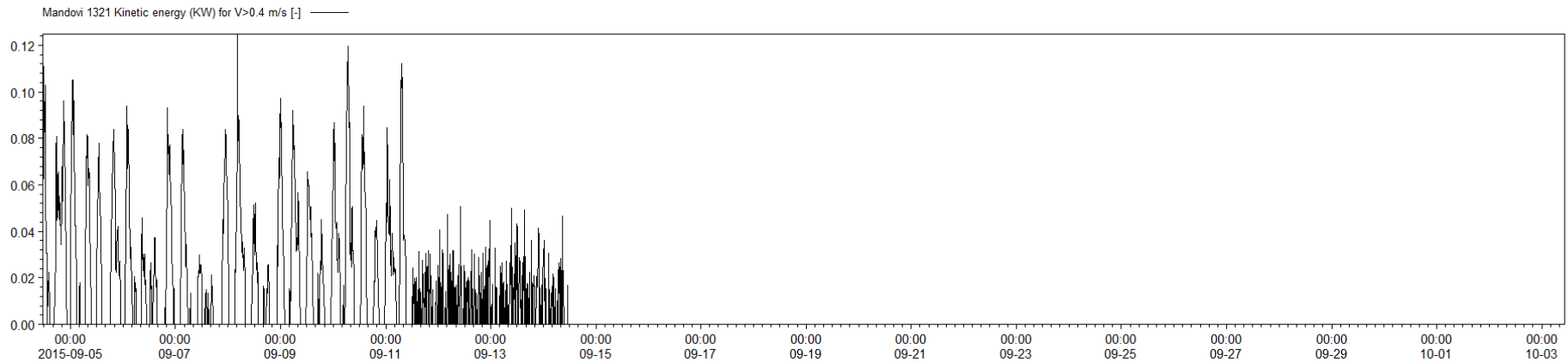
Table 3.5: Kinetic energy calculated/day for different threshold velocities

	Location	Kinetic energy per day for V>0.4m/s (kW)	Kinetic energy per day for V>0.5m/s (kW)	Kinetic energy per day for V>0.7m/s (kW)
From Measured	Chapora 1	0.00	0.00	0.00
	Chapora 2	1.54	1.17	0.42
	Mandovi 1321	2.76	2.21	0.84
	Mandovi 1420	1.05	0.744	0.12
	Zuari 1418	3.72	3.32	0.97
	Zuari 1420	5.56	5.24	3.68
	Zuari 1421	4.46	4.19	3.02
	Zuari 1422	6.90	6.54	5.07
From Modelled Currents	Chapora Point 1	11.68	10.91	7.56
	Chapora Point 2	10.11	9.29	5.50
	Chapora Point 3	5.17	4.18	1.98
	Chapora Point 4	4.72	3.86	1.22
	Mandovi Point 1	4.45	4.13	2.22
	Mandovi Point 2	0.25	0.10	0
	Mandovi Point 3	0.25	0.10	0
	Mandovi Point 4	3.60	3.15	1.50
	Mandovi Point 5	5.60	5.25	3.72
	Mandovi Point 6	2.70	2.32	1.09
	Zuari Point 1	0.00	0.00	0.00
	Zuari Point 2	25.64	25.50	24.82
	Zuari Point 3	24.72	24.58	23.87
	Zuari Point 4	0.01	0	0



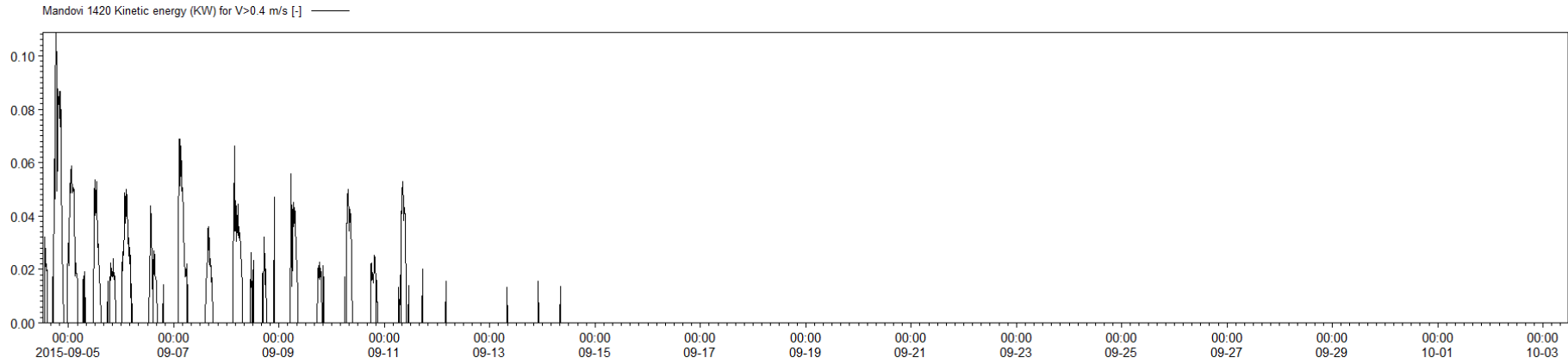
H:\Man\PHD\Measured Current data\Chapora\Chapora_river_current_dbs0

Figure 3.10a: Tidal stream energy (measured) at Chapora 2 having current speed greater than 0.4m/s



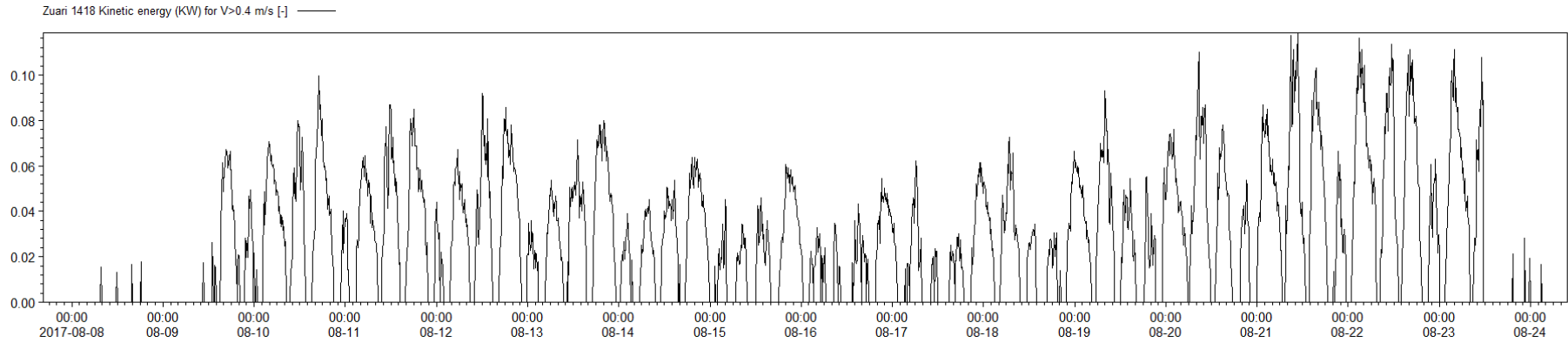
H:\Man\PHD\Measured Current data\Mandovi\1321_dbs0

Figure 3.10b: Tidal stream energy (measured) at Mandovi 1321 having current speed greater than 0.4m/s



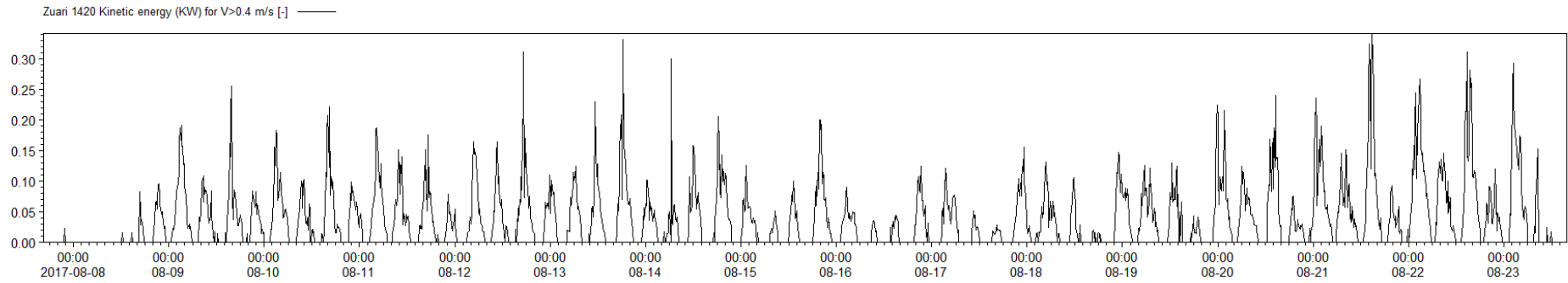
H:\Mus\PHD\Measured Current data\Mandovi\1420.dwg

Figure 3.10c: Tidal stream energy (measured) at Mandovi 1420 having current speed greater than 0.4m/s



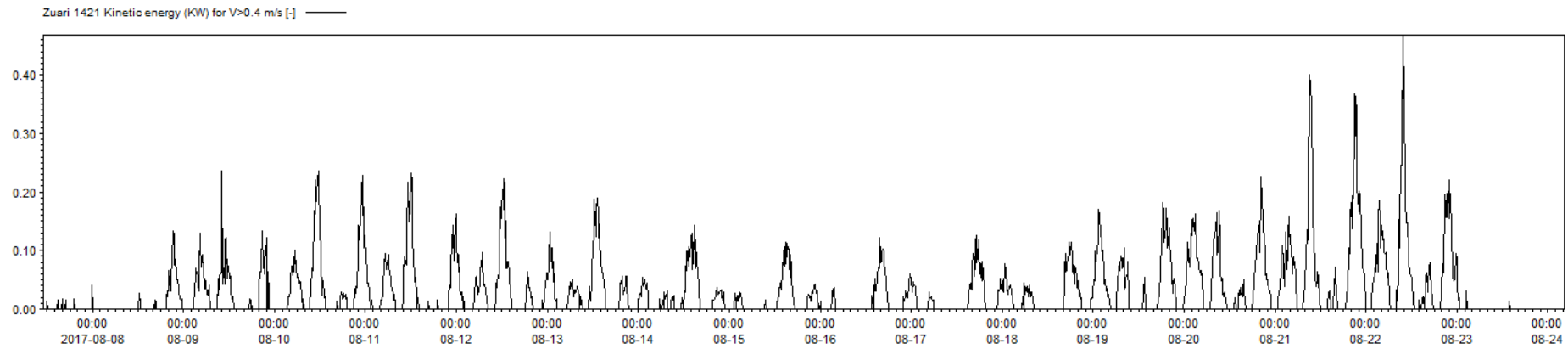
H:\Mus\PHD\Measured Current data\zuari\1418.dwg

Figure 3.10d: Tidal stream energy (measured) at Zuari 1418 having current speed greater than 0.4 m/s



H:\Kuan\PHD\Measured Current\data\uan1420.d80

Figure 3.10e: Tidal stream energy (measured) at Zuari 1420 having current speed greater than 0.4 m/s



H:\Kuan\PHD\Measured Current\data\uan1421.d80

Figure 3.10f: Tidal stream energy (measured) at Zuari 1421 having current speed greater than 0.4 m/s

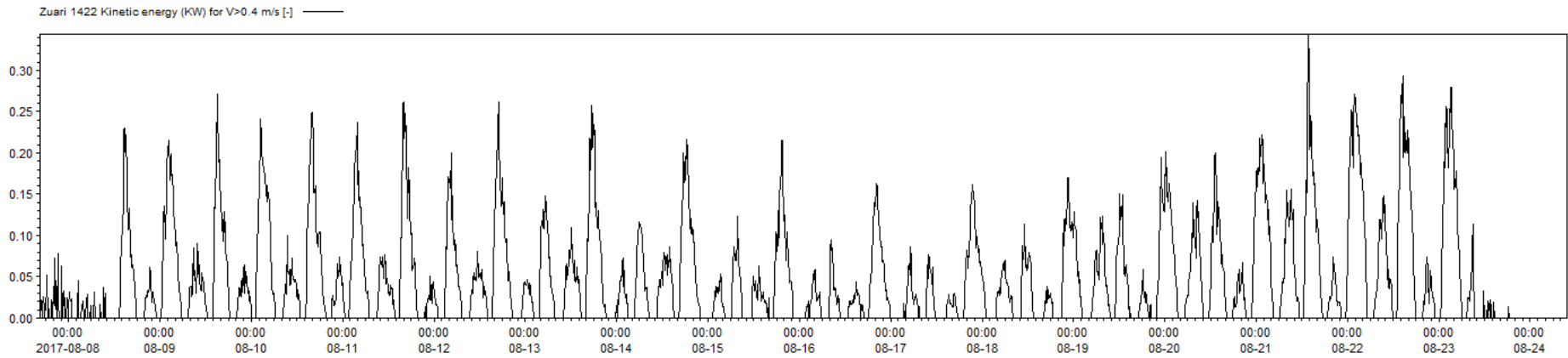


Figure 3.10g: Tidal stream energy (measured) at Zuari 1422 having current speed greater than 0.4 m/s

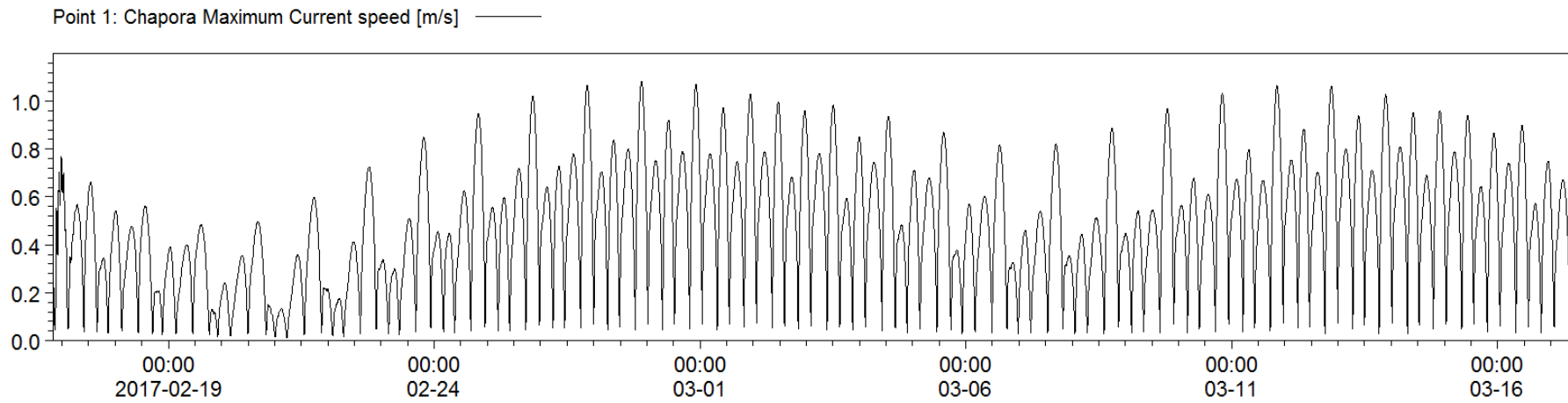


Figure 3.11a: Modelled currents at Point 1 in Chapora river

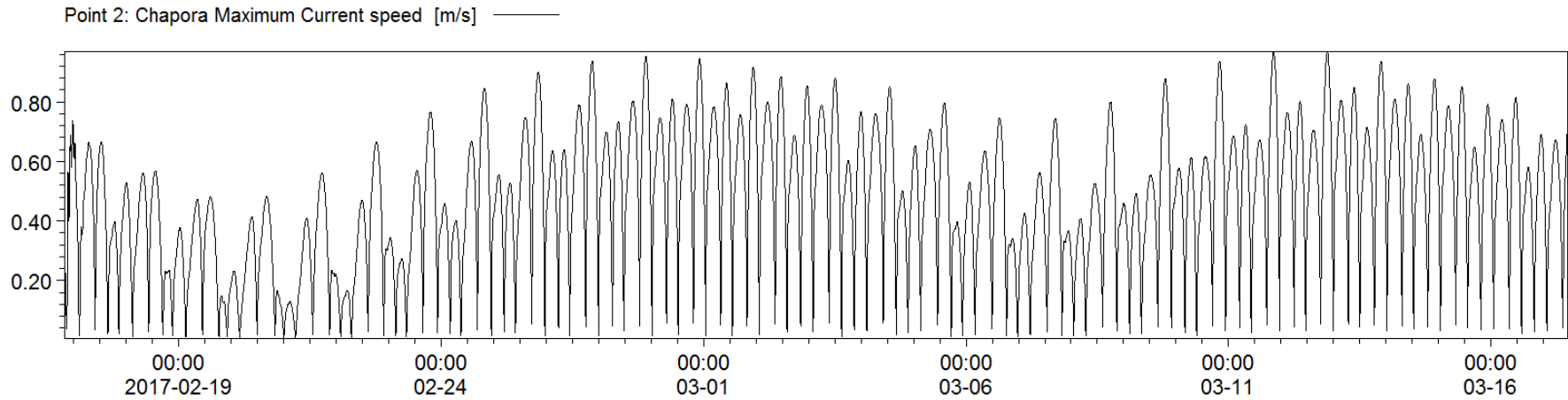


Figure 3.11b: Modelled currents at Point 2 in Chapora river

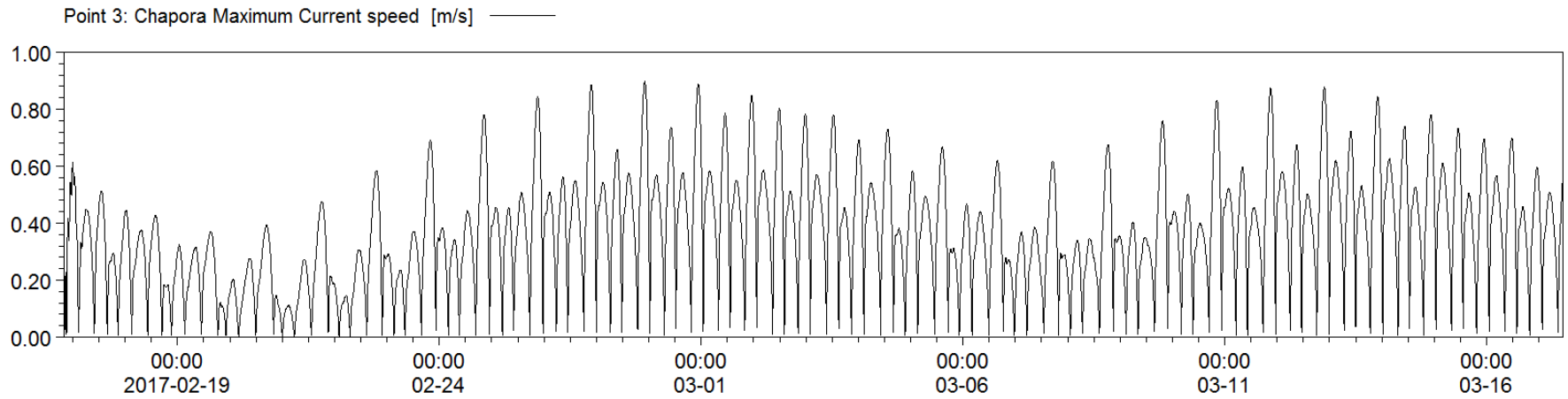


Figure 3.11c: Modelled currents at Point 3 in Chapora river

ata\chapora\MAXIMUM CURRENTS\Max_currents_2_ys.dfs0

ent_data\chapora\MAXIMUM CURRENTS\Max_currents_3.dfs0

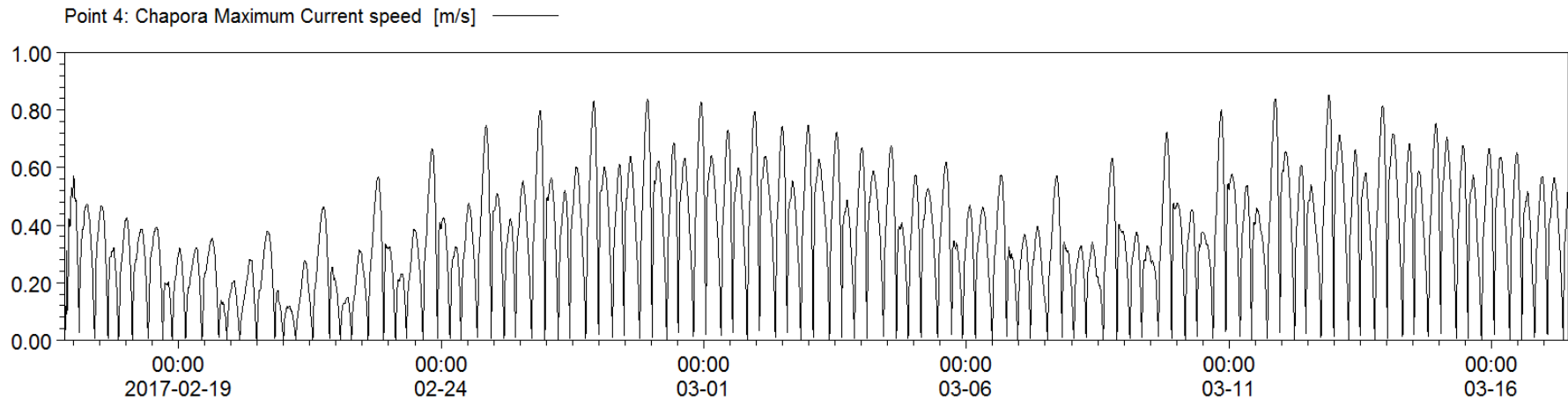


Figure 3.11d: Modelled currents at Point 4 in Chapora river

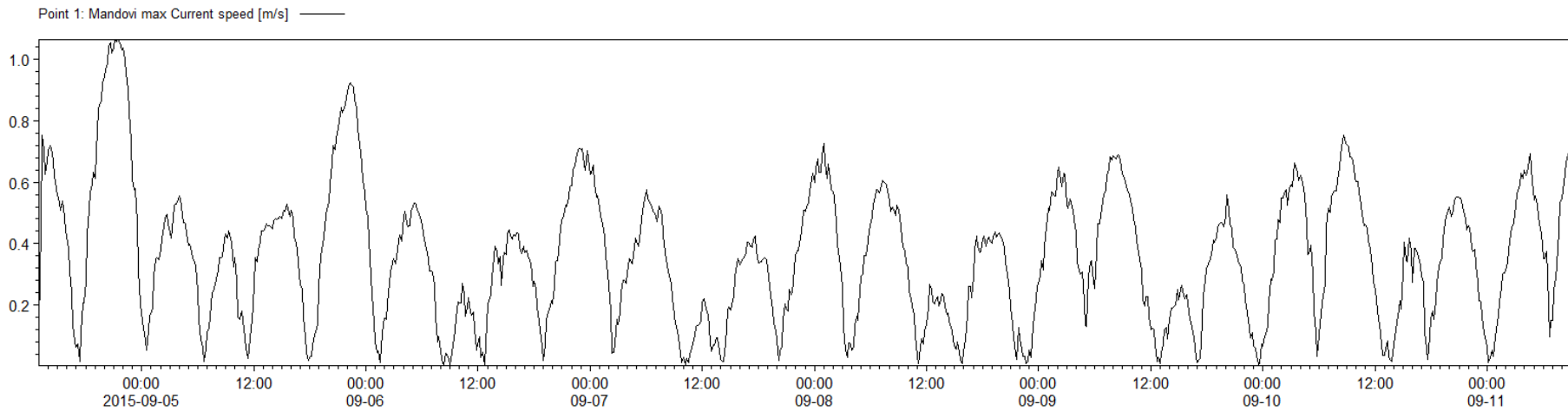
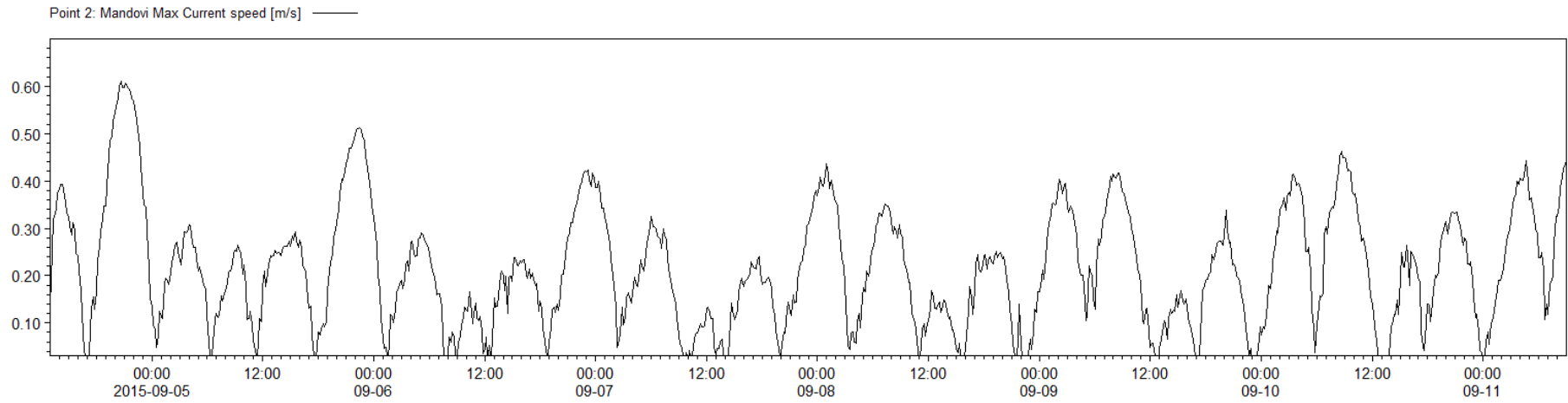


Figure 3.11e: Modelled currents at Point 1 in Mandovi river

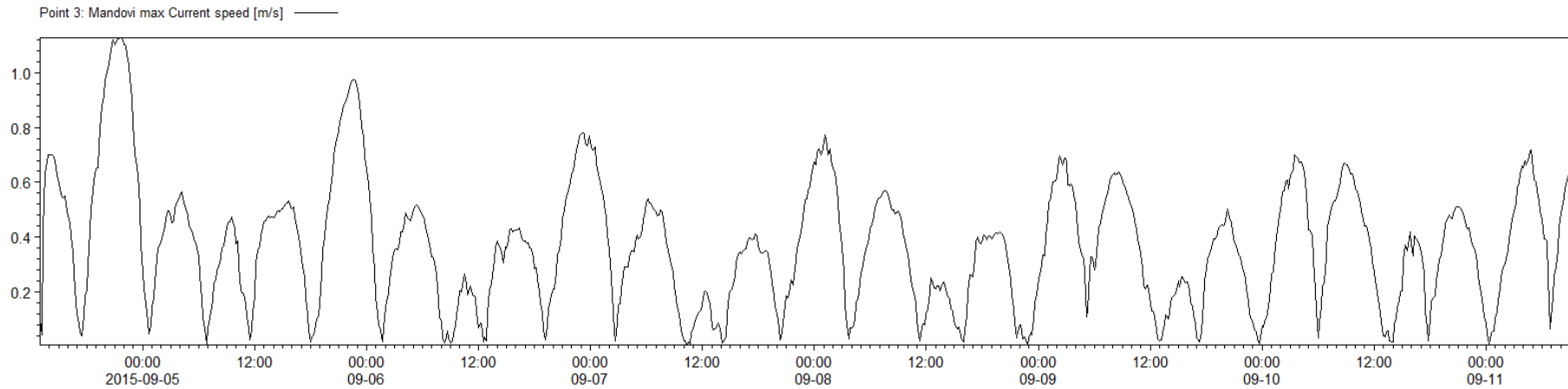
ent_data\chapora\MAXIMUM CURRENTS\Max_currents_4.dfs0

H:\kias\PhD\Measured Current data\Mandovi\Max_currents_6.dfs0



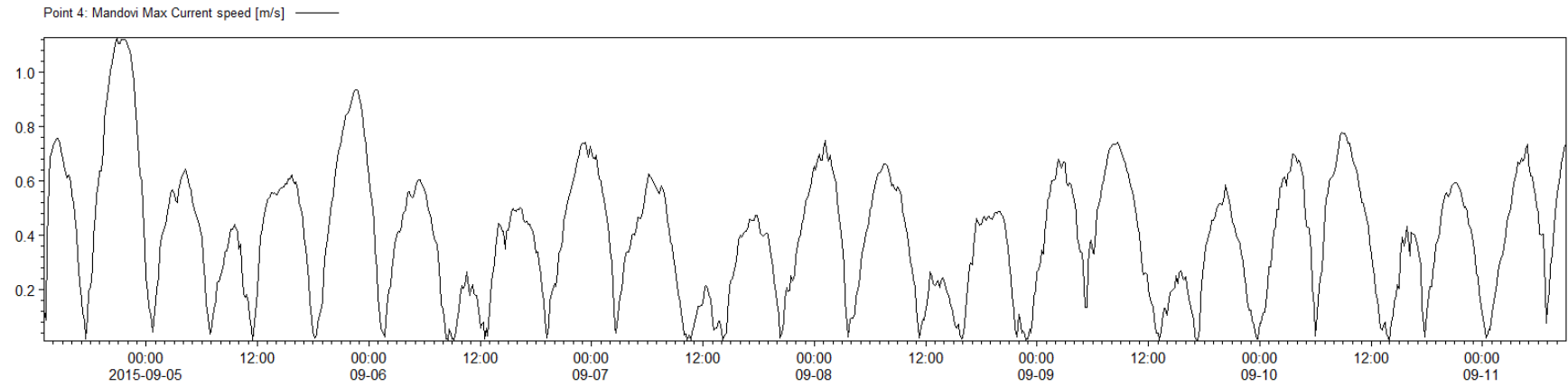
H:\Nkas\PHD\Measured Current data\MandoviMax_currents_2.dfs0

Figure 3.11f: Modelled currents at Point 2 in Mandovi river



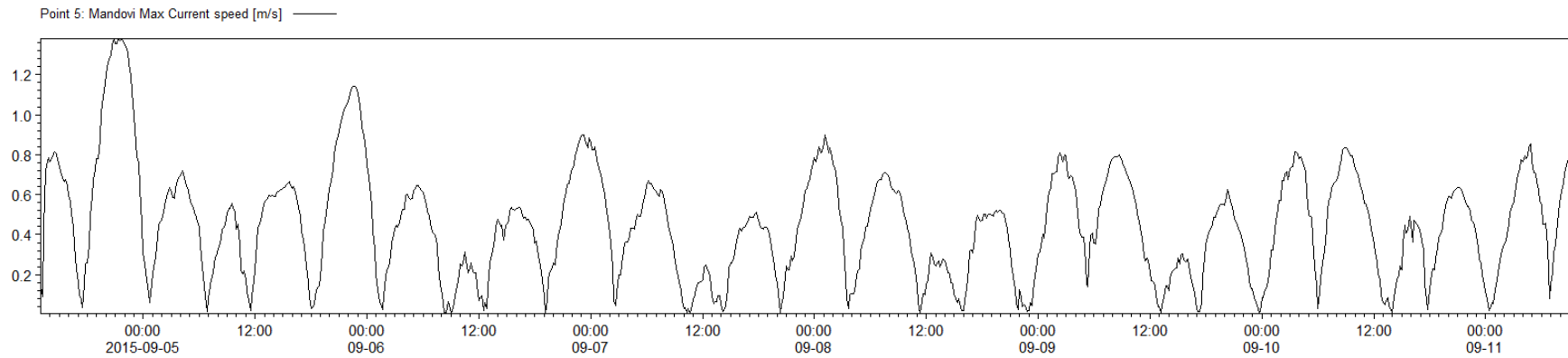
H:\Nkas\PHD\Measured Current data\MandoviMax_currents_3.dfs0

Figure 3.11g: Modelled currents at Point 3 in Mandovi river



H:\kias\PhD\Measured Current data\Mandovi\Max_currents_4.dfb

Figure 3.11h: Modelled currents at Point 4 in Mandovi river



H:\kias\PhD\Measured Current data\Mandovi\Max_currents_5.dfb

Figure 3.11i: Modelled currents at Point 5 in Mandovi river

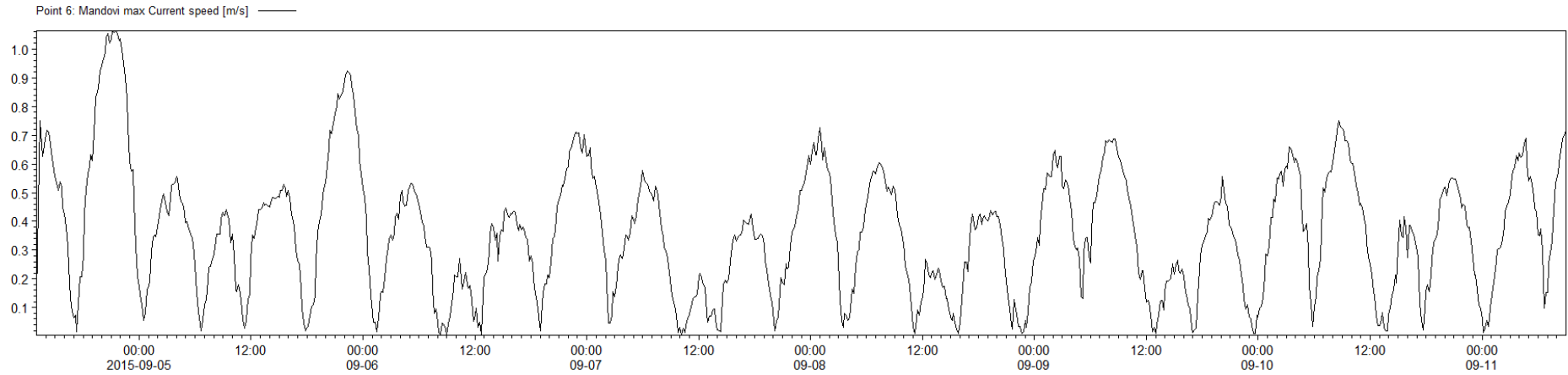


Figure 3.11j: Modelled currents at Point 6 in Mandovi river

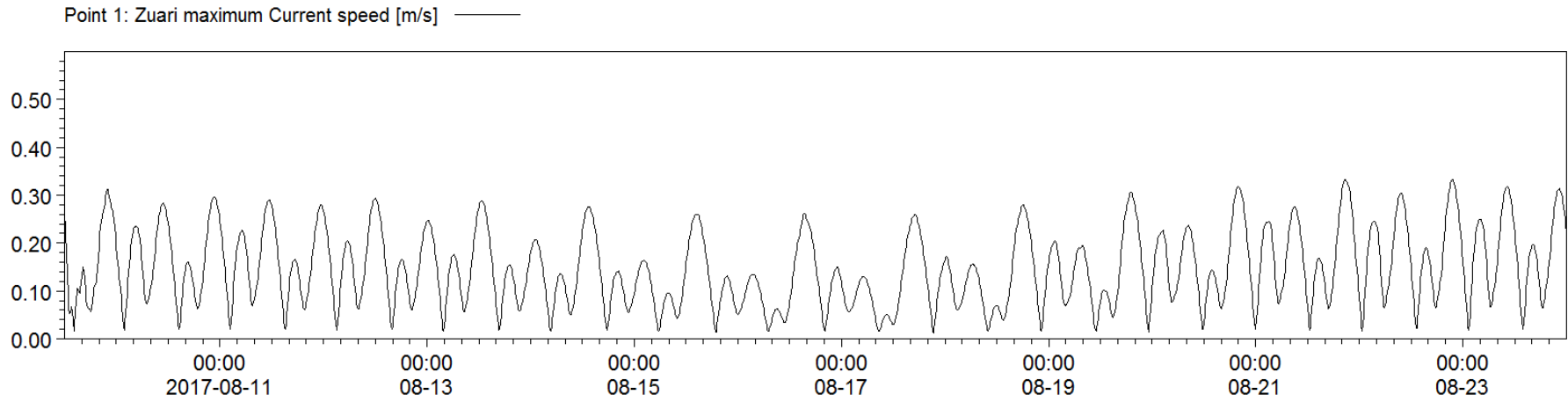
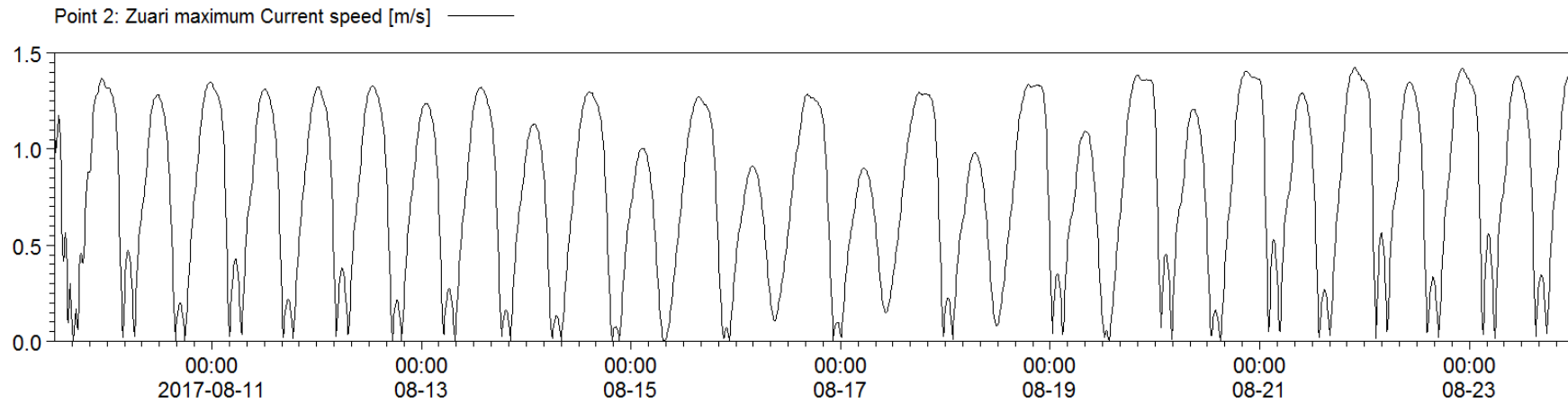
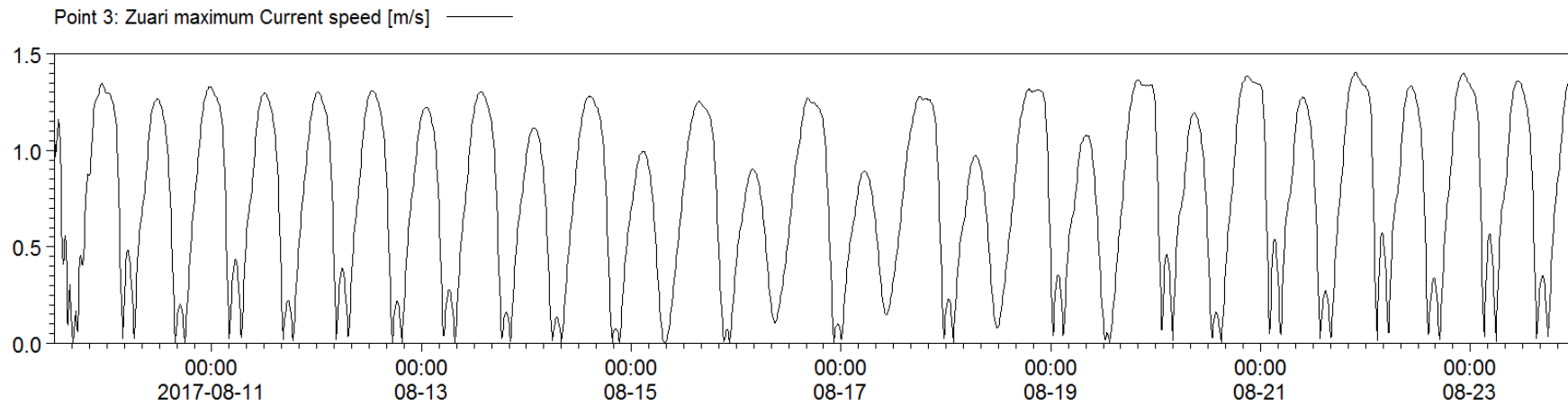


Figure 3.11k: Modelled currents at Point 1 in Zuari river



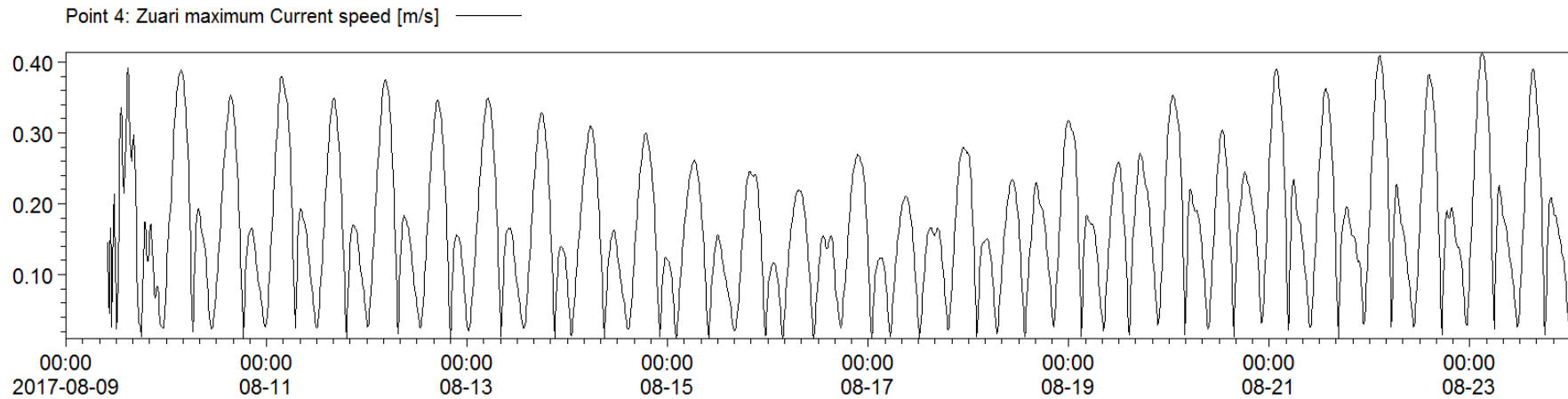
tazuan\Maximum modelled currents\Max_currents_2_ yes dfs0

Figure 3.11l: Modelled currents at Point 2 in Zuari river



nt_data\zuan\Maximum modelled currents\Max_currents_3_ dfs0

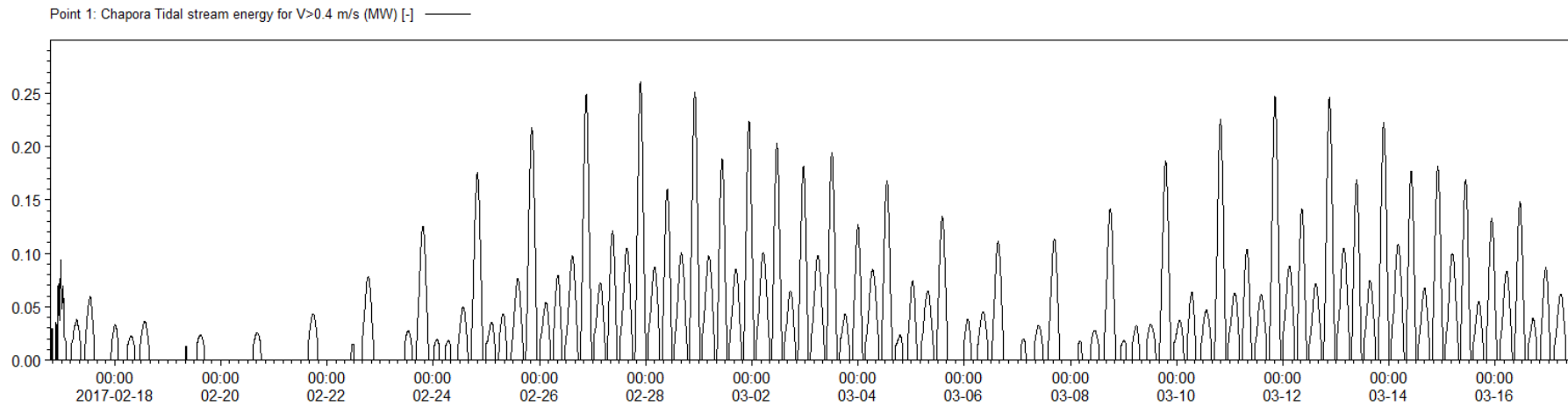
Figure 3.11m: Modelled currents at Point 3 in Zuari river



nt data\zuari\Maximum modelled currents\Max_currents_4.dfs0

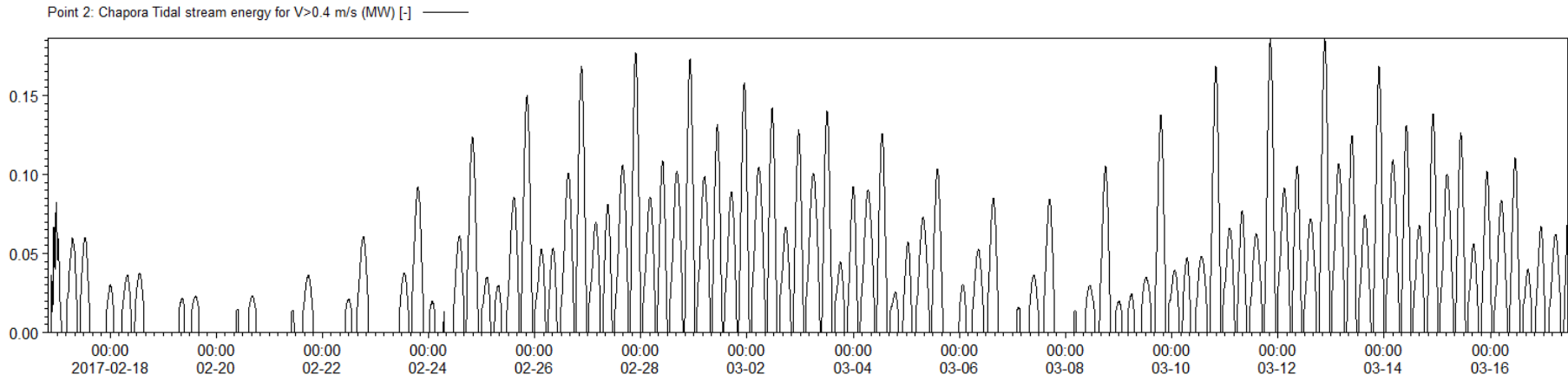
Figure 3.11n: Modelled currents at Point 4 in Zuari river

The stream energy is calculated from the points of maximum currents (modelled) as shown in **Figures 10a to 10n**. The currents less than 0.4 m/s are not considered.



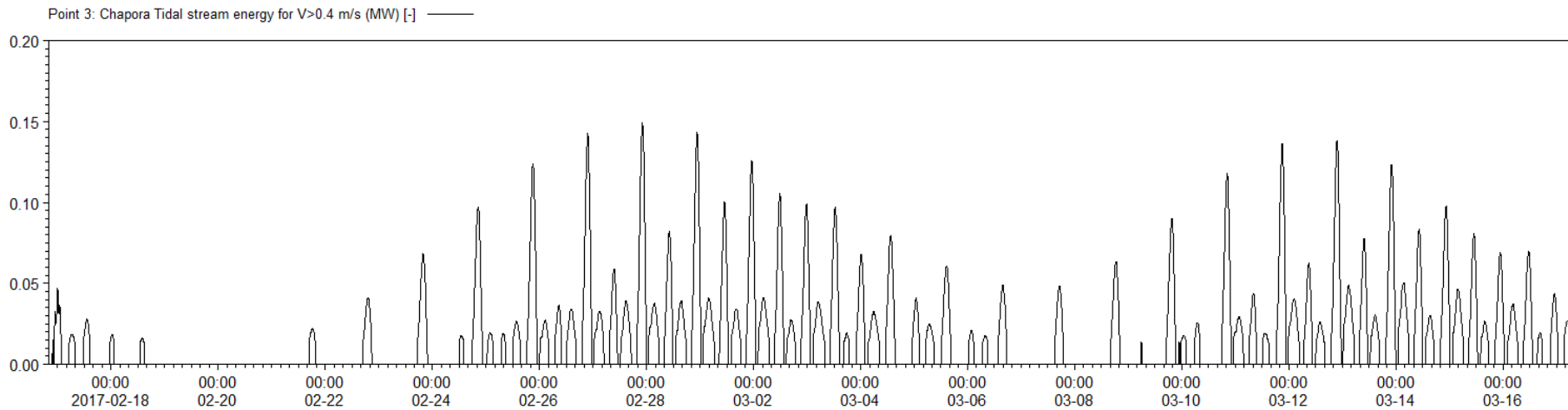
H:\Vikas\PhD\Measured Current data\chapora\Max_currents_1.dfs0

Figure 3.12a: Tidal stream energy (modelled) at Point 1 in Chapora River having current speed greater than 0.4 m/s



H:\Vikas\PhD\Measured Current data\chaporanMax_currents_2_yes.dfs0

Figure 3.12b: Tidal stream energy (modelled) at Point 2 in Chapora River having current speed greater than 0.4 m /s



H:\Vikas\PhD\Measured Current data\chaporanMax_currents_3.dfs0

Figure 3.12c: Tidal stream energy (modelled) at Point 3 in Chapora River having current speed greater than 0.4 m /s

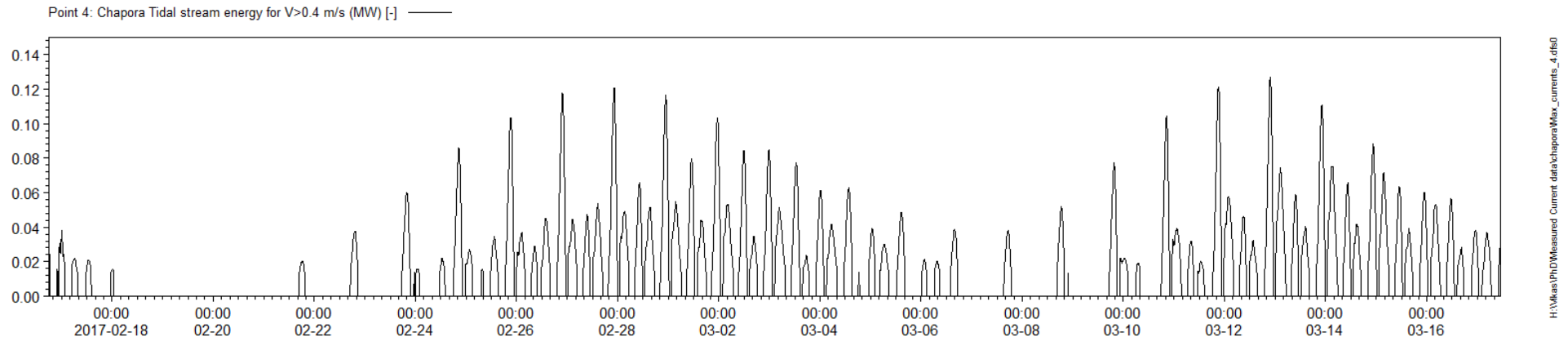


Figure 3.12d: Tidal stream energy (modelled) at Point 4 in Chapora River having current speed greater than 0.4 m /s

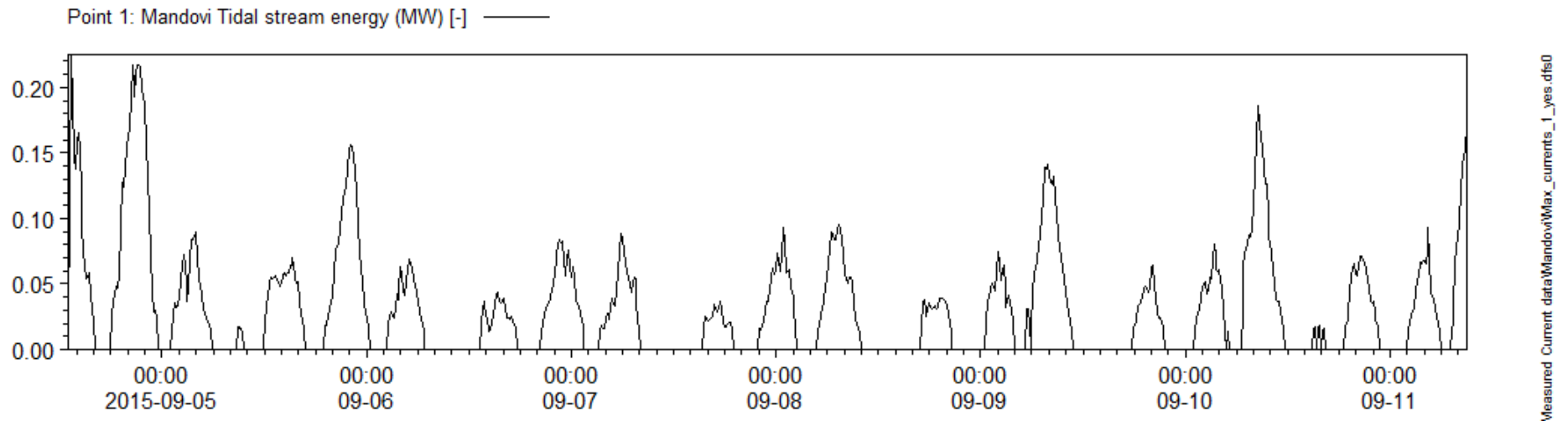


Figure 3.12e: Tidal stream energy (modelled) at Point 1 in Mandovi River having current speed greater than 0.4 m /s

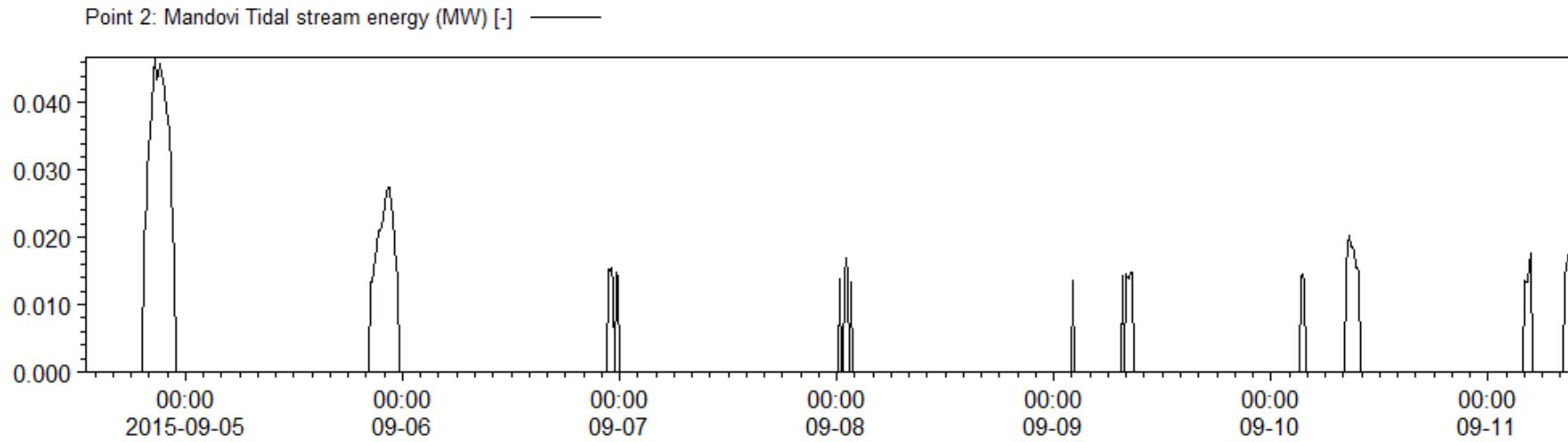


Figure 3.12f: Tidal stream energy (modelled) at Point 2 in Mandovi River having current speed greater than 0.4 m /s

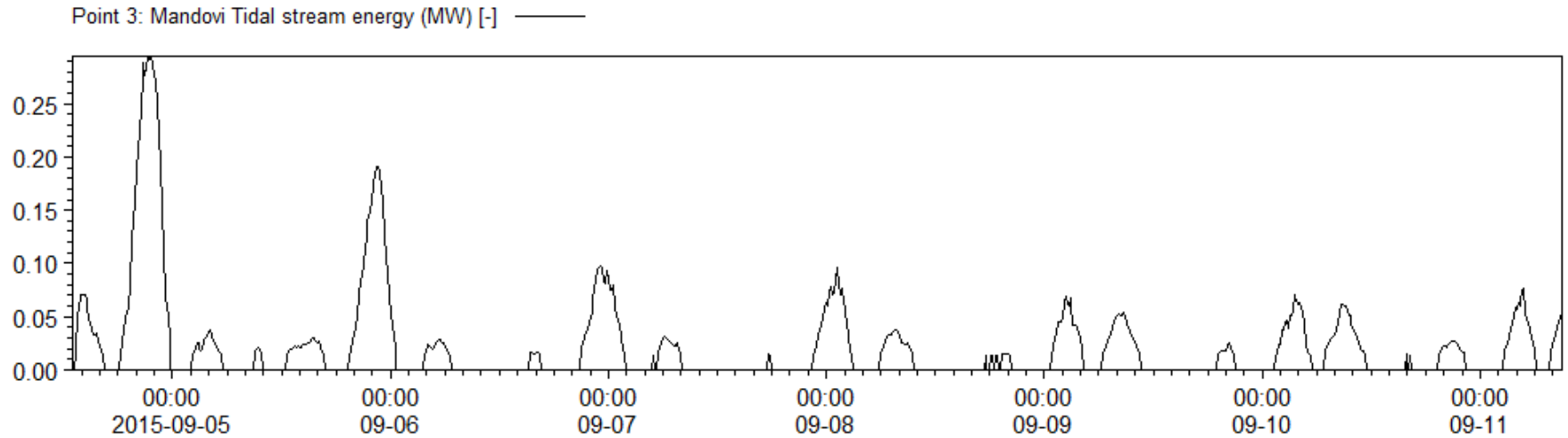


Figure 3.12g: Tidal stream energy (modelled) at Point 3 in Mandovi River having current speed greater than 0.4 m /s

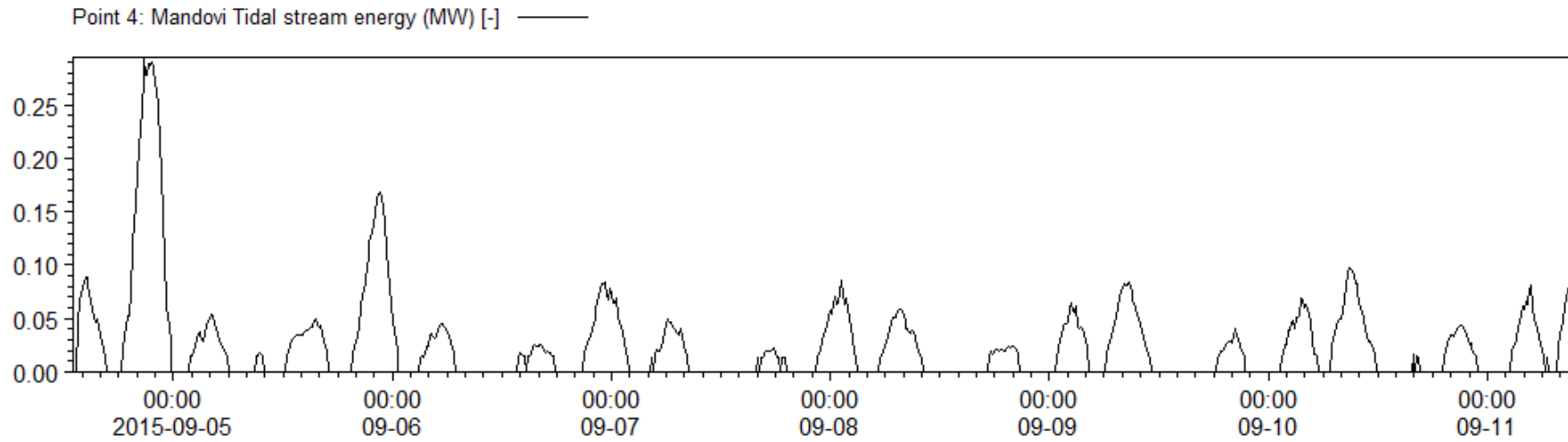


Figure 3.12h: Tidal stream energy (modelled) at Point 4 in Mandovi River having current speed greater than 0.4 m /s

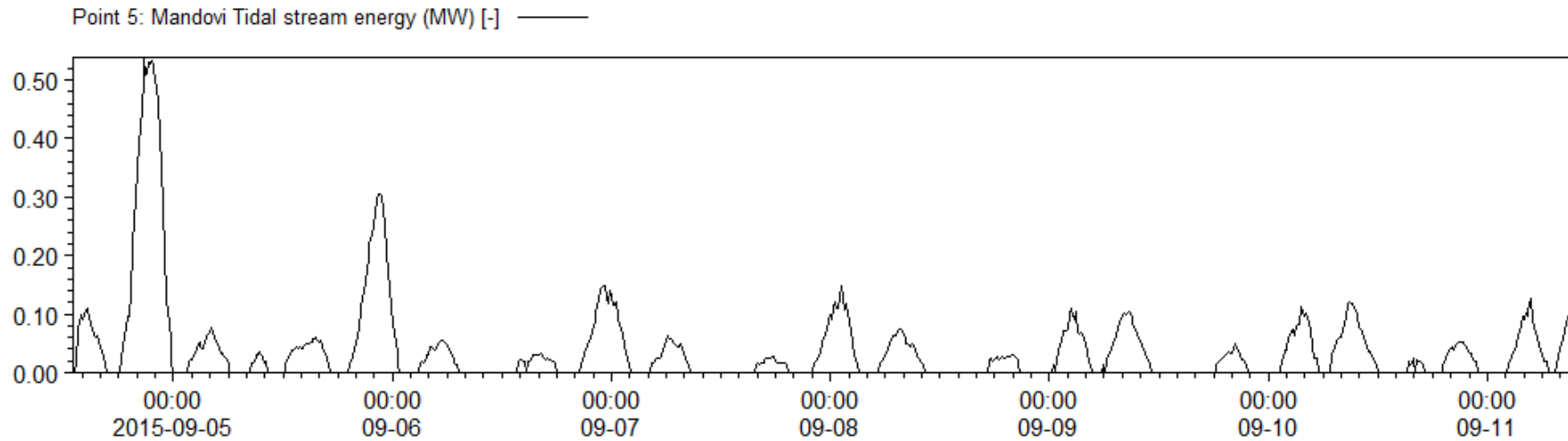


Figure 3.12i: Tidal stream energy (modelled) at Point 5 in Mandovi River having current speed greater than 0.4 m /s

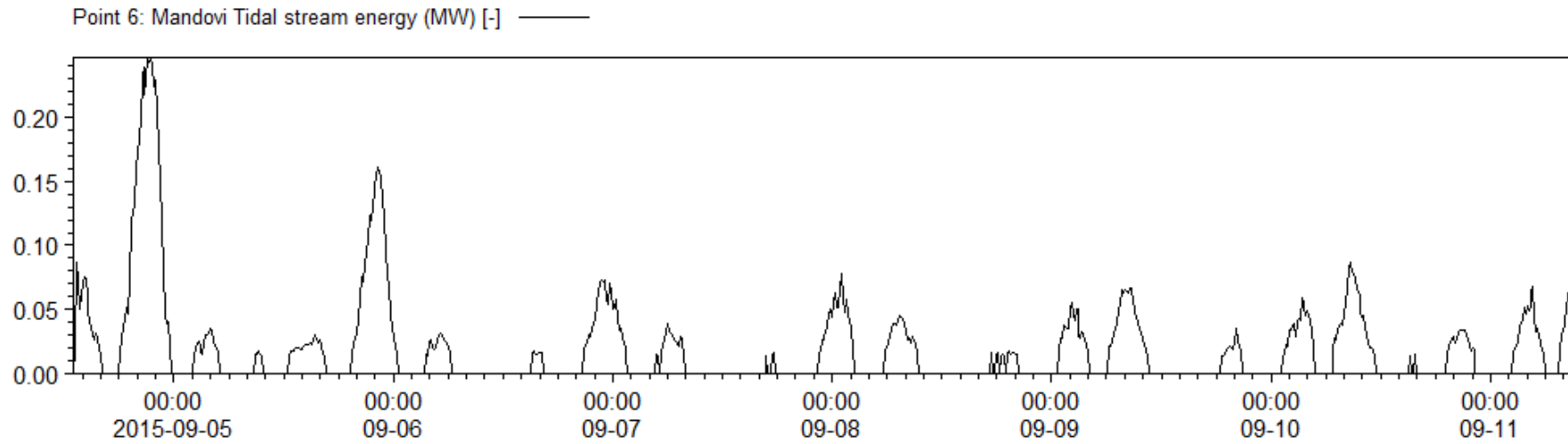


Figure 3.12j: Tidal stream energy (modelled) at Point 6 in Mandovi River having current speed greater than 0.4 m /s

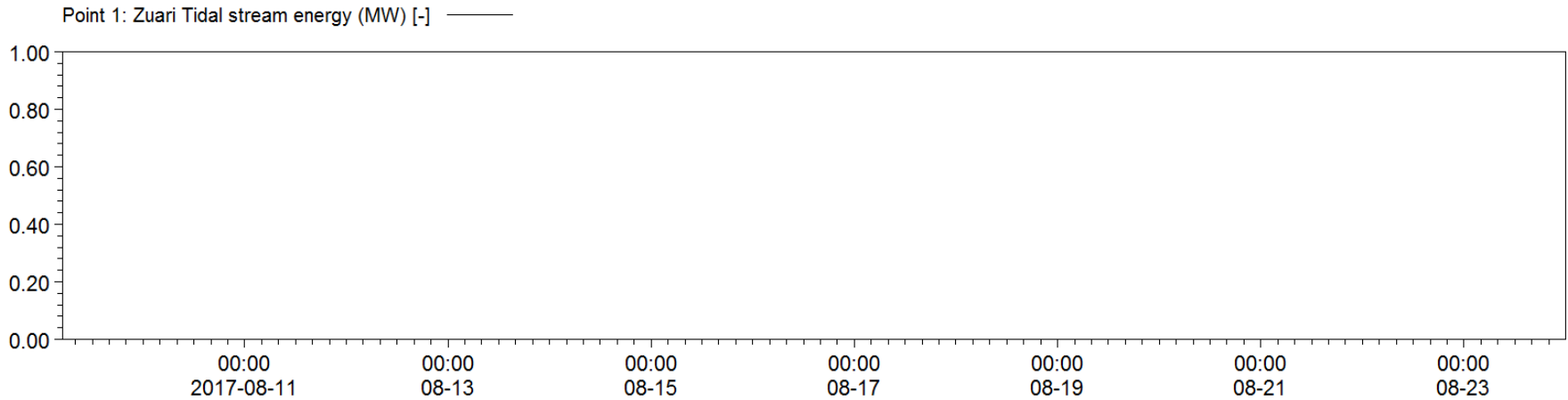


Figure 3.12k: Tidal stream energy (modelled) at Point 1 in Zuari River having current speed greater than 0.4 m /s

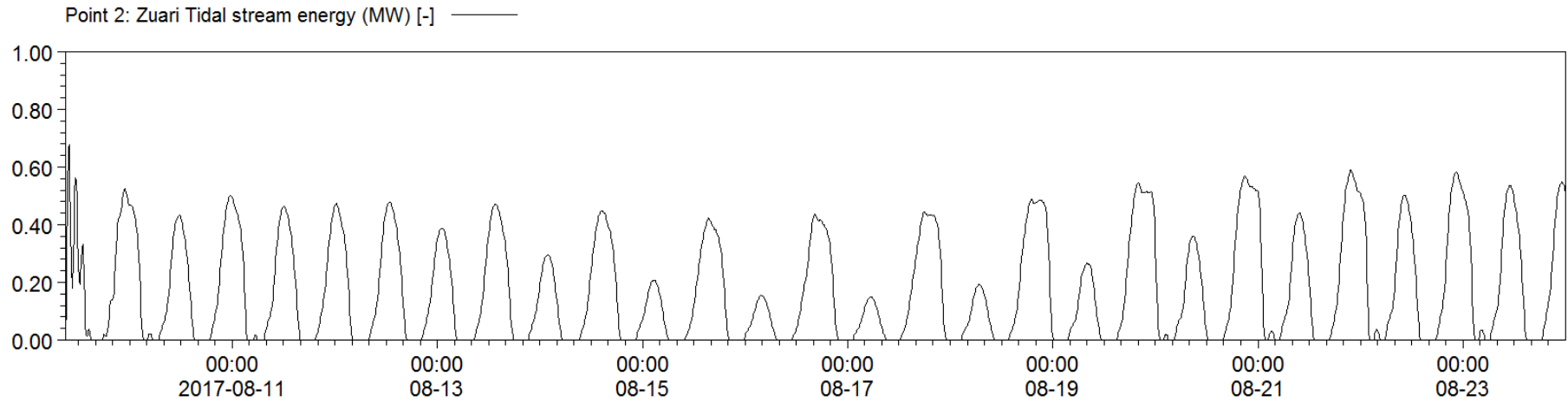


Figure 3.12l: Tidal stream energy (modelled) at Point 2 in Zuari River having current speed greater than 0.4 m /s

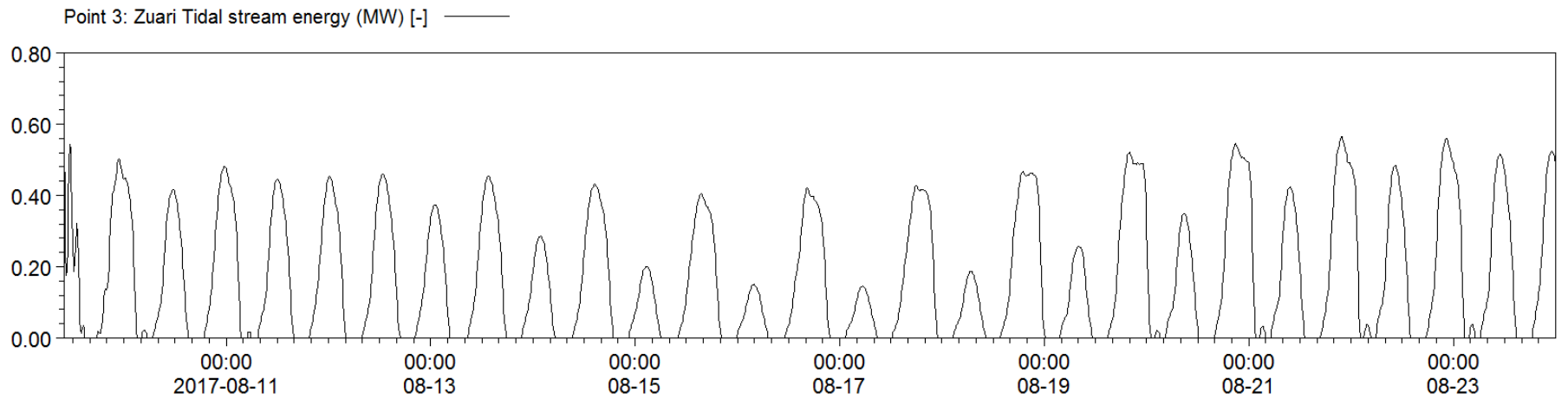
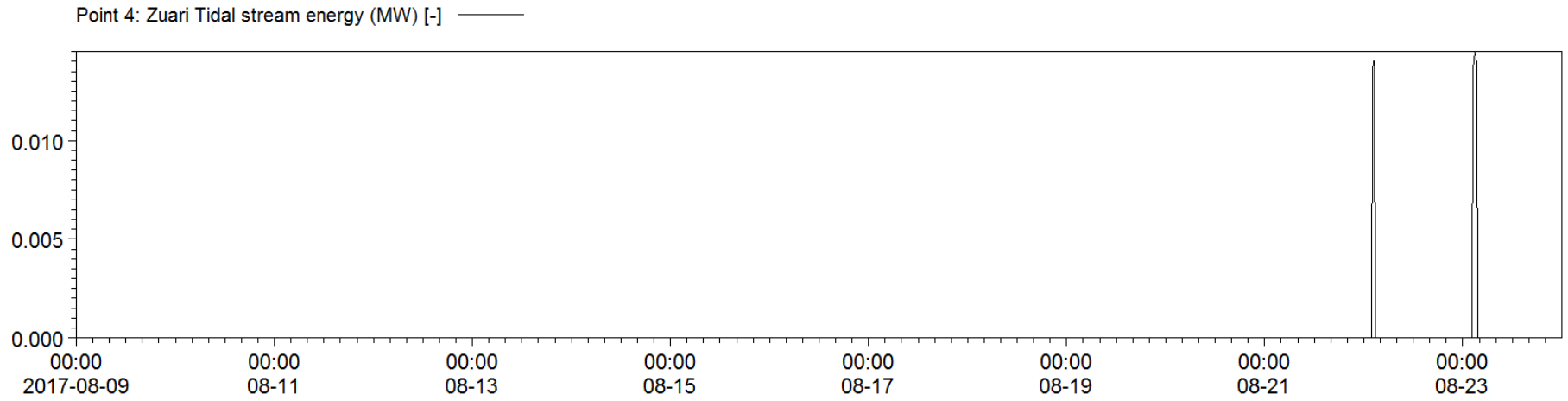


Figure 3.12m: Tidal stream energy (modelled) at Point 3 in Zuari River having current speed greater than 0.4 m /s



nt data\zuan\Maximum modelled currents\Max_currents_4.dfs0

Figure 3.12n: Tidal stream energy (modelled) at Point 4 in Zuari River having current speed greater than 0.4 m /s

3.7 Conclusions

- Tidal range, lagoon area and potential energy are calculated for 471 tidal inlets along the Indian coast and presented in Appendix 1.
- Out of 471 tidal inlets, 130 inlets are shortlisted and potential energy was estimated considering a threshold of 2.53 Mm^3 tidal prism and inlet width of 63m. However, the threshold value is an initial estimation that is considered based on the availability of existing tidal power plants. Tidal flux into a lagoon depends on the the depth and width of the inlet and the relative threshold values can be site specific.
- Total potential energy is 2254.906 MW. Further 107 inlets are shortlisted and potential energy is estimated considering both tidal prisms greater than 2.53 Mm^3 and inlet throat width greater than 63m. Total potential energy is 2127.281 MW.
- Currents are measured at three inlets (8 points) in Goa and the possible energy that could be generated is calculated for three inlets in Goa considering current speed 0.4m/s as a threshold.
- Currents are simulated at three locations in Goa, where the data is available for simulation, using MIKE21 flow model. The points of maximum currents are identified (14 locations) and tidal stream energy generated is calculated at these locations.
- Point 1 in Chapora, Point 5 in Mandovi and Point 2 in Zuari showed greater tidal stream energy extraction per day when considered 22 locations in 3 inlets from both measured and modelled data. The Kinetic energy estimated in these locations are 11.68 kW/day, 5.60 kW/day and 25.64 kW/day at Chapora, Mandovi and Zuari respectively.
- If the threshold speed is changed to 0.5 m/s or 0.7 m/s the total energy generation is observed to reduce by 37.78% and 64.53% which is observed from Table 3.5.

CHAPTER 4

IMPACT OF TIDAL ENERGY FARM ON LOCAL HYDRODYNAMICS AND ON ENERGY ESTIMATES

4.1 Introduction

The dynamic effects of extracting energy from tides present distinctive challenges to the improvement of tidal stream energy. The principle and mechanism of tidal turbines bear a resemblance to wind turbines and extract tidal energy from the ebb and flood of extreme currents which are driven by tides. Energy extraction will increase the resistance to flow, resulting in changes in tides, transport, mixing, and therefore the kinetic resource itself. These variations in turn have environmental, social, and economic implications that must be understood to develop a sustainable resource. The inlets have to be open throughout the year to aid energy extraction. Vu (2013) classified the tidal inlets as tide-dominated, wave-dominated, river-dominated, and ICOLLs (Intermittently Closed and Open Lakes and Lagoons) in New South Wales using different theoretical methods available and also suggested few more non-dimensional methods of classification. This classification would help to understand the inlet stability in a better way.

This chapter describes the development of a two-dimensional numerical model and its application to the study of morphodynamics covering select locations in Goa (India). Since the tidal stream flows are typically sub-critical, there are chances that the effects of it have an influence all over the estuary not simply at the location of extraction. The results of this study indicate that sediment transport at the site where turbines are located are dynamic due to energy extraction. In such sensitive surroundings, results inferred that there are possible modifications in tidal currents due to which energy extraction may have some effects on the existing morphodynamic regime.

The barrage method of construction generally involves huge installation costs, which is not practically feasible for installation at all the tidal inlets. Gulf of Kutch project is an example for this where a proposed 50MW plant was halted due to high tender cost. On the other hand, tidal stream technology is relatively less expensive, but a study on hydrodynamics becomes important. The energy estimates calculated by the tidal stream at a particular location may not be the same after the construction of the energy farm as the turbines that are installed will have an impact on the hydrodynamics and the theoretical power may not be achieved. So, it is important to study hydrodynamics and then revise the rated power of the energy farm. This

will be carried out by numerical modelling using MIKE by DHI software suite using flexible mesh for simulation as numerical models are well proven to mimic the prediction and conditions of ocean waters (Sannasiraj et al. 2004). For the modelling, bathymetry becomes an important factor that has to be available offshore, nearshore, inlet mouth, and inside the basin. Out of the 471 identified tidal inlets, the bathymetry data is very limited and field investigations are to be carried out to obtain the same. Mere interpolation of the bathymetry from hydrographic charts does not give us accurate results.

The Ministry of New and Renewable Energy (MNRE) in India says that “the total identified potential of Tidal Energy is about 12455 MW, with potential locations identified at Khambhat & Kutch regions, and large backwaters, where barrage technology could be used” [MNRE, <https://mnre.gov.in/new-technologies/overview>]. This clearly states that the explorations and estimates are only restricted to the northern part of India, i.e. Gujarat, and there is absolutely no information on the tidal energy potential in southern India and also about the tidal stream energy extraction which still seems to be in a nascent stage in India. Tidal stream energy, also being one of the potential and effective sources to extract the energy from moving waters, has substantial benefits when compared to the barrage method of energy extraction as mentioned by MNRE. Two major advantages of energy extraction from tidal currents are that; the construction costs are comparatively low and the pollution anticipated to happen in the sea waters that is caused during the construction is exponentially less in comparison to the barrage method of energy extraction. As a result, the cost per unit of the energy produced comes down and there are comparatively less environmental concerns to address if the energy is extracted from tidal currents. Figure 4.1 shows the study area in Goa (India) for the hydrodynamics of tidal stream energy assessment.

4.2 Methodology

Initial validation of the measured tidal currents is carried out to confirm the correctness of inputs provided to the numerical model to predict the tidal currents. MIKE21 flow model, that uses flexible mesh for the hydrodynamic model coupled with the sand transport. The turbines are placed at the locations where the highest tidal currents are observed as presented in chapter 2. Five different types of simulations are carried out to study the morphodynamic effects of the tidal turbines. Considering 0.5m diameter of the turbine with a drag coefficient of 0.4, the following are the typical cases considered:

- i. No turbines (as a base case for comparison).

- ii. One turbine.
- iii. An array of 3 turbines placed parallel to the flow.
- iv. An array of 3 turbines placed perpendicular to the flow.
- v. No turbines and decreased water depth at Zuari 3.

4.3 Numerical model

4.3.1 Hydrodynamic model

To evaluate the naturally occurring sediment movement patterns, a coupled Hydrodynamic (HD) and morphodynamic model is set up. The domain considered to study the morphodynamics included three tidal inlets in Goa, with a maximum water depth of ~ 28m on the seaside and ~ 16m on the lee side. This coupled mud/sand transport module in MIKE21 (flexible mesh) is used to simulate hydrodynamics due to energy extraction from tide induced currents in Goa. MIKE is developed by the Danish Hydraulic Institute. The flexible mesh flow model is a comprehensive modelling tool of MIKE21 for 2D and 3D hydrodynamic modelling. The two and three-dimensional numerical models are termed as MIKE21 and MIKE3 respectively and are based on finite volume method and they use flexible mesh for complex coastal area simulations. MIKE21 has proved to mimic the complex coastal environment in terms of many parameters. The flow model (FM) consists of the hydrodynamic module which is built based on the numerical solution of the 2D shallow water equations as shown below. (DHI Software 2012).

Integration of the horizontal momentum equations and the continuity equation over depth $h = \eta + d$ the following two dimensional equations are obtained.

$$\frac{\partial h}{\partial t} + \frac{\partial h\bar{u}}{\partial x} + \frac{\partial h\bar{v}}{\partial y} = hS \quad (4.1)$$

For the x and y components, the momentum equations can be written as

$$\begin{aligned} \frac{\partial h\bar{u}}{\partial t} + \frac{\partial h\bar{u}^2}{\partial x} + \frac{\partial h\bar{u}\bar{v}}{\partial y} = f\bar{v}h - gh\frac{\partial\eta}{\partial x} - \frac{h}{\rho_0}\frac{\partial p_a}{\partial x} - \frac{gh^2}{2\rho_0}\frac{\partial\rho}{\partial x} + \frac{\tau_{sx}}{\rho_0} - \frac{\tau_{bx}}{\rho_0} - \frac{1}{\rho_0}\left(\frac{\partial s_{xx}}{\partial x} + \frac{\partial s_{xy}}{\partial y}\right) + \\ \frac{\partial}{\partial x}(hT_{xx}) + \frac{\partial}{\partial y}(hT_{xy}) + hu_sS \end{aligned} \quad (4.2)$$

$$\begin{aligned} \frac{\partial h\bar{v}}{\partial t} + \frac{\partial h\bar{u}\bar{v}}{\partial x} + \frac{\partial h\bar{v}^2}{\partial y} = f\bar{u}h - gh\frac{\partial\eta}{\partial y} - \frac{h}{\rho_0}\frac{\partial p_a}{\partial y} - \frac{gh^2}{2\rho_0}\frac{\partial\rho}{\partial y} + \frac{\tau_{sy}}{\rho_0} - \frac{\tau_{by}}{\rho_0} - \frac{1}{\rho_0}\left(\frac{\partial s_{yx}}{\partial x} + \frac{\partial s_{yy}}{\partial y}\right) + \\ \frac{\partial}{\partial x}(hT_{xy}) + \frac{\partial}{\partial y}(hT_{yy}) + hv_sS \end{aligned} \quad (4.3)$$

Where, t – time, x, y – cartesian coordinates, η is the surface elevation, $h = \eta + d$
 u, v – flow velocity components, f – coriolis parameter, T – temperature
 ρ_0 – reference density of water, (τ_{sx}, τ_{sy}) and (τ_{bx}, τ_{by}) are x and y components
of the surface wind and bottom stresses.

g – gravitational acceleration

S – Magnitude of discharge due to point sources, u_s and v_s is the velocity by which
water is discharged into the ambient water.

The domain was forced with the predicted tides and simulated waves, measured winds
available at CSIR - National Institute of Oceanography, Goa.

4.3.2 Sediment transport model

The Sand Transport module picks up the flow rates from the HD module and calculates the
resulting transport of non-cohesive materials and wave conditions from wave calculations. A
mean sediment grain size, if available, can be given as input to the model over the entire domain
or varying in the domain. The model output consists of sediment transport rates, bed level
changes, amongst other parameters. In this study pure current formulation of sediment transport
is considered with the flow model providing the currents information obtained from the
hydrodynamic model.

4.4 Description of the model domain

The domain considered in this study contains Mandovi and Zuari Rivers between the
coordinates 73.68E, 15.33N and 74.00E, 15.53N covering over an approximate basin area of
91 km². The flexible mesh is generated with coarse grids in the offshore region and fine grids
inside the river. The maximum grid area offshore is 5090150 m³ and the minimum is 34 m³
with average grid lengths of 3692m and 3m respectively. A smaller grid, as shown in Figure
4.1, with a very fine mesh of the size of about 3m is considered at the location of deployment
of turbines for close examination of the parameters at the location. The width of the river mouth
of Mandovi is 3235m and that of Zuari is 4229m. The tidal signal in the area is semi-diurnal
with an oceanic spring tidal range of about 2.5m inside the estuary. However, in the simulation,
the turbines exist only in the Zuari River. Mandovi River also has been considered in the
simulation to ensure proper forcing of the tides into both the estuaries and also to maintain
discharge flow from both the inlets as both of them are adjacent to each other. Figure 4.1
presents the model domain considered in this study. The tides are forced from the north, west

and south boundaries along with the measured winds and simulated waves available at CSIR-National Institute of Oceanography. Four boundaries, two each are located on the lee side of Mandovi and Zuari inlets and a discharge of $800 \text{ m}^3/\text{s}$ is considered for the simulation through the boundaries.

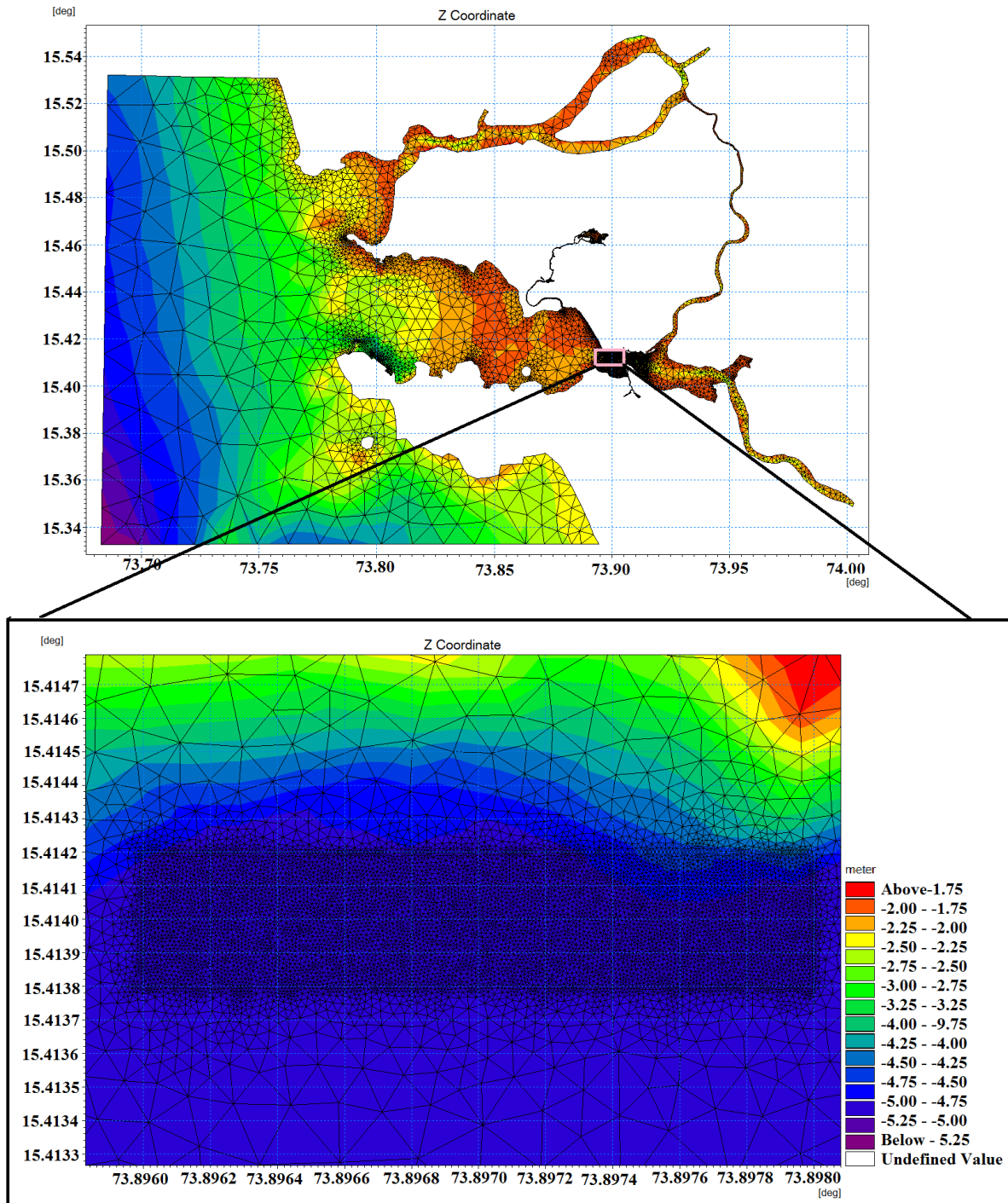


Figure 4.1: Model domain considered for simulation

4.5 Validation of modelled currents

The flow values obtained from the numerical model are validated with the current speeds that are measured using Aanderaa[®] RCM9 current meter to confirm that the modelled currents are similar to the measured currents. Measured tides, simulated waves and representative wind speeds are provided as input for the numerical model. The comparison of measured flow speeds with the model results (section 3.4) shows that the modelled currents are in good agreement with the measurements. However, due to unavailability of field data, the validation of bed level changes could not be carried out.

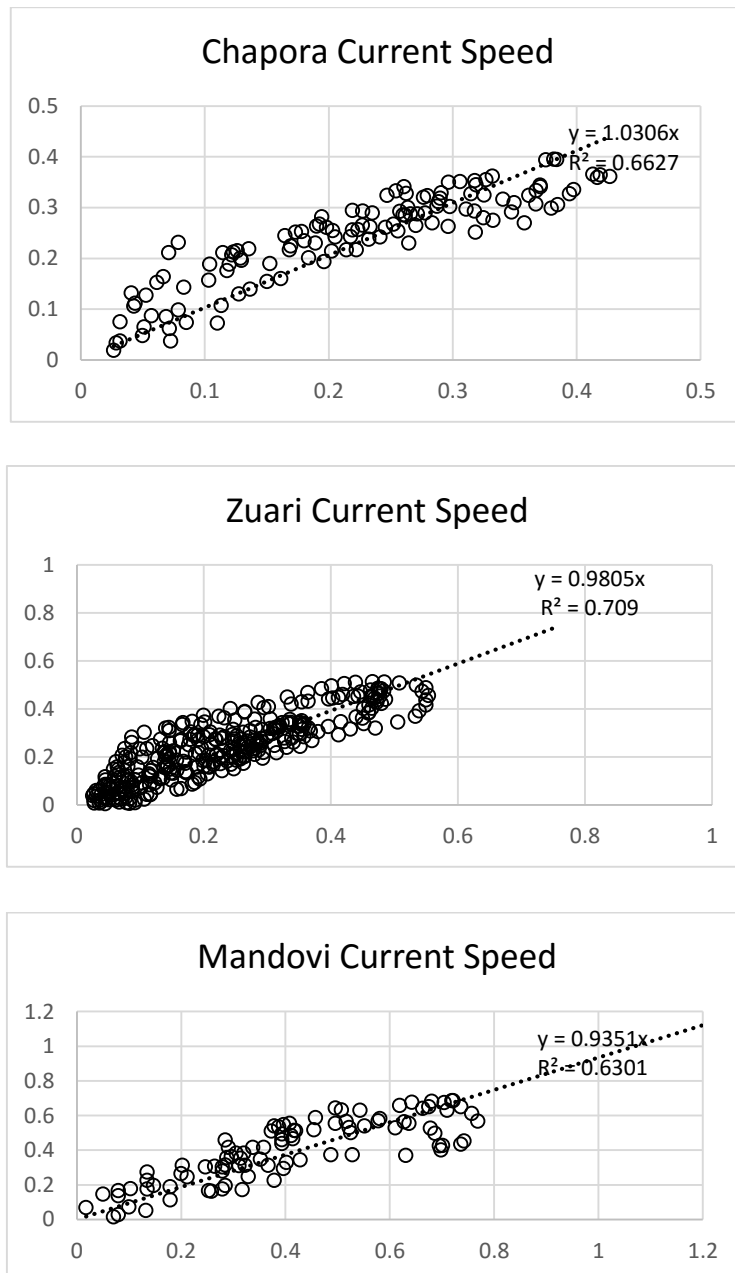


Figure 4.2: Validation of modelled currents with measured currents (scatter plot)

Table 4.0 r^2 values for the current speed and tide

	Current speed	Surface Elevation
	R-squared	R-squared
Chapora	0.66	0.6
Mandovi	0.63	0.9
Zuari	0.71	0.8

4.6 Results and discussion

MIKE21 flexible mesh Hydrodynamic model coupled with sand transport modules is used to study the impact of energy extraction on the morphodynamics. The simulation is carried out from 9 August 2017, 00:00:00 to 16 August 2017, 12:00:00 covering 7.5 days for the base case comprising of 1080 time steps for a duration of 10 minutes for each time step. 0.5m diameter of the turbine with a drag coefficient of 0.4 is considered. The location Zuari 2 has been identified along the navigation channel and hence it has not been considered for further morphodynamic study. As mentioned in the previous section, 5 typical cases are considered to study the impact of turbines on the morphodynamics, the results of which follows:

i. Domain with no turbines (as a base case for comparison)

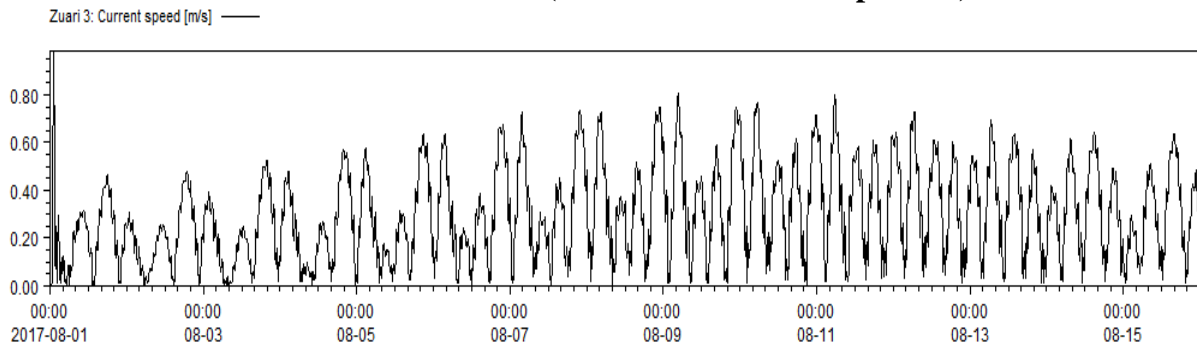


Figure 4.3: Modelled currents at Zuari 3 (Base case)

Figure 4.3 shows the modelled currents at Zuari 3 for possible energy extraction. The current data presented in Figure 4.3 is obtained by simulating the model domain in the absence of turbines and without making any alterations to the existing bathymetry. Hence the currents in Figure 4.3 will be considered as the base case and reference for all other simulations. The bed level change are observed at 6 points is shown in Table 4.1. The observation made from Figure 4.4 clarifies that there is bed level change for the base case during the simulation period.

Table 4.1 Data extraction locations for **case i** (no turbines) and **case iv** (decreased depth)

73.8962	15.414	Point 1
73.8963	15.414	Point 2

73.8964	15.414	Point 3
73.8965	15.414	Point 4
73.8966	15.414	Point 5
73.8967	15.414	Point 6

Point 1: Bed level change [m] ———
 Point 2: Bed level change [m] ———
 Point 3: Bed level change [m] ———
 Point 4: Bed level change [m] ———
 Point 5: Bed level change [m] ———
 Point 6: Bed level change [m] ———

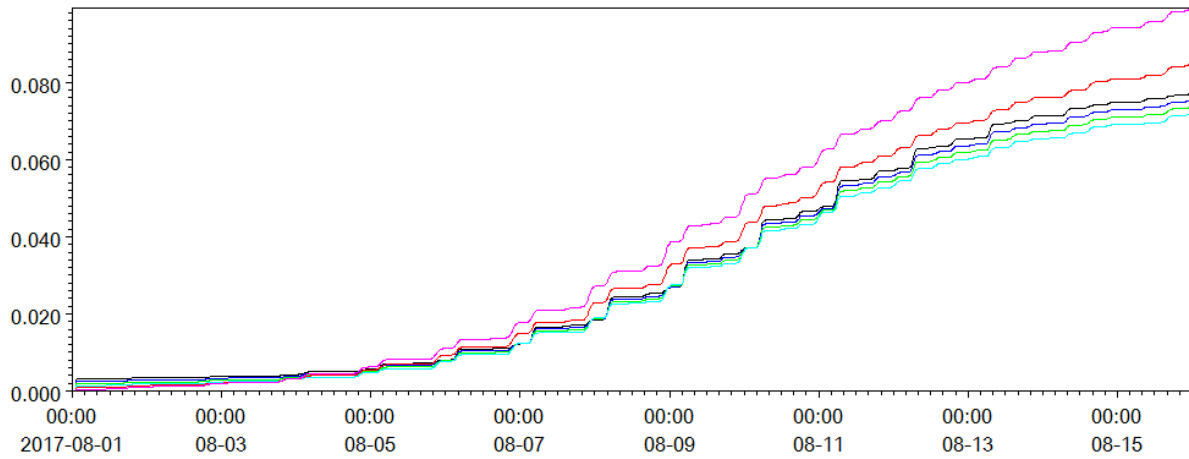


Figure 4.4: Bed level change for the base case

ii. Domain with one turbine at Zuari 3 which was observed to produce maximum currents

Figure 4.5 shows the location of the turbine in the model domain. Two cases are considered in this simulation. In the first case, a turbine having a diameter of 0.5m is used and for the same conditions, the diameter of the turbine is changed to 1m to observe if there is any change in the energy generated because of increasing the turbine diameter.

From Figure 4.6, it is observed that the current speeds at the 0.5m turbine reduced by 1% when a turbine of diameter 0.5m is used and from Figure 4.8, it is observed that the current speeds does not change with the increase in turbine diameter to 1m. Figure 4.9 presents the comparison of current speeds at 0.5m and 1m turbines with reference to the base case. The current speeds due to both the turbine showed less changes in comparison to the base case. The extraction of energy showed an impact on the bed level changes with sediment movement as observed in Figures 4.7 and 4.9. From the figures, it is observed that the bed level change is higher for a 1m diameter turbine in comparison to the 0.5m diameter turbine.

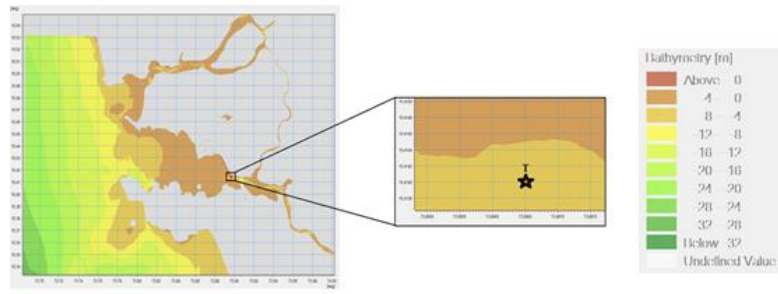


Figure 4.5: Turbine location in case ii

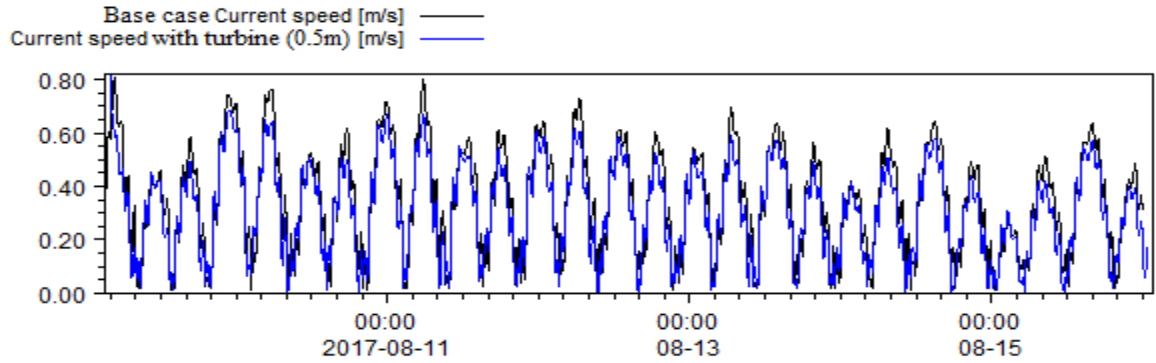


Figure 4.6: Comparison of current speeds for the base case with one turbine of 0.5m dia

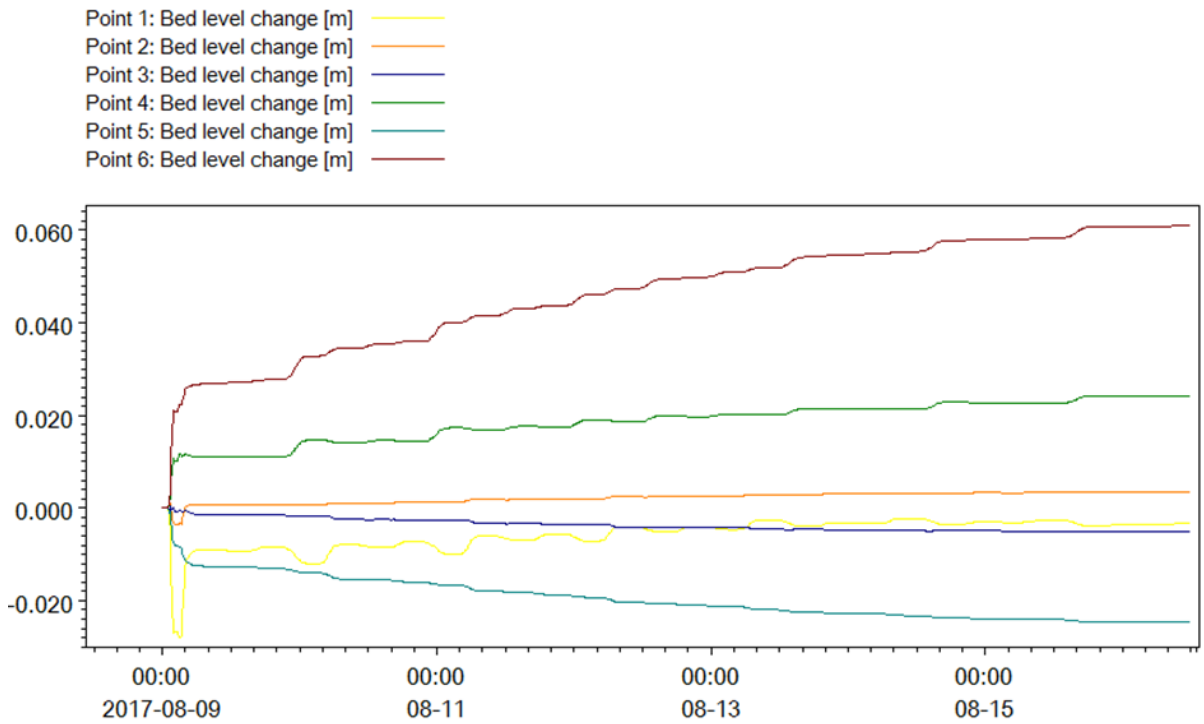


Figure 4.7: Bed level change when 0.5m dia turbine is deployed

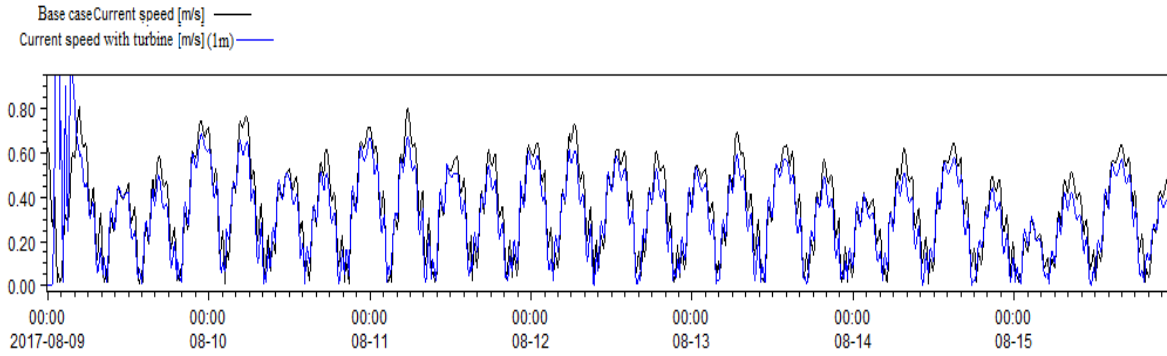


Figure 4.8: Comparison of current speeds for the base case with one turbine of 1m dia

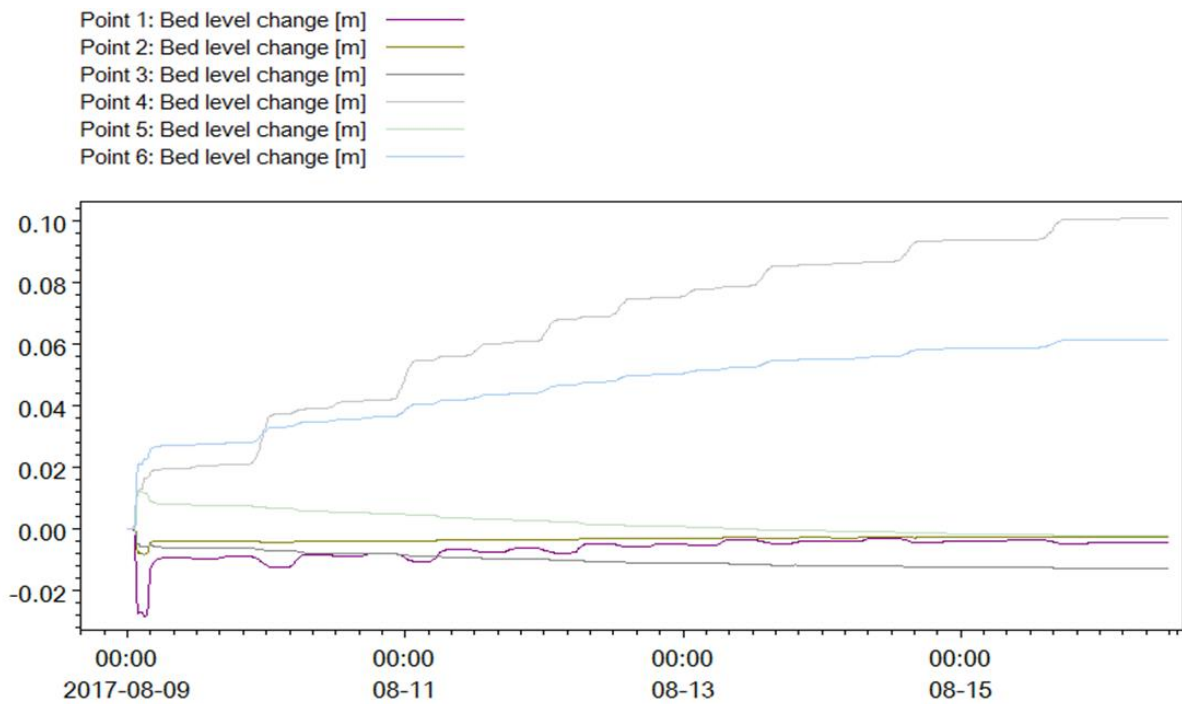


Figure 4.9: Bed level change when one turbine of 1m dia is deployed

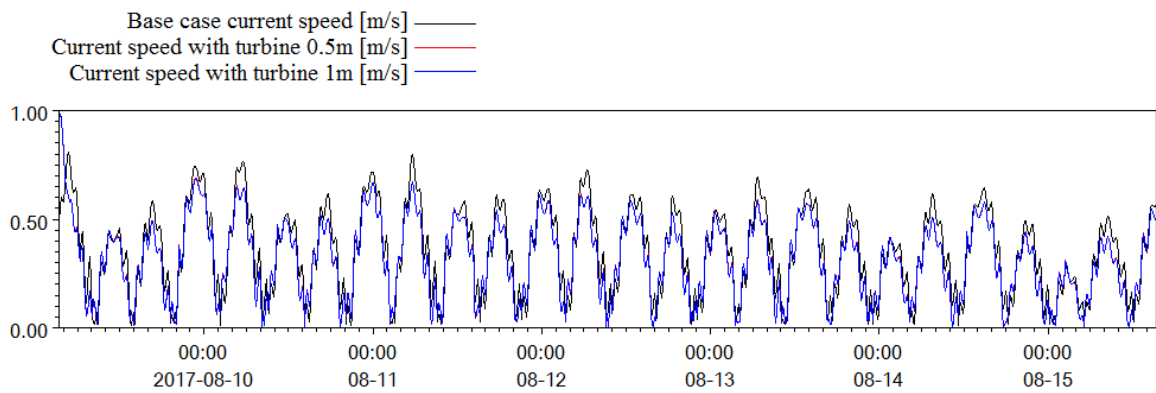


Figure 4.10: Comparison of current speeds for the base case with one turbine of 0.5m and 1m dia

iii. Domain with an array of turbines lined parallel to the flow.

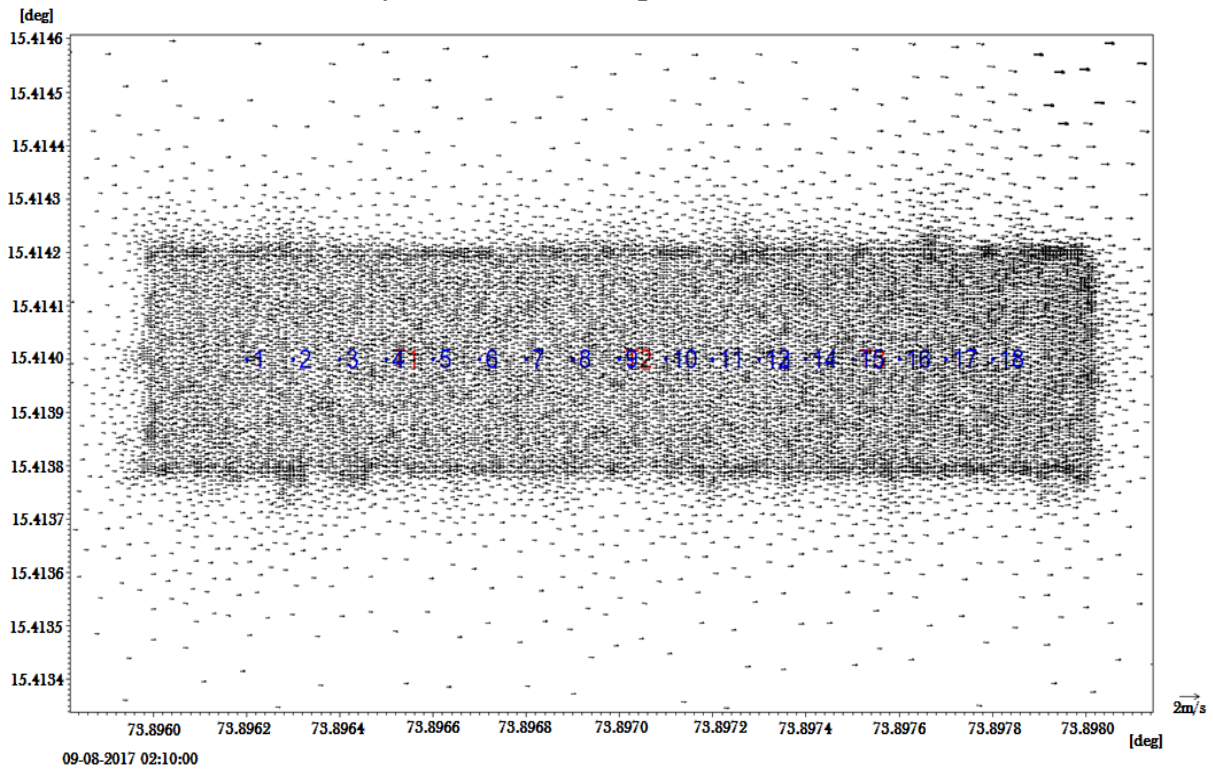


Figure 4.11: Turbines placed parallel to the flow

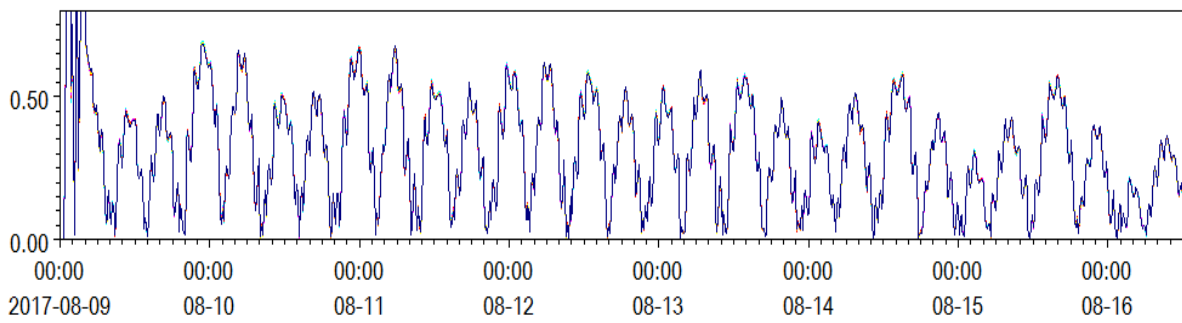
Three turbines T1 (Point 4), T2 (Point 9), and T3 (Point 15), as shown in Figure 4.11 are collinearly located such that they are lined parallel to the stream flow. The pattern of erosion and accretion was observed at points 1 to 18 shown in the figure 4.12. For the turbine T1, the current speeds and bed level changes are monitored at the points 1, 2, 3, 4, 5 and 6 where, point 4 is the location of turbine T1. For the turbine T2, the current speeds and bed level changes are monitored at the points 7, 8, 9, 10, 11 and 12 where, point 9 is the location of turbine T2. For the turbine T3, the current speeds and bed level changes are monitored at the points 13, 14, 15, 16, 17 and 18 where, point 15 is the location of turbine T3. Tables 4.2, 4.3 and 4.4 show the data extracted locations. The spacing between the turbines is considered as 50m as an experiment to observe the impact on each other. Figures 4.12 (a), 4.13 (a) and 4.14 (a) presents the comparison of current speeds from points 1 to 6. It can be observed that there is no change in the current speeds at these points. Table 4.5 presents the pattern of bed level change around the turbines T1, T2 and T3.

Table 4.2 Data extraction locations for T1 73.8965, 15.414

73.8962	15.414	Point 1
73.8963	15.414	Point 2
73.8964	15.414	Point 3
73.8965	15.414	Point 4
73.8966	15.414	Point 5
73.8967	15.414	Point 6

Point 1: Current speed [m/s] —
 Point 2: Current speed [m/s] —
 Point 3: Current speed [m/s] —
 Point 4: Current speed [m/s] —
 Point 5: Current speed [m/s] —
 Point 6: Current speed [m/s] —

(a)



Point 1: Bed level change [m] —
 Point 2: Bed level change [m] —
 Point 3: Bed level change [m] —
 Point 4: Bed level change [m] —
 Point 5: Bed level change [m] —
 Point 6: Bed level change [m] —

(b)

Turbine 1 at 73.8965, 15.414

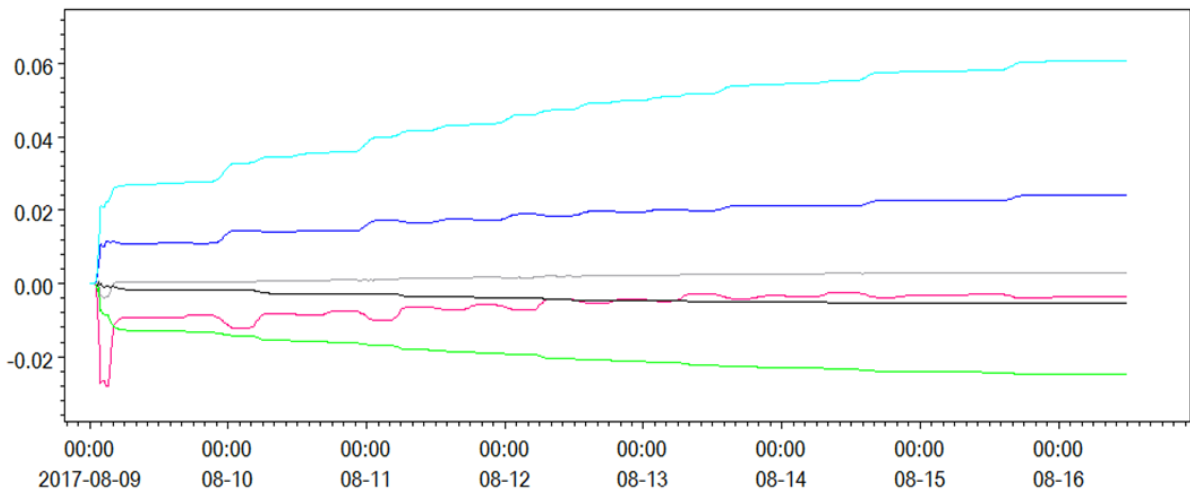


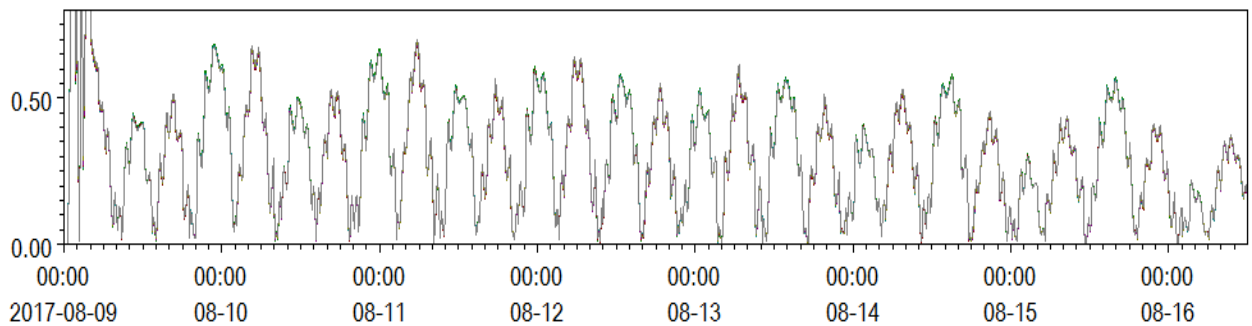
Figure 4.12 Variation of current speeds (a) and bed level changes (b) around T1

Table 4.3 Data extraction locations for T2 at 73.8970, 15.414

73.8968	15.414	Point 1
73.8969	15.414	Point 2
73.8970	15.414	Point 3
73.8971	15.414	Point 4
73.8972	15.414	Point 5
73.8973	15.414	Point 6

Point 1: Current speed [m/s] ———
 Point 2: Current speed [m/s] ———
 Point 3: Current speed [m/s] ———
 Point 4: Current speed [m/s] ———
 Point 5: Current speed [m/s] ———
 Point 6: Current speed [m/s] ———

(a)



Point 1: Bed level change [m] ———
 Point 2: Bed level change [m] ———
 Point 3: Bed level change [m] ———
 Point 4: Bed level change [m] ———
 Point 5: Bed level change [m] ———
 Point 6: Bed level change [m] ———

(b)

Turbine 2 at 73.8970, 15.414

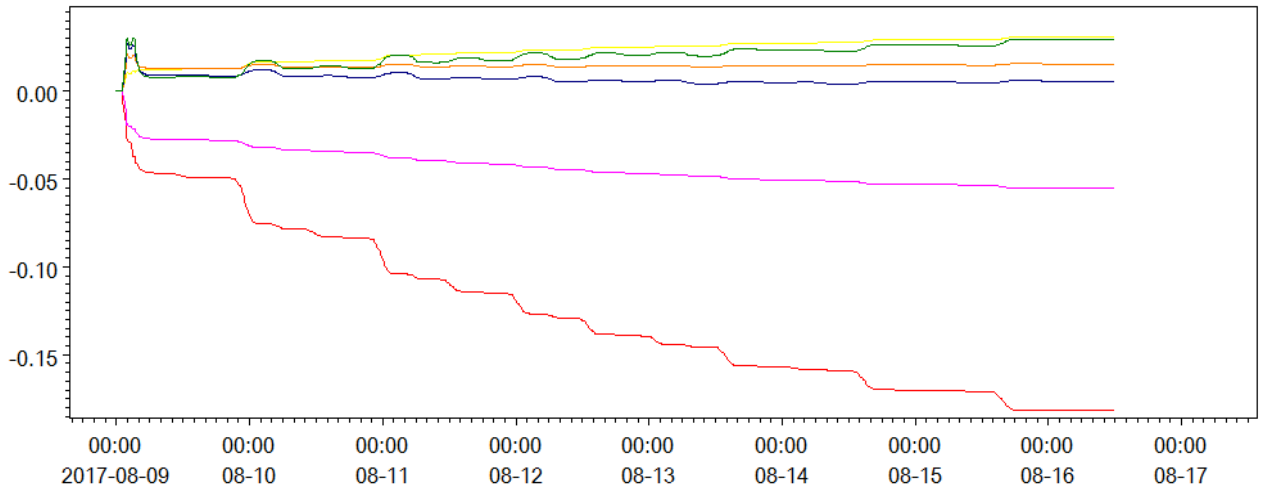


Figure 4.13 Variation of current speeds (a) and bed level changes (b) around T2

Table 4.4 Data extraction locations for T3 at 73.8975, 15.414.

73.8973	15.414	Point 1
73.8974	15.414	Point 2
73.8975	15.414	Point 3
73.8976	15.414	Point 4
73.8977	15.414	Point 5
73.8978	15.414	Point 6

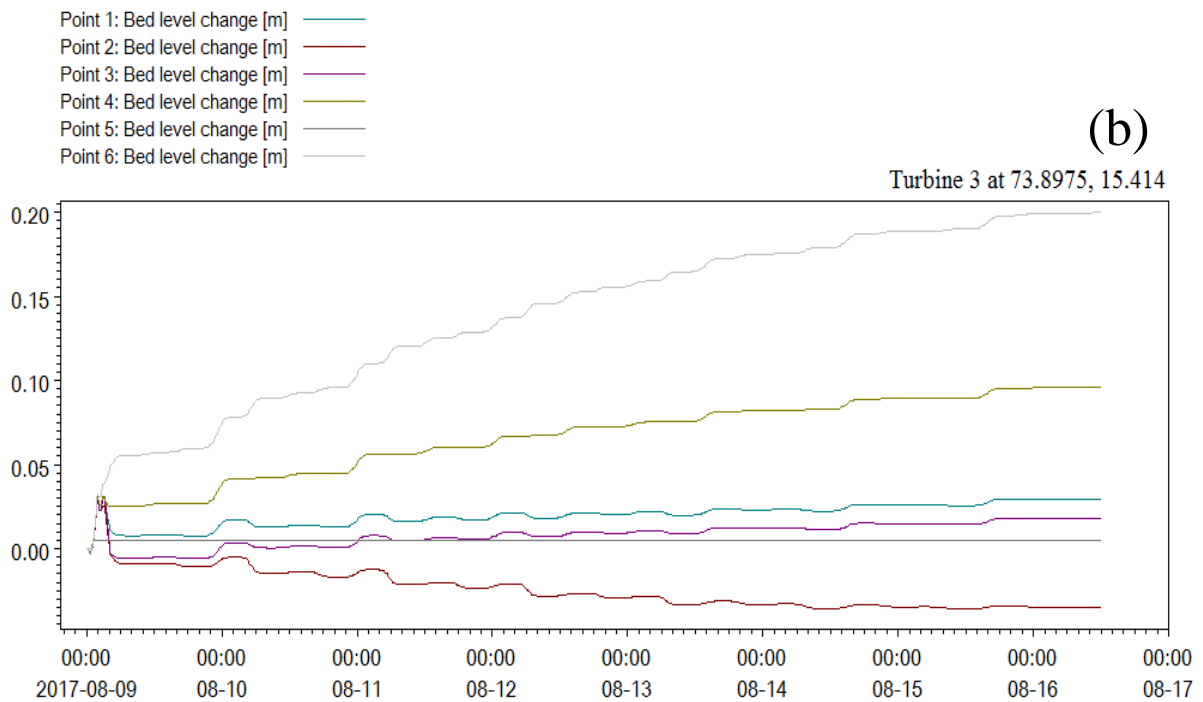
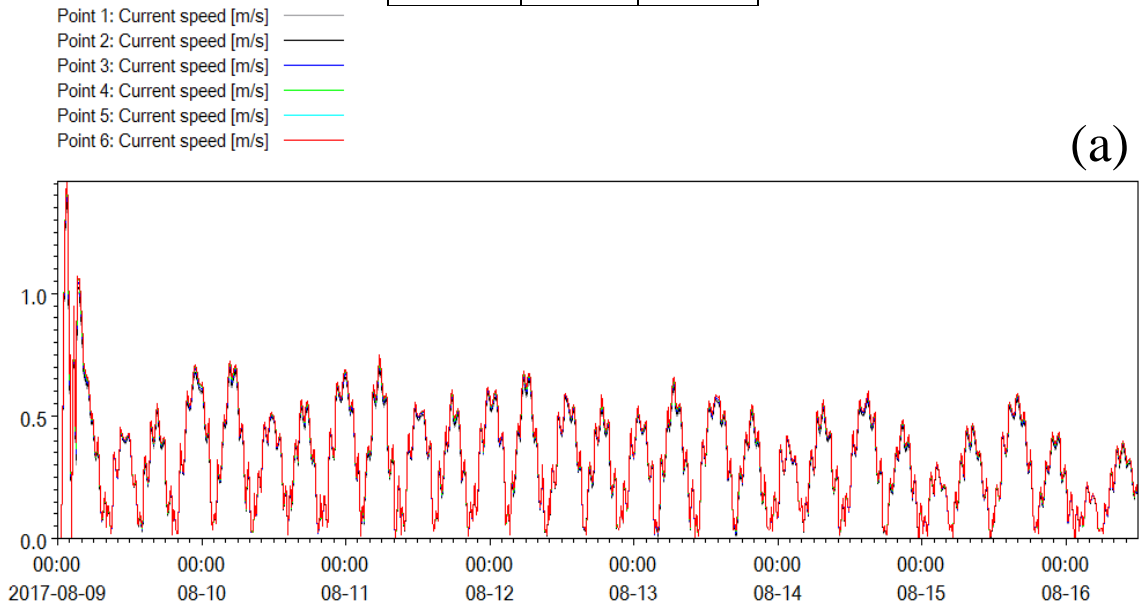


Figure 4.14 Variation of current speeds (a) and bed level changes (b) around T3

Table 4.5 Bed level changes observed at T1, T2 and T3

T1	Erosion	Accretion	T2	Erosion	Accretion	T3	Erosion	Accretion
1	√	-	1	√	-	1	-	-
2	-	-	2	√	-	2	√	-
3	√	-	3	-	√	3	-	-
4	-	√	4	-	-	4	-	√
5	√	-	5	-	-	5	-	-
6	-	√	6	-	-	6	-	√

iv. Domain with an array of turbines lined perpendicular to the flow

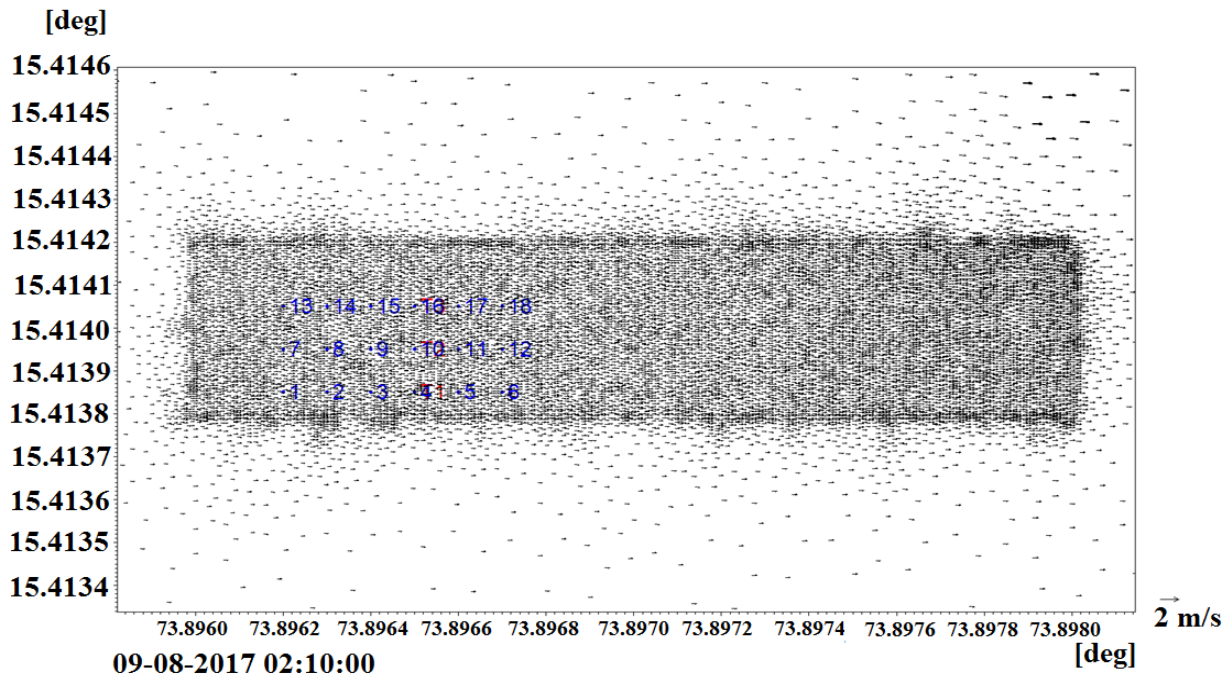


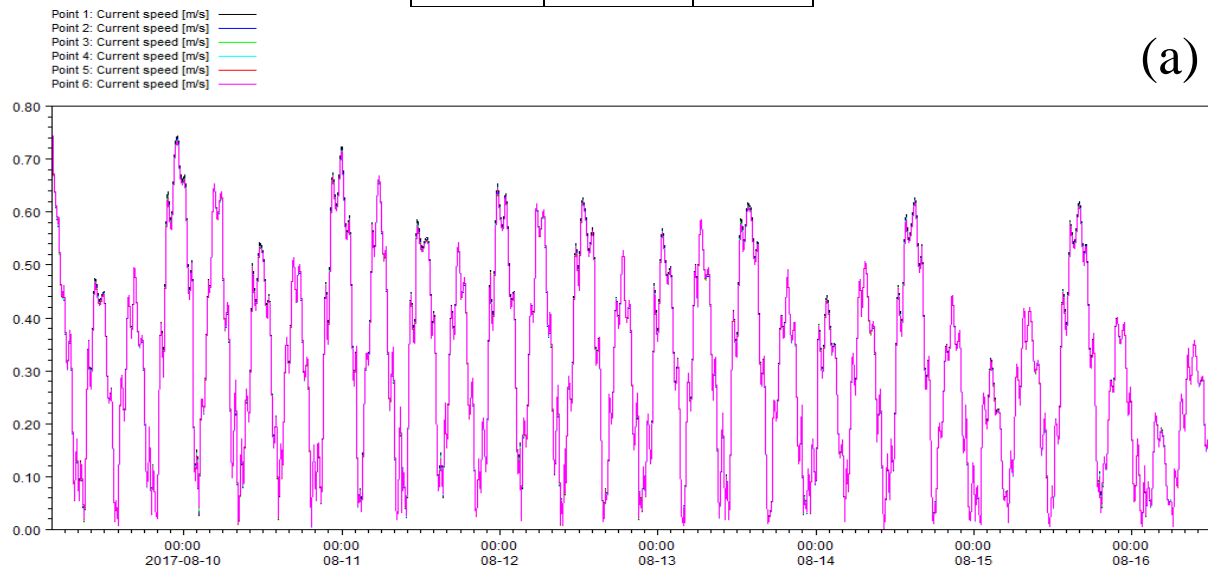
Figure 4.15: Turbines placed perpendicular to the flow

As shown in Figure 4.15, the turbines are collinearly placed such that they are lined perpendicular to the flow of water. Points T1 (point 4), T2 (point 10) and T3 (point 16) show the location of turbines and the labels 1 to 18 show the locations of tidal current and bed level change data extraction. For the turbine T1, the current speeds and bed level changes are monitored at the points 1, 2, 3, 4, 5 and 6 where, point 4 is the location of the turbine T1. For the turbine T2, the current speeds and bed level changes are monitored at the points 7, 8, 9, 10,

11 and 12 where, point 10 is the location of turbine T2. For the turbine T3, the current speeds and bed level changes are monitored at the points 13, 14, 15, 16, 17 and 18 where, point 16 is the location of turbine T3. Tables 4.6, 4.7 and 4.8 show the data extracted locations. The spacing between the turbines is considered as 10m as an experiment to observe the impact on each other. Figures 4.16 (a), 4.17 (a) and 4.18 (a) presents the comparison of current speeds from points 1 to 6 around T1, T2 and T3 respectively. It can be observed that there is no change in the current speeds at these points. Table 4.9 presents the pattern of bed level change around the turbines T1, T2 and T3.

Table 4.6 Data extraction locations for T1 at 73.8965, 15.41385.

73.8962	15.41385	Point 1
73.8963	15.41385	Point 2
73.8964	15.41385	Point 3
73.8965	15.41385	Point 4
73.8966	15.41385	Point 5
73.8967	15.41385	Point 6



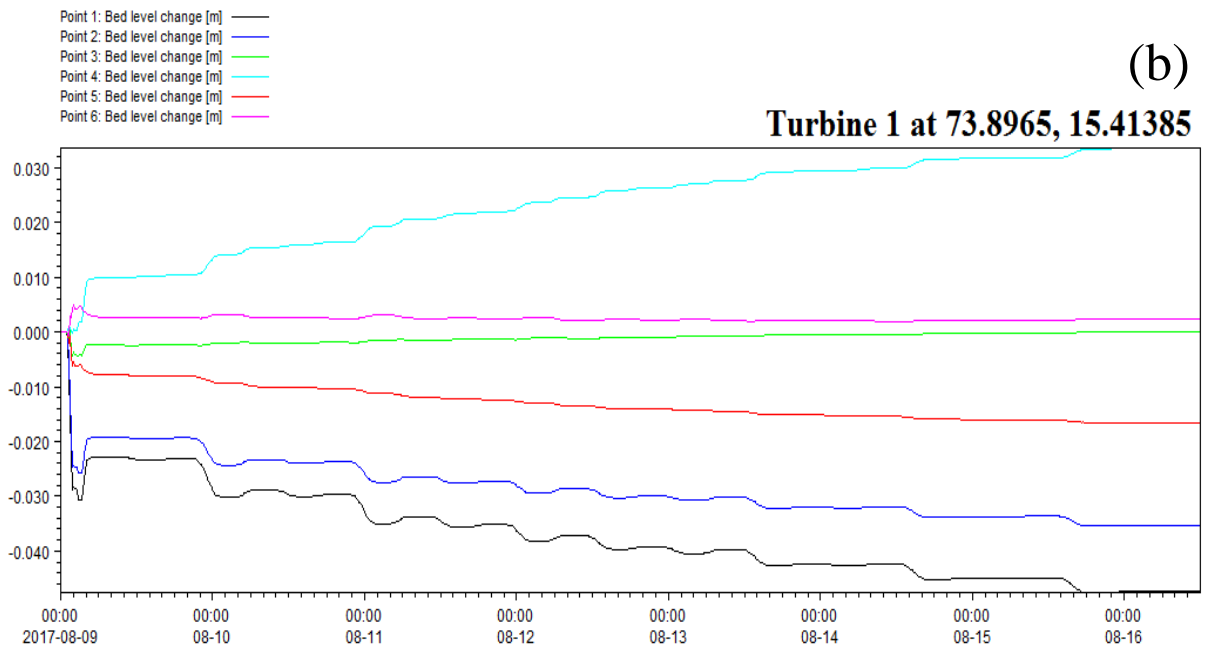


Figure 4.16 Variation of current speeds (a) and bed level changes (b) around T1

Table 4.7 Data extraction locations for T2 at 73.8965, 15.41395.

73.8962	15.41395	Point 1
73.8963	15.41395	Point 2
73.8964	15.41395	Point 3
73.8965	15.41395	Point 4
73.8966	15.41395	Point 5
73.8967	15.41395	Point 6

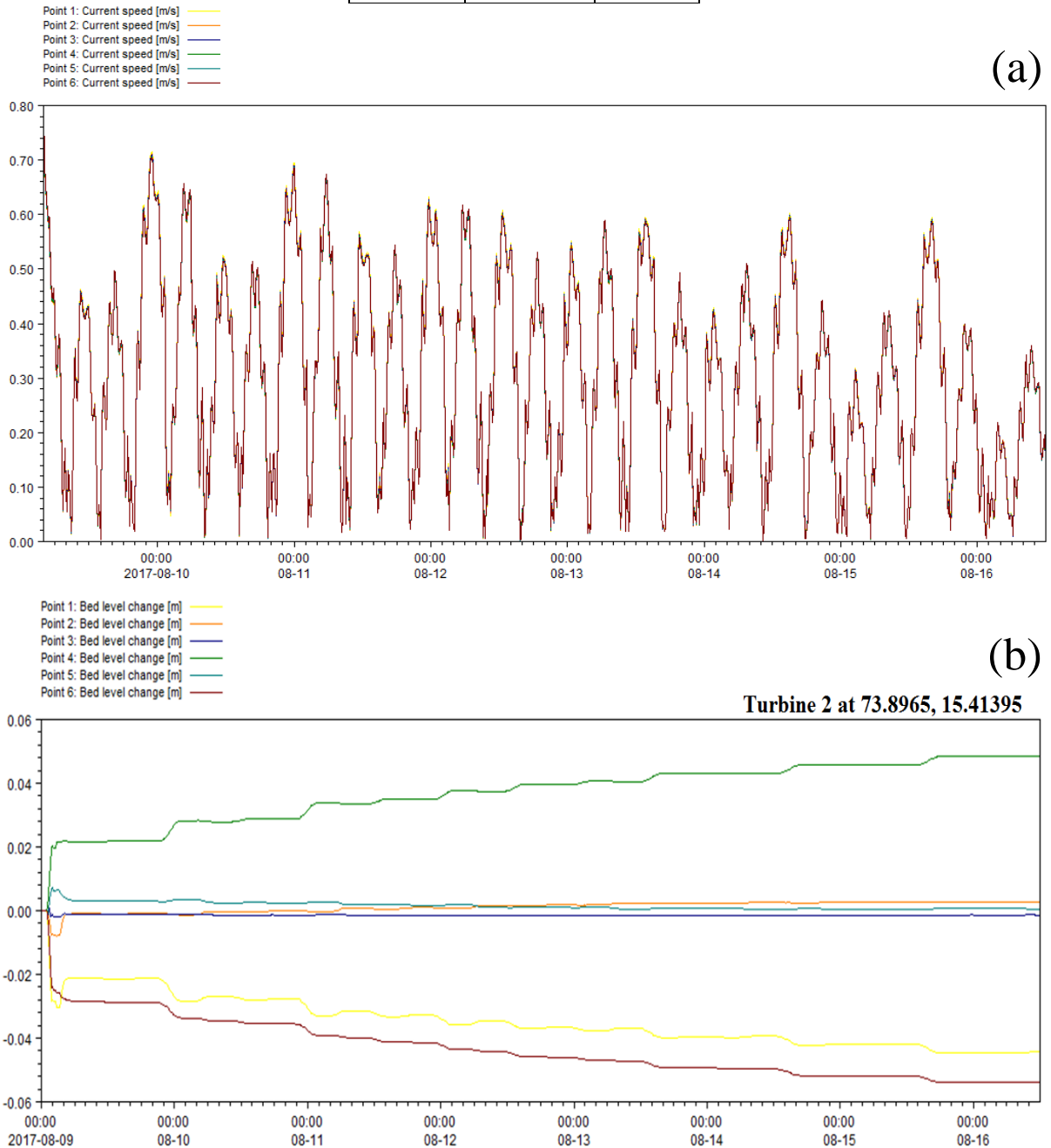


Figure 4.17 Variation of current speeds (a) and bed level changes (b) around T2

Table 4.8 Data extraction locations for T3 at 73.8965, 15.41405.

73.8962	15.41405	Point 1
73.8963	15.41405	Point 2
73.8964	15.41405	Point 3
73.8965	15.41405	Point 4
73.8966	15.41405	Point 5
73.8967	15.41405	Point 6

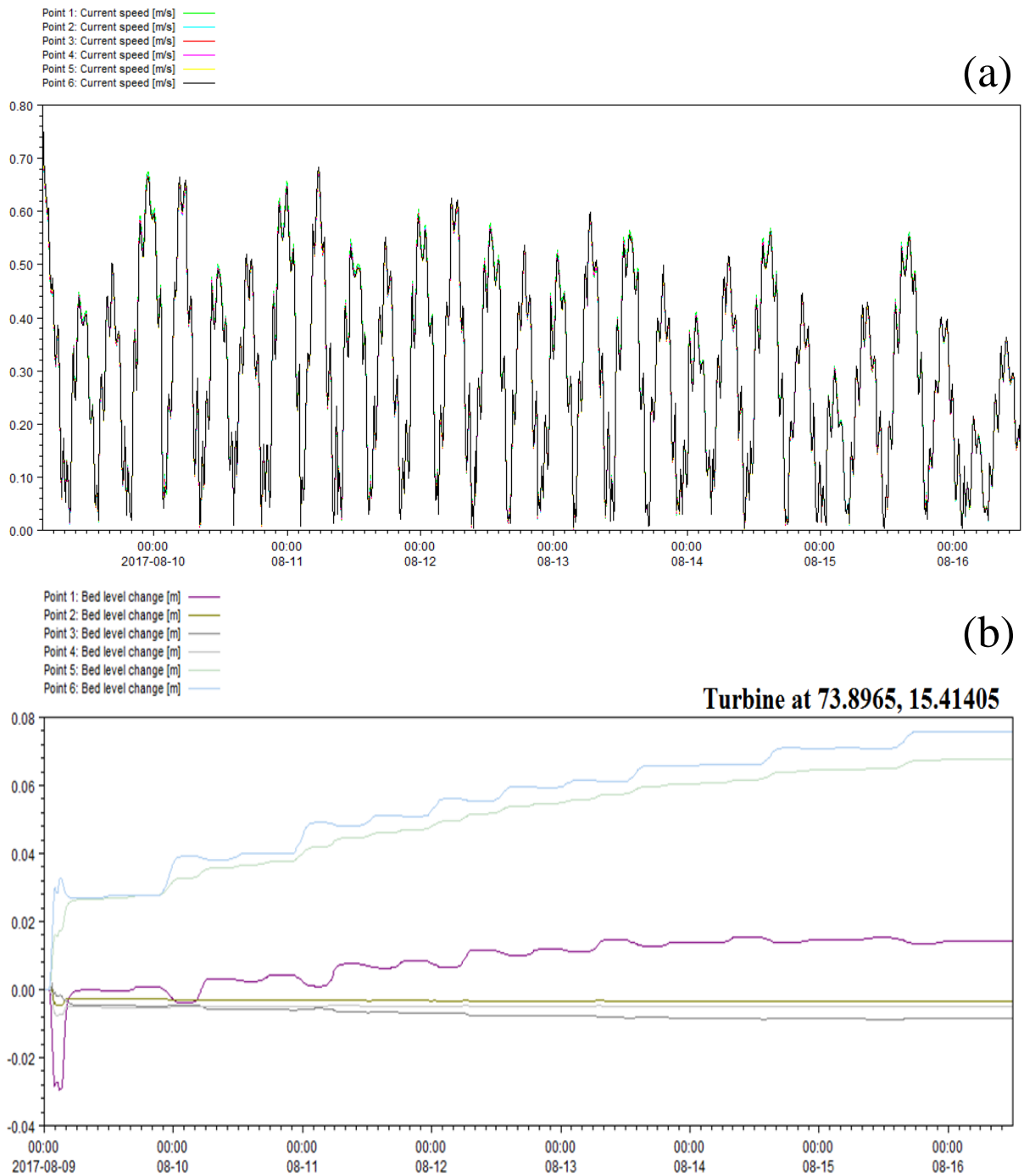


Figure 4.18 Variation of current speeds (a) and bed level changes (b) around T3

Table 4.9 Bed level changes observed at T1, T2 and T3

T1	Erosion	Accretion	T2	Erosion	Accretion	T3	Erosion	Accretion
1	√	-	1	√	-	1	-	√
2	√	-	2	-	-	2	-	-
3	-	-	3	-	-	3	-	-
4	-	√	4	-	√	4	-	-
5	√	-	5	-	-	5	-	√
6	-	-	6	√	-	6	-	√

v. Domain with NO turbines and decreased water depth at Zuari 3 to observe the improvement in flow velocities.

Bathymetry of the model domain was altered at the turbine location at Zuari 3 where a finer resolution of the mesh is considered. The water depth at the location is shallowed by 10 per cent and the bathymetry is interpolated to re-simulate the base case with the modified domain. The currents are extracted at points mentioned in table 4.1. By reducing the water depth, the flow speeds are observed to decrease and this is not favourable for energy extraction. However, other problems like navigation, erosion, depth required to place the turbines, etc. have to be addressed if the channel cross-sections are altered without proper preliminary survey.

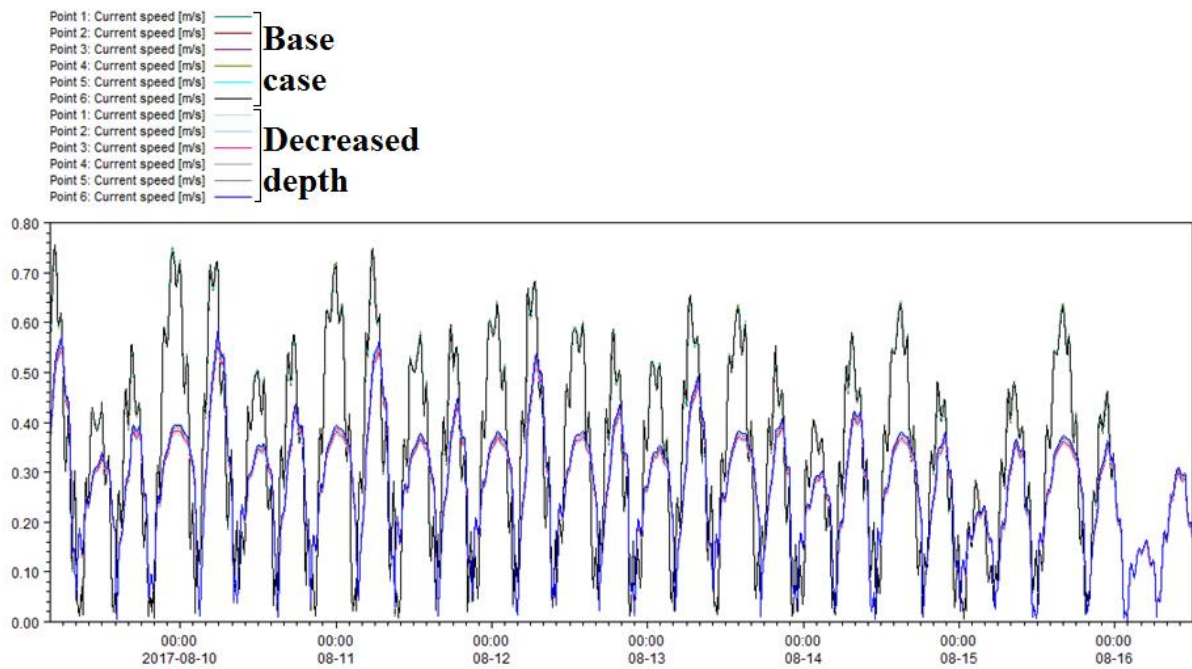


Figure 4.19: Comparison of current speeds for the base case and with a decrease in water depth by 10 percent

4.7 Conclusions

- A 2D hydrodynamic model MIKE21 is set up for the Zuari River (Goa, India) to examine the hydrodynamic and morphodynamic patterns pertinent to tidal energy extraction. A coupled model has been used to study the effects of tidal turbines that use the tidal stream energy on morphodynamics.
- An attempt has been made to reproduce the complex tidal current environment in the Zuari River. Five typical cases are considered where the simulations are carried for different locations of the tidal turbine. Total energy generated by 0.5m turbine is estimated to be 118kW in a year. Whereas the 1m turbine increased energy production to 470kW.
- The total energy estimates for case iii and case iv considering 0.4 m/s threshold for current speeds is approximated to 417.5kW and 409.35kW respectively.
- The morphodynamics is monitored and the sea bed morphology of Zuari River seen unstable to hydrodynamics during the simulation period.

The results of the coupled model proved that the location chosen for tidal energy extraction lies in an area that is highly sensitive sediment deposits. Hence, it becomes important to consider further investigation on the impacts of tidal energy extraction on the hydrodynamics and the morphodynamics of this area.

CHAPTER 5

TO ESTABLISH POTENTIAL SITES FOR TIDAL LAGOONS ALONG THE INDIAN COAST AND ITS INFLUENCE ON HYDRODYNAMICS

5.1 Introduction

Tidal energy is being majorly investigated and explored across the globe because of its immense advantages. Tidal energy extraction is well known for low maintenance costs, having a less environmental impact with little or no carbon emissions and is non-depleting. Tidal energy extraction takes place in various means and the method of extraction is insitu. The most conventional method of tidal energy extraction is the barrage method where a barrier is built across the channel and the energy is extracted by the potential energy of the stored water. In the recent past, tidal stream energy extraction is being explored at a rapid rate because of the advantage that the installation is easier and maintenance costs are lesser in comparison with the conventional barrage method. Another conceptual method is the “tidal pool or tidal lagoon method” where a pool of water is captured during the flooding phase in a tidal cycle and provisionally stored to release and extract the energy during the ebb phase.

Low head or low flow turbines are generally recommended for energy extraction using this method. The energy extraction from the tidal pools will alter the tides, tidal currents and the hydrodynamic parameters in the vicinity of the lagoon and the impacts may be reflected throughout the basin. The intensity of the impact on these parameters depends on the extent of the tidal pool established, its locality and the method adopted for energy extraction. These studies on the establishment and impacts have not been previously investigated along the Indian coastline.

This chapter contains a conceptual study on establishing a tidal lagoon along the Indian coast and conduct numerical modelling studies to understand the potential changes in the hydrodynamics due to the presence of tidal lagoon. A depth-averaged 2D hydrodynamic model is used for the simulation. The changes that will be reflected due to change in the size of the tidal pool, entrance conditions and mode of operation are comprehensively examined. The novelty of this study will help in providing the basic idea on the site selection, working, mode of operation and the effects on the local hydrodynamics due to the energy extraction from tidal pools.

5.2 Tides along the Indian coastline

Tides in India are mixed and are predominantly semidiurnal. The tidal range slightly increases from south to north. Fig. 5.1 shows the observed tides along the Indian coast. At Gujarat, the ranges are of the order of 5m at Okha port and increase to 6.5m towards the Gulf of Khambhat. At Mumbai, maximum ranges in tidal elevations are of about 5m. The tidal range decreases southward and reaches up to 2m at Marmagao. The tidal ranges are low in the south Indian coast. From Madras onwards the tidal range increases gradually towards the north, recording values higher than 5m at Haldia and Diamond Harbour in the Hooghly estuary.

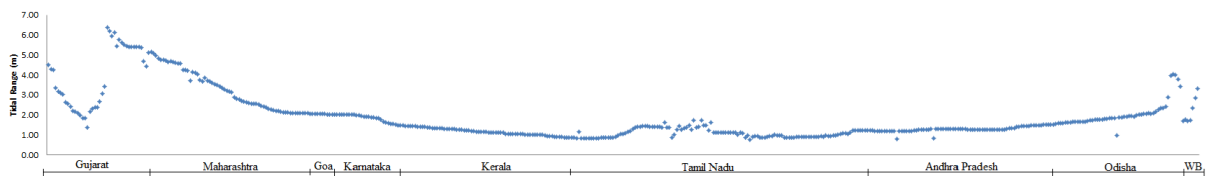


Figure 5.1: Variation of tidal range along the Indian coast

5.3 Construction of tidal lagoons

Tidal lagoon can be constructed in a number of ways. The construction of the tidal power lagoon depends on the priority and importance of the energy extraction. The shape of the tidal pool can be circular or elliptical. The location of the tidal pool is ideal where the tides are maximum.

- i. The simplest way to construct a tidal pool is by using the shoreline or naturally formed headlands. Partial construction can be made connecting the shoreline or headlands to form a circular/elliptical shaped pool.
- ii. A completely circular/elliptical pool can be constructed such that the opening (serves as inlet and outlet) of the pool to capture maximum water.
- iii. An offshore pool.

5.4 Site selection

Some preliminary standards are given by Couch and Bryden (2006) to identify sites that are suitable for the development of tidal energy extraction. The most important variables generally considered are:

1. *Location of rock/headland:* A tidal lagoon can be constructed either on an existing natural rock/headland or completely by artificial means. It can either be constructed nearshore/adjacent to the coast or in the offshore region of the tidal reservoir where conditions are feasible. The location should aid to capture large water mass.

2. *Presence of navigation channels and fishing harbours:* Inland navigation channels are the means of transport to many fishermen and also for local tourism. It is the livelihood for many fishermen and population residing in coastal areas. It should be preferred that the location is away from navigation channels and no fishing activity takes place.
3. *Location of beaches:* The establishment of tidal pools should not cause any interference to the existing beaches, nor they should lose accessibility because of the establishment of the tidal pools.
4. *The local water depth:* The technology that is currently available for the extraction of tidal energy is limited to shallow water depths. The turbines should preferably be installed at the water depths of about 25-45 meters.
5. *The location of the nearest exploitable grid connection:* For an immature industry, the economics of tidal energy extraction require easy access to a nearby grid connection with spare capacity; otherwise the capital cost cannot be viably recouped across the life of the project.
6. *An energetic and persistent resource:* Large mean spring and neap tide velocities are highly desirable. Some sites have the added advantage of minimizing the low-velocity periods of the tidal cycle as the local dynamics ensure that the tidal flow reverses through the slack period at an accelerated rate. The sites that the developers are interested to extract energy tend to have peak spring tidal velocities greater than or equal to 1.5 m/s.

If these six primary criteria are met, a site can be considered to have the potential for tidal energy extraction using tidal pools.

5.5 Identification of locations for tidal pools

Based on the criterion mentioned in the above section, the locations feasible for the construction of tidal pools are proposed. Two locations presented in Figure 5.2, Figure 5.3 and mentioned in Table 5.1 are chosen to conduct a morphodynamic study based on the availability of the bathymetry and tide data for numerical simulation.

Table 5.1: Locations of tidal pools chosen for assessment and potential energy estimation

Location ID	Latitude (°N)	Longitude (°E)	Basin area (m²)	Tidal range (m)	Tidal Prism (m³)	Energy generation potential/time in 1 day (MW)
Jaigad 1	17°24'48.50"	73°10'43.96"	4343561	2.7	11727615	3.69
Jaigad 2	17°16'38.18"	73°15'14.33"	1526679	2.7	4122033	1.3

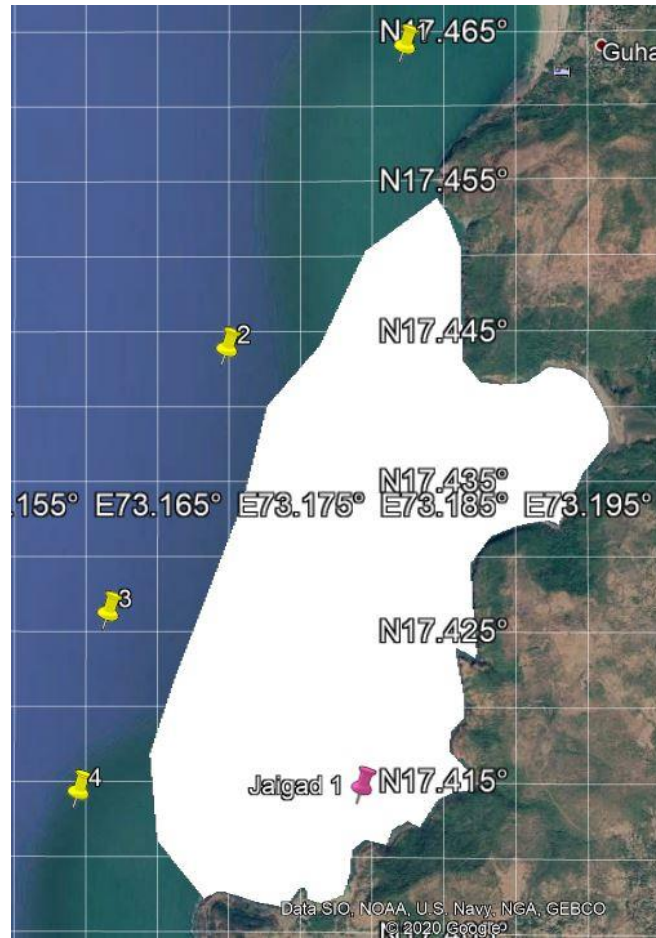


Figure 5.2: Tidal pools at Jaigad 1

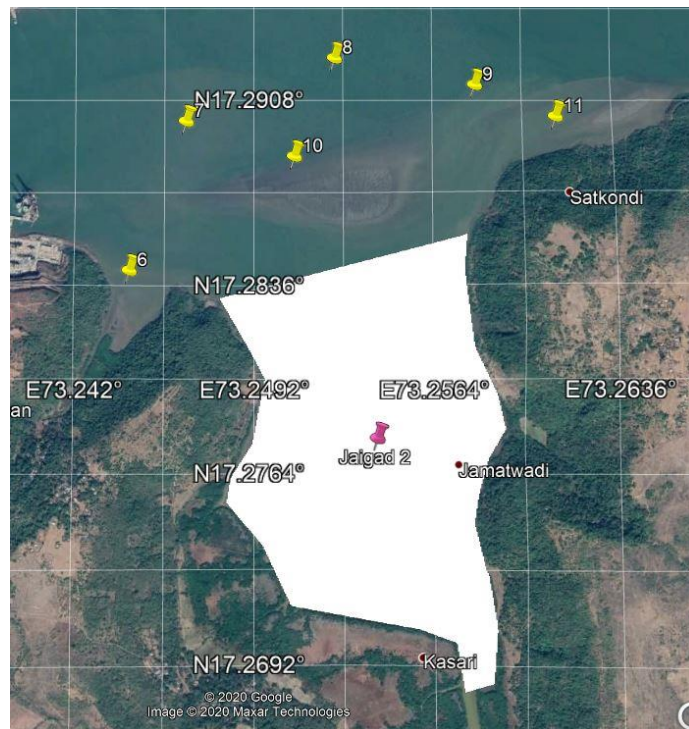


Figure 5.3: Tidal pools at Jaigad 2

5.6 Description of the model domain

The domain considered for this study is in Maharashtra state on the west coast of India located at Jaigad between the coordinates 73E, 17.18N and 73.30E, 17.66N. The domain consists of two tidal pools considered for energy estimation and morphology change.

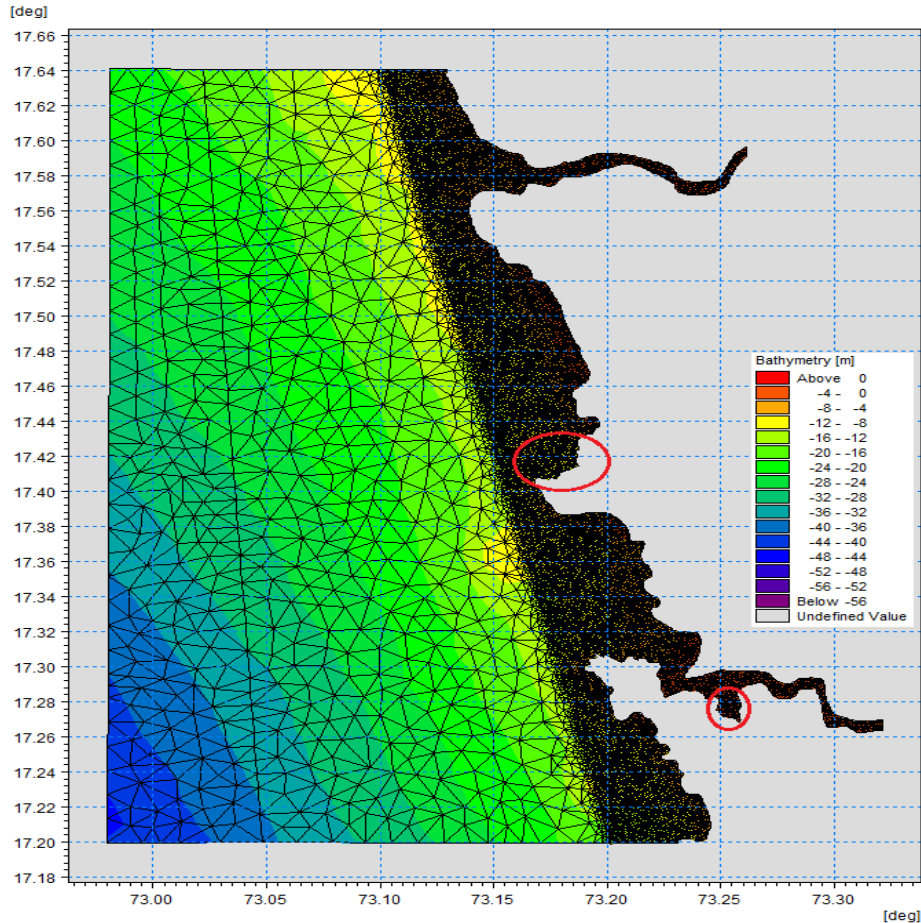


Figure 5.4: Model domain considered for the study

MIKE21 flexible mesh hydrodynamic model coupled with sand transport module is used to study the morphodynamics at Jaigad due to the construction of tidal pools at locations mentioned in Table 5.1. The consideration of the same in the model domain is presented in Figure 5.4. The simulation is carried out for 20 days with the results stored every 10 minutes. The domain as shown in Figure 5.5 and Figure 5.6 was forced with tides at north, west and south are taken as input from the global tide toolbox of MIKE21, bathymetry is considered from hydrographic charts published by Indian Naval Hydrographic Office, Dehradun.

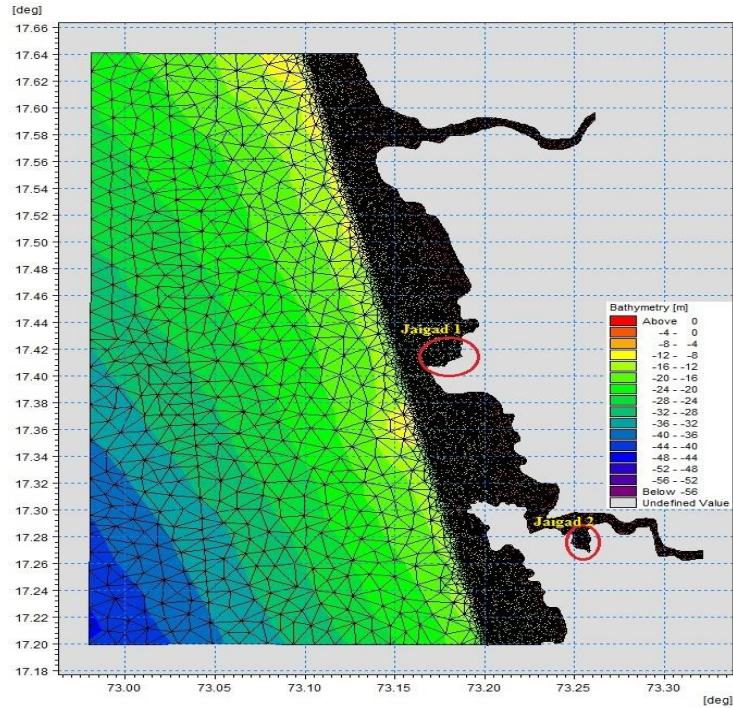


Figure 5.5: Simulation for base case – without tidal pool at Jaigad1 and Jaigad 2

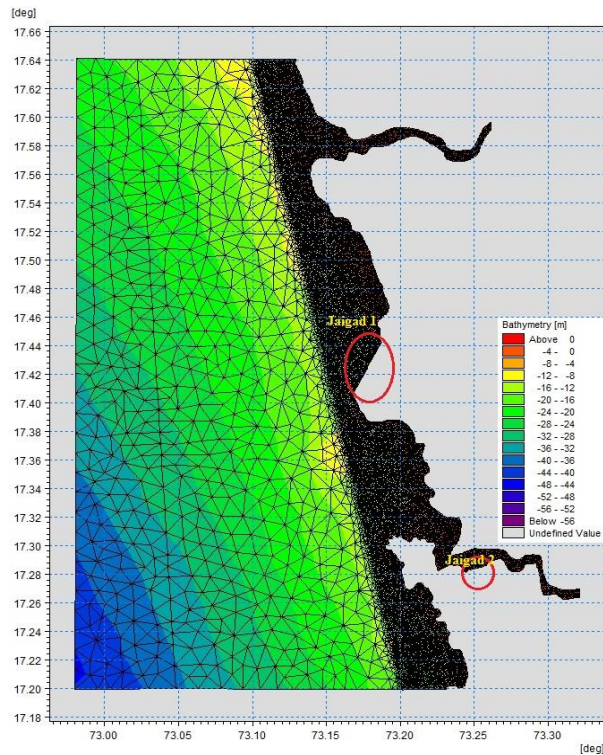


Figure 5.6: Simulation by considering tidal pool at Jaigad 1 and Jaigad 2

Current speeds are extracted at 11 locations as shown in Figure 5.7 around the tidal pools to observe the effect on the current speeds and morphodynamics due to the construction of tidal barrage.

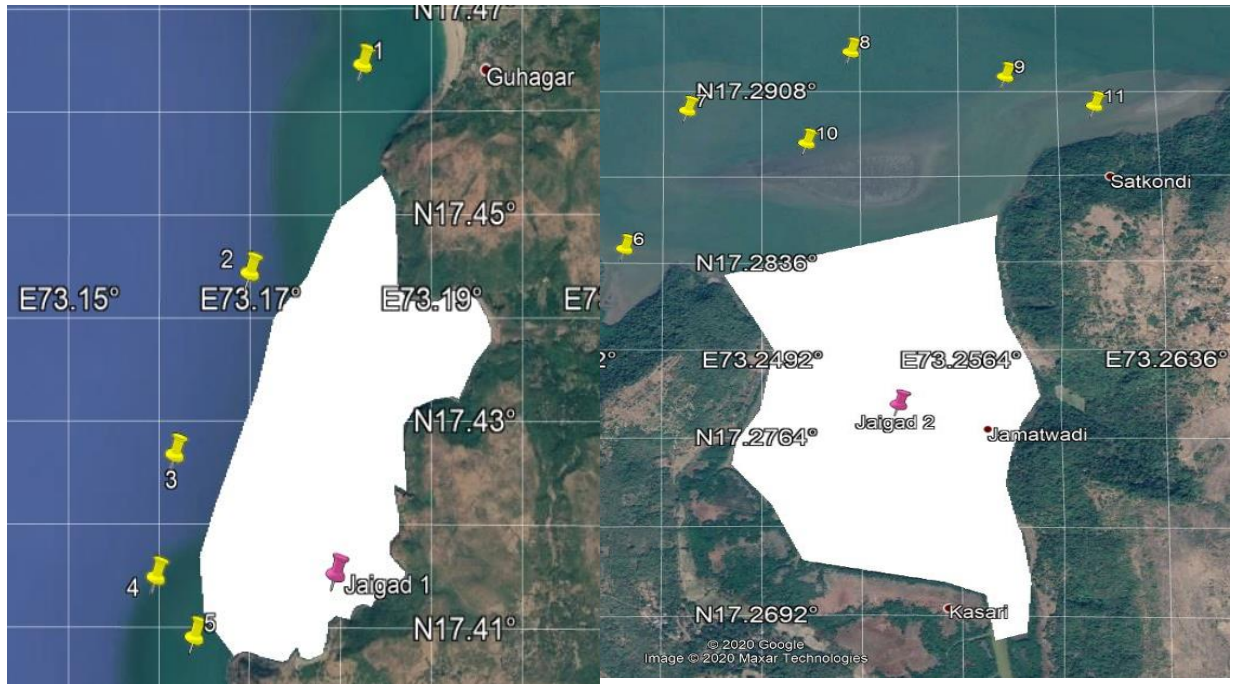


Figure 5.7: Locations of current speed extraction (Points 1 to 11)

Figures 5.8 and 5.9 show the comparison of current speeds before and after the construction of the tidal pools at 11 points near Jaigad 1 and Jaigad 2 respectively. At Jaigad 1, maximum currents are observed at point 5 with a peak flow of 0.34 m/s. At Jaigad 2, maximum currents are observed at point 5 with a peak flow of 0.44 m/s. Figure 10 shows the percentage change in current speeds at these locations. It is observed from Figure 10 that at Jaigad 1, the percentage change in current speeds before and after the construction of the tidal pool is maximum at point 5. At Jaigad 2, the percentage change in current speeds at points 6, 7 are maximum. These locations can further be considered for assessment and can be used as the entrance/exit points to tidal pools which can aid maximum flow.

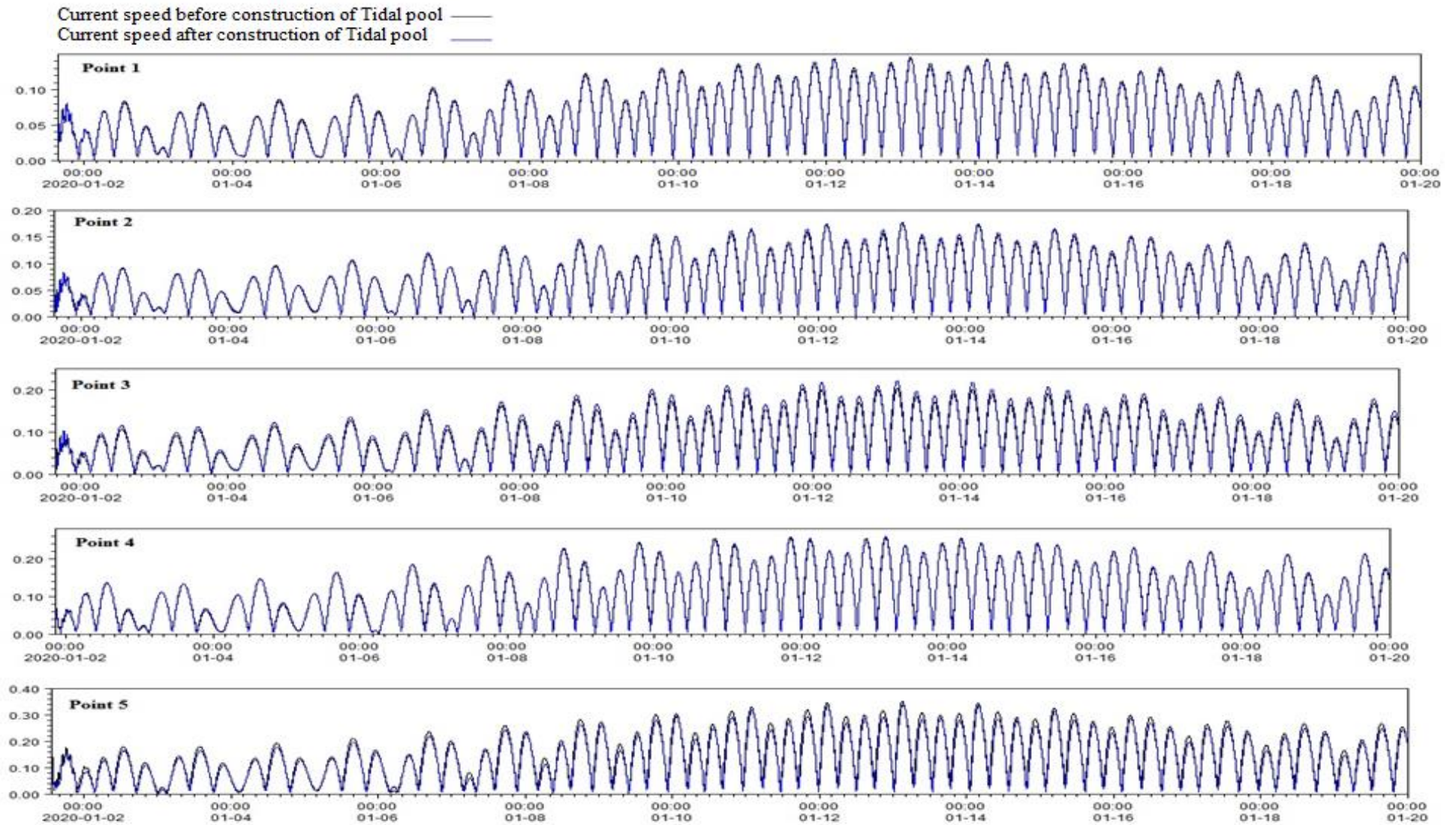


Figure 5.8: Current speeds comparison before and after construction of the tidal pool at Jaigad 1

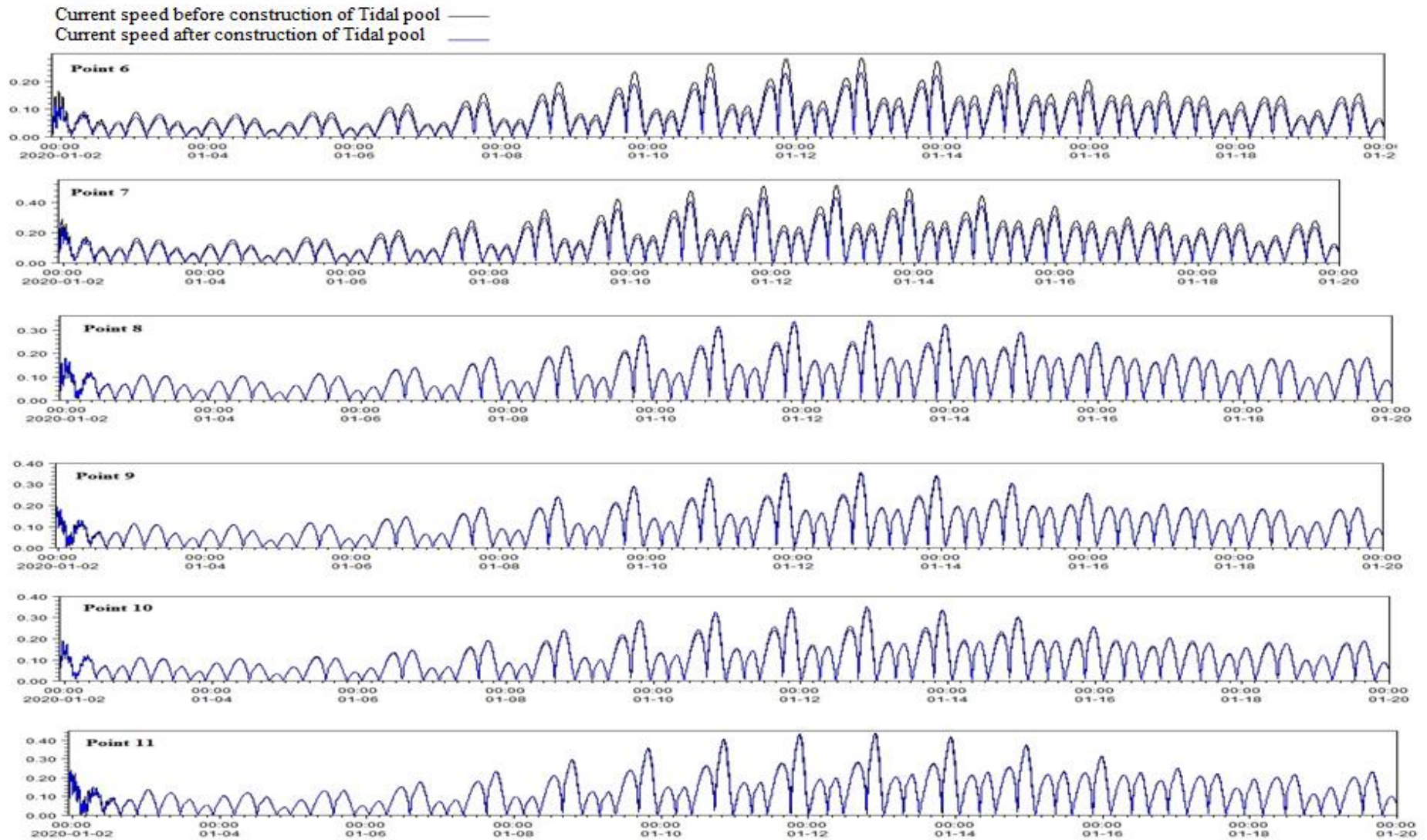


Figure 5.9: Current speeds comparison before and after construction of the tidal pool at Jaigad 2

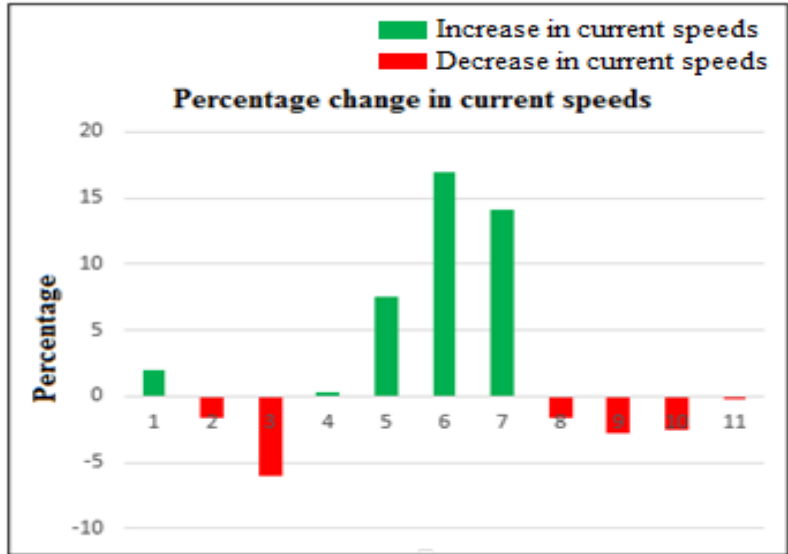
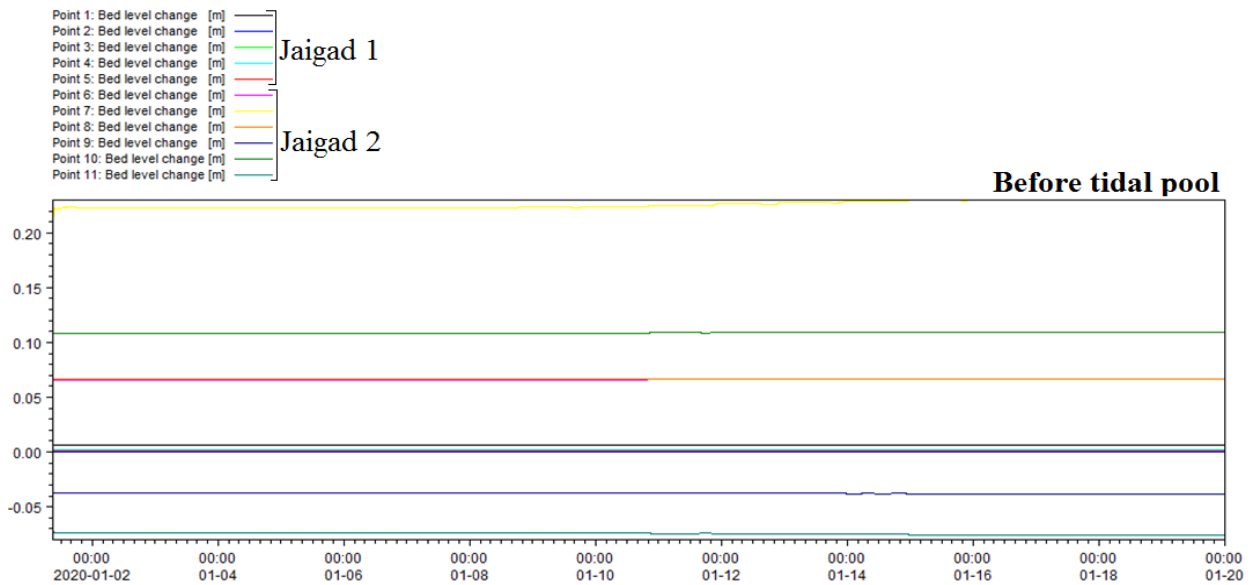


Figure 5.10: Percentage change in current speeds

5.7 Morphodynamic study at the tidal pool

MIKE21 hydrodynamic model coupled with sediment transport module is used to analyze the morphodynamics at Jaigad 1 and Jaigad 2. Results of morphodynamic study for 20 days are presented in figure 5.11. The bed level changes observed at Jaigad 1 (left) and Jaigad 2 (right) in figure 5.11 prove less sensitive to hydrodynamics. Bed level changes observed unaffected due to the construction of tidal barrage.



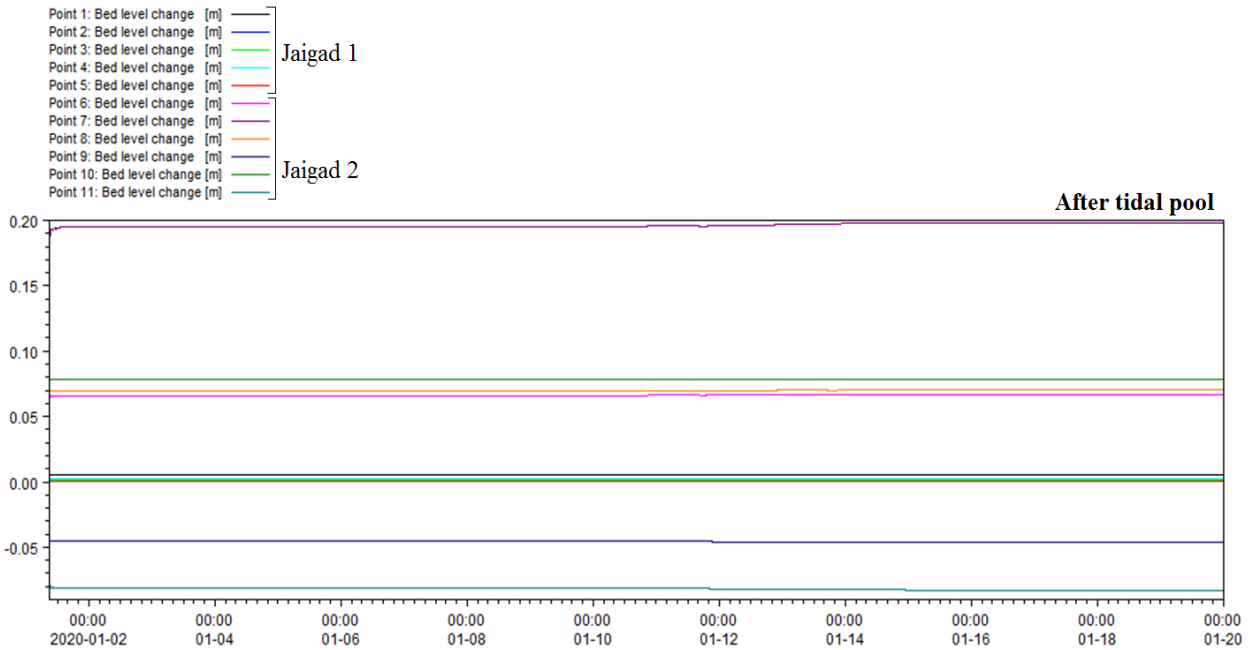


Figure 5.11: Bed level changes at Jaigad 1 and Jaigad 2 before and after construction at the tidal pool

5.8 Summary and Conclusions

- The concept of tidal pools is explored and two locations are chosen for the assessment of tidal energy form tidal energy.
- Morphodynamics are studied to look at the impact of the extraction of the tidal energy from tidal pools.
- Jaigad 1 and Jaigad 2 in Maharashtra are chosen for the study. Tidal pools are created using the naturally available area a barrage was constructed to close the pool that allows to and fro movement of water.
- Current speeds at eleven locations are extracted to locate the entrance for the barrages to achieve maximum tidal prism. Point 5 at Jaigad-1, Points 6 and 7 at Jaigad-2 showed higher current speeds among the eleven locations after the construction of the tidal barrage. These locations can be considered as the entrances for the tidal pools.
- The theoretical energy is estimated to be 3.69MW and 1.3MW respectively. On theoretically achieving this energy potential, an analysis is carried out to study the bed level changes due to the construction of the barrage.
- The rate of bed level change observed during the simulation period does not reduce and hence it can be concluded that the morphology is unaffected due to the energy extraction

from tidal pools. These locations proved less sensitive to hydrodynamics and the bed level changes observed unaffected due to the construction of tidal barrage. However, study of bed level changes for longer duration helps to assess the sensitivity of the bed level changes in a better way.

CHAPTER 6

SUMMARY AND CONCLUSIONS

6.1 Summary

- The first objective mainly focuses on tidal energy resource availability and the energy that can be harnessed from tides along the coast of India. Two methods are considered viz. tidal barrage and tidal stream energy. Out of 471 tidal inlets identified in 9 maritime states along the Indian coast, 130 inlets are shortlisted considering a threshold of 2.53 Mm³ tidal prism and potential energy was estimated. Total potential energy estimate considering 130 inlets is 2254.906 MW. Further 107 inlets are shortlisted considering both tidal prism greater than 2.53Mm³ and inlet throat width greater than 63m and the corresponding potential energy is estimated as 2127.281 MW. The Kinetic energy estimated was 11.68kW, 5.60kW and 25.64kW at Chapora, Mandovi and Zuari respectively.
- The second objective intends to study the impact of tidal energy of local hydrodynamics. The turbines are placed at the locations where highest tidal currents are observed as presented in objective 1. Five cases are considered where the simulations are carried for different locations of the tidal turbine. Total energy generated by 0.5m diameter turbine is estimated to be 118kW in a year. Whereas the 1m diameter turbine increased the energy by 470kW. The total yearly estimates for 3 turbines in parallel and 3 turbines in tandem considering 0.4 m/s threshold for current speeds is approximated to 417.5kW and 409.35kW respectively. The morphodynamics are simulated and the sea bed morphology of Zuari creek was found to be unstable to hydrodynamics. The results of the coupled model proved that the location chosen for tidal energy extraction lie in area which is highly sensitive sediment deposits.
- In the third objective, tidal lagoons are established and the morphodynamics due the energy extraction are studied. A tidal lagoon can be constructed either on an existing natural rock/headland or completely by artificial means. It can either be constructed nearshore adjacent to the coast of in the tidal reservoir where conditions are feasible. Locations for the construction of tidal lagoons are identified along in Maharashtra (Jaigad 1 and Jaigad 2). The potential energy that can be extracted from the established tidal pools is estimated

to be 3.69MW and 1.3MW respectively. Results of morphodynamic study for 20 days are analyzed. The bed level changes observed at Jaigad 1 and Jaigad 2 prove less sensitive to hydrodynamics.

6.2 Conclusions

The following are the salient conclusions based on the studies carried out and reported in various chapters in this thesis.

- The potential locations to extract tidal energy from potential and kinetic energy concepts are identified along both the coasts of India.
- Out of the identified 471 tidal inlets, 107 inlets are chosen for the final assessment of potential energy based on the tidal prism and the entrance width criteria of 63m.
- A 2D hydrodynamically coupled model MIKE21 is used to examine the hydrodynamic and morphodynamic patterns relevant to tidal energy extraction. The complex tidal current environment in the Zuari creek was convincingly replicated.
- Eight points at 3 locations in Goa are studied for tidal stream energy potential and the energy estimated in these locations are 11.68 kW, 5.60 kW and 25.64 kW by considering a threshold current speed on 0.4 m/s. If the threshold speed is considered as 0.5 m/s or 0.7 m/s the total energy generation is observed to reduce by 37.78% and 64.53%. Five cases are considered for the simulation at selected locations in Goa, considering 0.5m and 1m diameter of turbines. Total energy generated by 0.5m turbine is estimated to be 118kW in a year. Whereas the 1m turbine increases energy production by 470kW.
- The morphodynamics is studied using sand transport module coupled with the hydrodynamic model. The results indicated that energy extraction caused morphodynamic changes at the location of energy extraction to a lesser extent.
- Tidal pools suitability along the Maharashtra and Goa coast is explored and locations along Jaigad coast are found suitable. Energy extraction from the tidal pools is estimated and the dynamics of the sediment deposits are studied due to the construction of tidal pools.
- The potential energy that can be extracted from the established tidal pools at two locations along Jaigad coast is estimated to be 3.69MW and 1.3MW respectively.

- Results of morphodynamic study for 20 days are analyzed. Bed level changes observed unaffected due to the construction of tidal barrage. The bed level changes observed at Jaigad 1 and Jaigad 2 prove less sensitive to hydrodynamics.

6.3 Scope for future work

- Tidal stream energy assessment can be carried out in all states of India. It is however, subject to availability of high resolution bathymetry data.
- Detailed assessment can be carried out at locations that showed high potential for energy extraction (potential energy and kinetic energy).
- Studies on low flow turbines are required to be carried out to suit the tidal conditions for the south Indian coast.
- 3D modelling studies can be carried out to study the location of the turbines, location of sluice gates, weir on the tidal barrage constructed for the purpose of tidal pools.
- Further, this study can be extended to a variety of energy extraction situations by varying the array configurations and turbine locations in the water column for which a 3D model would be appropriate to examine and calculate the possible variations to the present morphodynamic regime at the test location. Also, resulting morphodynamic changes could be effectively correlated with the current field to map notable relationships between altered currents and seabed change.

6.4 Limitations of the study

- The value of tidal range ‘h’ used in the computation of the potential energy is the mean tidal range considered during the simulation period. However, the average tide is not attained throughout the tidal cycle and the assessment done considering LWL and LLWL will give better results.
- The threshold of 63m considered for tidal energy extraction is assumed by considering the existing operating tidal power plants across the world. This threshold, however is site specific.
- The basin area is computed from the Google Earth® satellite imagery in 2016. The high and low water levels were not considered because of the unavailability of the satellite imagery at specific times. Computation of the basin area using high and low water levels will give more accurate values of tidal prism.

6.5 Contributions from the present study

- Assessment of tidal energy has been carried out. Both potential and kinetic energy have been assessed.
- Studies on the impact of tidal energy farm on local hydrodynamics and energy estimates are carried out.
- Tidal pools are established and the impact on hydrodynamics has been assessed.

REFERENCES

- Bahaj, A. S., Myers, L. E., Thomson, M. D., and Jorge, N. (2007). "Characterising the wake of horizontal axis marine current turbines." *7th Eur. Wave Tidal Energy Conf.*, (January).
- Batten, W. M. J., Bahaj, A. S., Molland, A. F., and Chaplin, J. R. (2007). "Experimentally validated numerical method for the hydrodynamic design of horizontal axis tidal turbines." *Ocean Eng.*, 34(7), 1013–1020.
- Behera, M. R., and Tkalich, P. (2014). "Assessment of Kinetic Tidal Energy Resources Using SELFE." *Int. J. Ocean Clim. Syst.*, 5(3), 141–149.
- Blunden, L. S., and Bahaj, A. S. (2006). "Initial evaluation of tidal stream energy resources at Portland Bill, UK." *Renew. Energy*, 31(2), 121–132.
- Bonar, P. A. J., Adcock, T. A. A., Venugopal, V., and Borthwick, A. G. L. (2018). "Performance of non-uniform tidal turbine arrays in uniform flow." *J. Ocean Eng. Mar. Energy*, 4(3), 231–241.
- Bonar, P. A. J., Chen, L., Schnabl, A. M., Venugopal, V., Borthwick, A. G. L., and Adcock, T. A. A. (2019). "On the arrangement of tidal turbines in rough and oscillatory channel flow." *J. Fluid Mech.*, 865, 790–810.
- Bryden, I. G., and Couch, S. J. (2007). "How much energy can be extracted from moving water with a free surface: A question of importance in the field of tidal current energy?" *Renew. Energy*, 32(11), 1961–1966.
- Bryden, I., and Melville, G. T. (2004). "Choosing and evaluating sites for tidal current development." *Proc. Inst. Mech. Eng. Part A J. Power Energy*, 218(8), 567–577.
- Callaghan, J. (2006). *Future marine energy: results of the marine energy challenge: cost competitiveness and growth of wave and tidal stream energy.*
- Carballo, R., Iglesias, G., and Castro, A. (2009). "Numerical model evaluation of tidal stream energy resources in the Ría de Muros (NW Spain)." *Renew. Energy*, 34(6), 1517–1524.
- Charlier R H (2007). *Renewable and Sustainable Energy Reviews* 11 2032–2057.
- Charlier R. H. and Finkl C. W. (2009). *Ocean Energy-Tide and Tidal power. Civ. Eng. New York, N.Y.*

- Chatzirodou, A., and Karunarathna, H. (2014). “Impacts of Tidal Energy Extraction on Sea Bed Morphology.” *Coast. Eng. Proc.*, 1(34), 33.
- Chiou, M. Da, Chien, H., Centurioni, L. R., and Kao, C. C. (2010). “On the simulation of shallow water tides in the vicinity of the Taiwan banks.” *Terr. Atmos. Ocean. Sci.*, 21(1), 45–69.
- Cornett, A., Cousineau, J., and Nistor, I. (2011). “Hydrodynamic Impacts due to Tidal Power Lagoons in the Upper Bay of Fundy , Canada.” *Eur. Wave Tidal Energy Conf. Southampton, UK*, Southampton, UK.
- Cornett, A., Durand, N., and Serrer, M. (2010). “3-D Modelling and Assessment of Tidal Current Resources in the Bay of Fundy , 3-D Modelling and Assessment of Tidal Current Resources in the Bay of Fundy , Canada.” *3rd Int. Conf. Ocean Energy, 6 October, Bilbao 3-D*, 1–6.
- Couch, S. J., and Bryden, I. (2006). “Tidal current energy extraction: Hydrodynamic resource characteristics.” *Proc. Inst. Mech. Eng. Part M J. Eng. Marit. Environ.*, 220(4), 185–194.
- Cousineau, J., Nistor, I., and Cornett, A. (2012). “Hydrodynamic impacts of tidal power lagoons in the bay of fundy.” *Proc. Coast. Eng. Conf.*
- DHI Software. (2012). “MIKE 21 & MIKE 3 FLOW MODEL FM, Mud Transport Module Scientific Documentation.” 46.
- Discusser, O., Andersen, M., Argyriadis, K., Butterfield, S., Fonseca, N., Kuroiwa, T., Boulluec, M. Le, Liao, S., and Turnock, S. (2006). “Ocean Wind and Wave Energy Utilization.” *16Th Int. Sh. Offshore Struct. Congr.*, 2(August), 253.
- Douglas, C. A., Harrison, G. P., and Chick, J. P. (2008). “Life cycle assessment of the Seagen marine current turbine.” *Proc. Inst. Mech. Eng. Part M J. Eng. Marit. Environ.*, 222(1), 1–12.
- Draycott, S., Payne, G. S., Steynor, J., Nambiar, A., Sellar, B., Davey, T., Noble, D. R., and Venugopal, V. (2019a). “Environmental & load data: 1:15 Scale tidal turbine subject to a variety of regular wave conditions.” *Data Br.*, 23, 103732.
- Draycott, S., Payne, G., Steynor, J., Nambiar, A., Sellar, B., and Venugopal, V. (2019b). “An experimental investigation into non-linear wave loading on horizontal axis tidal turbines.” *J. Fluids Struct.*, 84, 199–217.

Draycott, S., Sutherland, D., Steynor, J., Sellar, B., and Venugopal, V. (2017). “Re-creating waves in large currents for tidal energy applications.” *Energies*, 10(11).

Fairley, I., Masters, I., and Karunarathna, H. (2015). “The cumulative impact of tidal stream turbine arrays on sediment transport in the Pentland Firth.” *Renew. Energy*, 80, 755–769.

Falconer, R. A., Xia, J., Lin, B., and Ahmadian, R. (2009). “The Severn Barrage and other tidal energy options: Hydrodynamic and power output modeling.” *Sci. China, Ser. E Technol. Sci.*, 52(11), 3413–3424.

Fraenkel, P. L. (2002). “Power from marine currents.” *Proc. Inst. Mech. Eng. Part A J. Power Energy*, 216(1), 1–14.

Gorlov, A. M. (2003). “and Near-surface Turbulence. Heat and Momentum Fluxes at the Sea Surface. Heat Transport and Climate. Indian Ocean Equatorial Currents. Internal Waves. Island Wakes. Langmuir Circulation and Instability. Mesoscale Eddies. Open Ocean Convection. Pacific.” *Photogramm. Fernerkundung, Geoinf.*, 2955–2960.

Greenberg, D. A. (1979). “A Numerical Model Investigation of Tidal Phenomena in the Bay of Fundy and Gulf of Maine.” *Mar. Geod.*, 2(2), 161–187.

Hagerman, G., and Polagye, B. (2006). “Methodology for estimating tidal current energy resources and power production by tidal in-stream energy conversion (TISEC) devices.” *Electr. Power Res. Inst.*

Haverson, D., Bacon, J., Smith, H. C. M., Venugopal, V., and Xiao, Q. (2017). “Cumulative impact assessment of tidal stream energy extraction in the Irish Sea.” *Ocean Eng.*, 137, 417–428.

Haverson, D., Bacon, J., Smith, H. C. M., Venugopal, V., and Xiao, Q. (2018). “Modelling the hydrodynamic and morphological impacts of a tidal stream development in Ramsey Sound.” *Renew. Energy*, 126, 876–887.

Fairley, H. K. and A. C. (2017). “Modelling the Effects of Marine Energy Extraction on Non-Cohesive Sediment Transport and Morphological Change in the Pentland Firth and Orkney Waters.” *Scottish Mar. Freshw. Sci. Vol 8 No 7*, 8(7), 1–34.

Jaya Kumar Seelam, Vikas M, A. R. N. and S. R. (2015). “Classification of tidal inlets along the

Indian coast.” *Int. Symp. Indian Ocean CSIR-National Inst. Oceanogr. Goa, 30th Novemb. – 4th December.*

Jena, B. K., Sivakholundu, K. M., and Rajkumar, J. (2018). “A description of tidal propagation in Hooghly estuary using numerical and analytical solutions.” *Ocean Eng.*, 169(August), 38–48.

Karsten, R. H., Mcmillan, J. M., Lickley, M. J., and Haynes, R. D. (2008). “Assessment of tidal current energy in the Minas Passage , Bay of Fundy.” *Proc. IMechE Vol. 222 Part A J. Power Energy*, 493–508.

Karunarathna, H., Chatzirodou, A., and Reeve, D. E. (2017). “Computational modelling of hydrodynamics of a proposed tidal stream energy extraction site.” *Proc. Int. Offshore Polar Eng. Conf.*, 1307–1312.

Kumar, V. S., Dora, G. U., Philip, S., Pednekar, P., and Singh, J. (2011). “Variations in Tidal Constituents along the Nearshore Waters of Karnataka, West Coast of India.” *J. Coast. Res.*, 276(5), 824–829.

L. Sheela Nair, V. Sundar, N. P. K. (2010). “Numerical Model Studies on Coastal Processes in a Critically Eroding Sector of South West Coast of India.” *IXth Int. Conf. Hydro-Science Eng.*

Lalander, E., Thomassen, P., and Leijon, M. (2013). “Evaluation of a model for predicting the tidal velocity in fjord entrances.” *Energies*, 6(4), 2031–2051.

Lumborg, U., and Pejrup, M. (2005). “Modelling of cohesive sediment transport in a tidal lagoon - An annual budget.” *Mar. Geol.*, 218(1–4), 1–16.

MacKay. (2007). “Enhancing Electrical Supply by Pumped Storage in Tidal Lagoons.” <http://www.inference.phy.cam.ac.uk/mackay/Environment>, <<http://www.inference.phy.cam.ac.uk/mackay/Environment>>.

Masters, I., Williams, A., Croft, T. N., Togneri, M., Edmunds, M., Zangiabadi, E., Fairley, I., and Karunarathna, H. (2015). “A comparison of numerical modelling techniques for tidal stream turbine analysis.” *Energies*, 8(8), 7833–7853.

McPherson, B., Young, S., Modra, B., Couriel, E., You, B., Hanslow, D., Callaghan, D., Baldock, T., and Nielsen, P. (2013). “Penetration of Tides and Tidal Anomalies in New South Wales

Estuaries.” *Coasts and Ports*, (October 2016), 537–542.

Mendi, V. (2015). “Classification of tidal Inlets along the Indian coast.” National Institute of Technology Karnataka, Surathkal, India.

Muni Reddy, M. G., Sannasiraj, S. A., and Natarajan, R. (2007). “Numerical investigation on the dynamics of a vertical wall defenced by an offshore breakwater.” *Ocean Eng.*, 34(5–6), 790–798.

Murali, K., and Sundar, V. (2017). “Reassessment of tidal energy potential in India and a decision-making tool for tidal energy technology selection.” *Int. J. Ocean Clim. Syst.*, 8(2), 85–97.

Nicholls-Lee, R. F., and Turnock, S. R. (2008). *Tidal energy extraction: Renewable, sustainable and predictable. Sci. Prog.*

O’Doherty, T., O’Doherty, D. M., and Mason-Jones, A. (2017). “Tidal energy technology.” *Wave Tidal Energy*, (June), 105–150.

Pradhan, U. K., Mishra, P., Mohanty, P. K., Panda, U. S., and Ramanamurthy, M. V. (2020). “Modeling of tidal circulation and sediment transport near tropical estuary, east coast of India.” *Reg. Stud. Mar. Sci.*, 37, 101351.

Provost C., M. L. G. and F. L. Le. (1994). “Spectroscopy of the world ocean tides from a finite element hydro dynamic model.” *J. Geophys. Res.*, 99(24), 777–797.

Ranasinghe, R., Pattiaratchi, C., and Masselink, G. (1999). “A morphodynamic model to simulate the seasonal closure of tidal inlets.” *Coast. Eng.*, 37(1), 1–36.

Reddy, N. A., Vikas, M., Rao, S., and Seelam, J. K. (2015). “Classification of tidal inlets along the central east coast of India.” *Procedia Eng.*, 116(1), 922–931.

Rose, L., and Bhaskaran, P. K. (2017). “Tidal asymmetry and characteristics of tides at the head of the Bay of Bengal.” *Q. J. R. Meteorol. Soc.*, 143(708), 2735–2740.

Rose, L., Bhaskaran, P. K., and Kani, S. P. (2015). “Tidal analysis and prediction for the Gangra location, Hooghly estuary in the Bay of Bengal.” *Curr. Sci.*, 109(4), 745–758.

Sannasiraj, S. A., Zhang, H., Babovic, V., and Chan, E. S. (2004). “Enhancing tidal prediction accuracy in a deterministic model using chaos theory.” *Adv. Water Resour.*, 27(7), 761–772.

SatheeshKumar, J., and Balaji, R. (2017). “Estimation of tidal current energy along the Gulf of Khambhat using three-dimensional numerical modeling.” *Int. J. Ocean Clim. Syst.*, 8(1), 10–18.

Sun, X., Chick, J. P., and Bryden, I. G. (2008). “Laboratory-scale simulation of energy extraction from tidal currents.” *Renew. Energy*, 33(6), 1267–1274.

Thuỳ, V. T. T. (2013). “Aspects of Inlet Geometry and Dynamics.” Ph.D. Thesis, The University of Queensland, Australia.

Tidal stream energy review (ETSU). (1993). *Tidal stream energy review*.

Tousif, S. R., and Taslim, S. B. (2011). “Tidal Power: An Effective Method of Generating Power 2 G ENERATION OF TIDAL ENERGY.” *Int. J. Sci. Eng. Res.*, 2(5), 1–5.

Vikas, M., Reddy, N. A., Rao, S., and Seelam, J. K. (2015). “Classification of tidal inlets along the central west coast of India.” M.Tech Thesis, *Procedia Eng.*, 116(1), 912–921.

Vriend, H. J. de, Dronkers, J., Stive, M. J. F., and Wang, J. H. (2002). “Coastal inlets and Tidal basins.” *Delft Univ. Technol.*, 1, 1–84.

Waldman, S., Bastón, S., Nimalidinne, R., Chatzirodou, A., Venugopal, V., and Side, J. (2017). “Implementation of tidal turbines in MIKE 3 and Delft3D models of Pentland Firth & Orkney Waters.” *Ocean Coast. Manag.*, 147, 21–36.

Xia, J., Falconer, R. A., and Lin, B. (2010a). “Hydrodynamic impact of a tidal barrage in the Severn Estuary, UK.” *Renew. Energy*, 35(7), 1455–1468.

Xia, J., Falconer, R. A., and Lin, B. (2010b). “Impact of different operating modes for a Severn Barrage on the tidal power and flood inundation in the Severn Estuary, UK.” *Appl. Energy*, 87(7), 2374–2391.

Xia, J., Falconer, R. A., and Lin, B. (2010c). “Impact of different tidal renewable energy projects on the hydrodynamic processes in the Severn Estuary, UK.” *Ocean Model.*, 32(1–2), 86–104.

www.universetoday.com (accessed on 24-03-2017)

www.usna.edu (accessed on 24-03-2017)

https://en.wikipedia.org/wiki/File:M2_tidal_constituent.jpg (accessed on 02-12-2018)

www.power-technology.com (accessed on 24-03-2017)

www.bv.com (accessed on 24-03-2017)

PUBLICATIONS BASED ON PRESENT WORK

1. Vikas M, Subba Rao and Jaya Kumar Seelam, (2016), "Tidal Power: A Review", Hydro 2016 International, 21st Conference on Hydraulics, Water resources & Environmental Engineering. (Dec. 8-10, 2016), Organized by Central Water & Power Research Station, Pune, INDIA; (Paper ID HYD16-633).
2. Vikas Mendi, Jaya Kumar Seelam, Subba Rao, "Estimation of tidal energy along the west coast of India", World Scientific, 9th International Conference on Asian and Pacific Coasts (APAC 2017), Pages 343-355, Philippines. https://doi.org/10.1142/9789813233812_0032. (Scopus Indexed)
3. Vikas Mendi, Subba Rao, Jaya Kumar Seelam "General considerations for tidal energy extraction", 2nd International Conference on Climate Change, 15-16 February 2018, Colombo, Sri Lanka. (Poster presentation)
4. Vikas Mendi, N Amarnatha Reddy, Jaya Kumar Seelam, Subba Rao "Tidal energy figure estimation of potential tidal inlets along the east coast of India", 4th International Conference in Ocean Engineering, 18-21 February, 2018, IIT Madras, India. https://doi.org/10.1007/978-981-13-3134-3_49. (Scopus Indexed)
5. Vikas Mendi, Jaya Kumar Seelam, Subba Rao "Evaluation of tidal stream energy at major tidal inlets of Goa, India", ISH Journal of Hydraulic Engineering, November 2019. ISSN:0971-5010 (Print) 2164-3040 (Online) <https://doi.org/10.1080/09715010.2019.1692313>. (Scopus Indexed)
6. Vikas Mendi, Seelam Jaya Kumar, Subba Rao, Jyoti Kerkar "Hydrodynamic impacts of tidal pools along the Indian coast" International Conference on Hydraulics, Water Resources and Coastal Engineering (HYDRO2020), NIT Rourkela, 16-18 December 2020.

APPENDIX -1

Notations used in Table A1 to Table A9:

- WD- Wave dominated tidal inlet
 TD- Tide dominated tidal inlet
 RD- River dominated tidal inlet
 ME- Mixed energy
 ICOLL- Intermittently Close and Open Lakes and Lagoons
 Col 1- Inlet number
 Col 2- Inlet name
 Col 3- Latitude (°N)
 Col 4- Longitude (°E)
 Col 5- Geomorphological Classification
 Col 6- Tidal range (m)
 Col 7- lagoon area (m²)
 Col 8- Potential energy/ day (MW)
 Col 9- Inlet throat width

Table A1: Tidal inlets along Gujarat coast

Col 1	Col 2	Col 3	Col 4	Col 5	Col 6	Col 7	Col 8	Col 9
1	Gandhiya	22°22'24.74"	69°31'00.26"	TD	4.51	84752.28	0.201	18
2	Kalawad	22°20'15.65"	69°29'22.81"	TD	4.28	15080.3	0.032	68
3	Panero	22°19'58.58"	69°27'27.42"	TD	4.25	537291.31	1.130	-
4	Mithapur	22°24'12.82"	68°58'39.24"	TD	3.34	60189.36	0.078	27
5	Makanpur	22°21'11.88"	68°57'34.30"	ICOLL	3.18	247462.64	0.291	116.5
6	Dwaraka	22°15'20.92"	68°57'33.43"	TD	3.09	36485.34	0.041	23
7	Hari kund	22°14'07.26"	68°57'55.39"	TD	3.03	379599.93	0.406	43
8	Goji	21°58'58.62"	69°11'44.70"	ICOLL	2.62	138855.89	0.111	35
9	Navadra	21°56'02.00"	69°14'42.80"	ICOLL	2.55	98306.59	0.074	30
10	Miyani	21°49'52.61"	69°22'14.90"	ICOLL	2.43	22872621.21	15.721	142
11	Porbandar	21°38'20.22"	69°35'28.17"	ME	2.21	366437.1	0.208	104
12	Tukada	21°32'12.73"	69°42'21.71"	ICOLL	2.15	2352104.93	1.266	-
13	Chikasa	21°27'37.87"	69°46'35.66"	WD	2.09	1002576.79	0.510	118
14	Shil	21°10'38.96"	70°01'47.76"	ICOLL	1.96	569724.64	0.255	330
15	Ravon	20°54'58.10"	70°20'45.12"	TD	1.86	131292.63	0.053	-
16	Prabhas	20°52'51.13"	70°24'39.02"	TD	1.86	66500.78	0.027	1865
17	Mul Dwarka	20°45'42.59"	70°40'22.49"	TD	1.38	152316.37	0.034	2705
18	Sarkhadi	20°42'32.80"	70°52'16.25"	TD	2.17	5125180.47	2.809	18
19	Diu	20°43'11.68"	70°59'13.56"	TD	2.31	6548911.94	4.068	1000
20	Bandar	20°44'35.99"	71°04'33.79"	TD	2.38	114062.7	0.075	-
21	Rajput	20°45'22.00"	71°05'07.98"	WD	2.38	87766.85	0.058	355
22	Rajpara	20°47'52.91"	71°12'14.39"	TD	2.65	428795.74	0.351	113

23	Jafrabad	20°52'03.14"	71°22'18.34"	TD	3.07	2395996.47	2.629	234
24	Chanch	20°57'08.10"	71°32'18.40"	TD	3.43	2237793.75	3.065	110
25	Tena river	21°13'40.12"	72°36'29.15"	TD	6.37	1359769.79	6.422	22
26	Mindhola river	21°03'59.65"	72°41'24.75"	TD	6.19	2372001.44	10.579	1150
27	Puma river	20°54'32.08"	72°46'42.98"	TD	5.96	10515856.67	43.480	72
28	Kavai creek	20°48'16.88"	72°50'02.88"	TD	6.11	744537.83	3.235	215
29	Ambika river	20°45'09.94"	72°51'06.84"	TD	5.45	4902604.5	16.950	283
30	Auranga river	20°37'59.02"	72°53'19.71"	TD	5.75	1018925.07	3.921	144
31	Umarsadi	20°31'57.29"	72°53'19.62"	ME	5.61	1027770.09	3.765	167
32	Kolak river	20°28'01.27"	72°51'27.38"	ME	5.51	269626.67	0.953	91
33	Daman	20°24'41.47"	72°49'50.96"	ME	5.44	1145286.19	3.945	143
34	Bhathaiya	20°23'06.00"	72°49'35.44"	TD	5.42	55020.9	0.188	17
35	Kalu river	20°22'05.88"	72°49'16.63"	TD	5.41	379403.82	1.293	133
36	Kalai	20°21'17.96"	72°48'41.14"	TD	5.4	13631.33	0.046	33
37	Kalgam 1	20°19'27.77"	72°46'31.09"	TD	5.4	17881.22	0.061	20
38	Kalgam 2	20°20'02.08"	72°46'36.88"	TD	5.4	7803.08	0.026	13
39	Maroli	20°18'08.68"	72°46'23.57"	TD	5.36	11750.19	0.039	47
40	Varoli river	20°15'40.21"	72°45'08.94"	TD	4.66	19532.33	0.049	36
41	Nargol	20°12'09.18"	72°44'51.00"	TD	4.45	1296535.61	2.989	121
42	Deheri	20°09'54.97"	72°44'31.92"	TD	5.1	21212.96	0.064	20

Table A2: Tidal inlets along Maharashtra coast

Col 1	Col 2	Col 3	Col 4	Col 5	Col 6	Col 7	Col 8	Col 9
43	Zai	20°07'42.89"	72°44'18.81"	TD	5.14	40822.22	0.126	90
44	Gholvad	20°04'55.60"	72°43'34.53"	TD	5.09	5225.6	0.016	18
45	Dahanu	19°58'09.91"	72°43'33.52"	TD	4.96	1973969.28	5.653	383
46	Navapur	19°47'32.14"	72°41'47.30"	WD	4.84	653884.4	1.783	80
47	Dudh river	19°43'47.60"	72°43'07.00"	WD	4.76	1662026.76	4.383	500
48	Darapada	19°37'13.80"	72°43'44.81"	TD	4.74	55553.26	0.145	66
49	Kelwa	19°35'53.92"	72°45'35.45"	TD	4.72	633620.28	1.643	256
50	Bhadve	19°29'35.95"	72°47'40.71"	TD	4.65	32590059.19	82.025	1921
51	Rajodi	19°25'01.74"	72°45'41.27"	TD	4.66	7089.45	0.018	19
52	Bhuigaon Kh.	19°23'34.91"	72°46'03.57"	TD	4.65	232398.29	0.585	92
53	Vasai	19°19'01.34"	72°48'12.01"	TD	4.62	43904492.1	109.081	2291
54	Malad	19°11'52.98"	72°48'01.66"	TD	4.59	4652036.14	11.408	304
55	Versova	19°08'40.27"	72°50'02.88"	TD	4.58	1283028.8	3.133	130
56	Revas	18°53'43.55"	72°53'00.05"	TD	4.25	249331458.2	524.216	7670
57	Mandve	18°50'09.28"	72°57'33.40"	TD	4.25	30577769	64.289	1684
58	Awass	18°46'10.60"	72°51'52.17"	TD	4.23	6261.06	0.013	63
59	Surekhar	18°45'27.00"	72°52'01.58"	WD	3.7	92708.98	0.148	33
60	Navgaon	18°42'04.28"	72°51'48.01"	WD	4.14	46181.18	0.092	44

61	Navapada	18°40'07.18"	72°52'00.98"	WD	4.1	98102.08	0.192	110
62	Akshi	18°38'18.24"	72°53'19.62"	TD	4.02	794766.67	1.495	137
63	Bagmala	18°34'42.10"	72°55'29.89"	TD	3.74	70494.61	0.115	94
64	Revdanda	18°32'18.35"	72°55'58.00"	TD	3.69	11964373.54	18.963	549
65	Wandeli	18°30'12.20"	72°54'37.73"	WD	3.87	96788.46	0.169	124
66	Surulpeth	18°22'23.88"	72°55'46.98"	TD	3.72	129229.89	0.208	97
67	Eakdara	18°19'12.47"	72°58'23.06"	TD	3.67	283118.82	0.444	103
68	Rajapuri	18°16'53.15"	72°58'48.79"	TD	3.61	56897200.44	86.310	1637
69	Velas Agar	18°11'44.52"	72°59'18.88"	TD	3.53	192119.66	0.279	189
70	Diveagar	18°09'32.72"	73°00'00.61"	TD	3.5	59649.73	0.085	30
71	Walavati kh.	18°04'20.10"	73°01'00.09"	TD	3.41	136399.12	0.185	43
72	Shrivardhan	18°01'34.86"	73°02'31.35"	TD	3.35	1398745.51	1.827	134
73	Bankot	17°58'59.52"	73°02'59.86"	TD	3.28	19776854.19	24.766	701
74	Sakhari	17°55'54.52"	73°04'08.17"	TD	3.22	924282.18	1.116	163
75	Koliwada	17°53'25.37"	73°05'27.49"	TD	3.19	162176.19	0.192	83
76	Jaikar	17°50'30.62"	73°10'06.76"	TD	3.13	848256.4	0.967	108
77	Dabhol	17°34'47.14"	73°10'36.96"	TD	2.87	18361936.31	17.605	664
78	Mouje	17°30'54.72"	73°11'51.31"	WD	2.81	109356.5	0.101	27
79	Palshet	17°26'15.97"	73°13'15.74"	TD	2.76	34913.76	0.031	38
80	Muslondi	17°21'16.13"	73°13'37.22"	TD	2.71	37271.69	0.032	12
81	Jaigad	17°17'32.78"	73°14'24.96"	TD	2.67	18327896.14	15.209	931
82	Bhandrawada	17°11'58.02"	73°15'42.85"	TD	2.62	298025.69	0.238	32
83	Bhandarpule	17°09'30.49"	73°16'29.11"	WD	2.6	113697.39	0.089	63
84	Kajitbhati	17°06'00.40"	73°17'17.98"	WD	2.57	172901.4	0.133	67
85	Sadye	17°04'40.84"	73°17'33.98"	TD	2.55	324633.56	0.246	47
86	Sadamirya	17°02'17.30"	73°17'03.86"	TD	2.55	2375265.74	1.798	314
87	Karle	16°59'09.17"	73°18'02.16"	TD	2.51	2940577.62	2.156	215
88	Bhatiwadi	16°53'27.60"	73°18'59.66"	TD	2.46	2682646.4	1.890	79
89	Khsheli	16°48'23.26"	73°19'38.43"	TD	2.42	4655405.02	3.174	219
90	Wadativare	16°41'13.74"	73°21'26.23"	TD	2.37	299052.68	0.196	105
91	Vijayadurg	16°34'14.38"	73°19'47.99"	TD	2.3	18997595.28	11.698	1639
92	Phanase	16°26'36.31"	73°22'21.04"	WD	2.26	335757.57	0.200	36
93	Padavne	16°23'34.26"	73°23'10.95"	WD	2.24	7921668.34	4.627	730
94	Taramumbari	16°21'36.50"	73°24'40.81"	TD	2.22	1284779.6	0.737	100
95	Morve	16°16'28.34"	73°26'03.17"	WD	2.19	931059.72	0.520	53
96	Pirawadi	16°12'04.03"	73°27'46.55"	TD	2.16	1563059.12	0.849	117
97	Sariekot	16°05'16.91"	73°27'56.98"	WD	2.13	6939686.12	3.665	183
98	Malvan	16°04'15.67"	73°29'26.36"	TD	2.13	248313.22	0.131	33
99	Kalethar	16°00'36.72"	73°30'13.56"	TD	2.11	11688.69	0.006	10
100	Bhogwa	15°58'01.20"	73°32'02.41"	WD	2.11	5507266.63	2.854	392
101	Shriramwadi	15°56'17.45"	73°34'03.09"	TD	2.1	140353.62	0.072	27

102	Khalchiwadi	15°55'08.80"	73°35'11.19"	TD	2.1	46345.03	0.024	-
103	Kelus 1	15°54'37.76"	73°35'48.19"	TD	2.1	177248.43	0.091	40
104	Kelus 2	15°53'42.32"	73°36'40.63"	ICOLL	2.09	38102.21	0.019	-
105	Dabholi	15°51'56.74"	73°39'12.07"	WD	2.09	111712.46	0.057	27
106	Tank	15°47'37.82"	73°39'49.45"	WD	2.08	632315.22	0.318	77
107	Khalchikar	15°45'12.49"	73°41'23.10"	TD	2.07	654420.81	0.326	120

Table A3: Tidal inlets along Goa coast

Col 1.	Col 2	Col 3	Col 4	Col 5	Col 6	Col 7	Col 8	Col 9
108	Terekhol	15°43'16.82"	73°44'10.86"	WD	2.07	4250000	2.120	270
109	Chapora	15°36'38.81"	73°44'53.07"	WD	2.06	9079000	4.485	550
110	Baga	15°33'46.08"	73°47'24.54"	WD	2.06	93500	0.046	25
111	Mandovi	15°29'08.81"	73°48'56.41"	TD	2.05	57650000	28.201	3235
112	Zuari	15°25'36.88"	73°57'03.30"	WD	2.05	32700000	15.996	4229
113	Mobor	15°08'30.41"	73°58'47.73"	WD	2.04	1910000	0.925	166
114	Cola	15°03'15.66"	74°00'56.30"	WD	2.04	214000	0.104	38
115	Anjadip	15°00'48.28"	74°02'07.85"	WD	2.03	41000	0.020	13
116	Canacona 2	14°59'36.53"	74°02'19.25"	WD	2.03	980000	0.470	8
117	Canacona 1	14°59'02.65"	74°02'59.10"	WD	2.03	76000	0.036	46
118	Mashem	14°57'27.72"	74°07'19.97"	WD	2.03	300000	0.144	60

Table A4: Tidal inlets along Karnataka coast

Col 1.	Col 2	Col 3	Col 4	Col 5	Col 6	Col 7	Col 8	Col 9
119	Karwar	14°50'29.72"	74°09'31.59"	WD	2.03	12380000	5.938	680
120	Chendia	14°45'08.89"	74°13'41.79"	WD	2.02	570000	0.271	30
121	Todur	14°44'41.14"	74°15'51.25"	WD	2.02	116000	0.055	75
122	Belekeri	14°42'42.52"	74°16'45.48"	ME	2.03	670000	0.321	59
123	Ankola	14°39'41.98"	74°17'02.63"	WD	2.02	220000	0.104	24
124	Belambar	14°38'49.38"	74°17'32.99"	WD	2.02	275000	0.131	7
125	Manjaguni	14°36'00.86"	74°21'28.42"	WD	2.02	4413000	2.096	75
126	Tadadi Port	14°31'11.78"	74°23'34.51"	ME	2.01	15700000	7.383	595
127	Alvekodi 2	14°25'03.94"	74°25'27.75"	ME	2.00	340000	0.158	33
128	Karki	14°17'56.65"	74°28'11.32"	WD	1.98	13310000	6.074	155
129	Nakhuda	14°11'20.62"	74°30'05.06"	ME	1.96	40000	0.018	6
130	Alvekodi 1	14°01'36.62"	74°31'04.58"	WD	1.92	1550000	0.665	60
131	Jali	13°59'05.53"	74°32'05.18"	ME	1.9	48000	0.020	15
132	Mavakurve	13°58'01.81"	74°33'59.88"	WD	1.89	265000	0.110	159
133	Hadin	13°56'59.86"	74°35'08.18"	WD	1.89	36000	0.015	55
134	Alivey Gadde	13°55'20.78"	74°36'25.66"	ME	1.88	310000	0.128	17
135	Paduvari	13°52'05.52"	74°37'27.52"	ME	1.85	1200000	0.478	100
136	Koderi	13°47'38.69"	74°40'11.33"	ME	1.84	700000	0.276	85

137	Gangoli	13°38'02.83"	74°41'43.50"	WD	1.77	21000000	7.658	203
138	Kundapura	13°27'00.94"	74°44'11.12"	WD	1.68	15400000	5.059	183
139	Malpe	13°20'50.24"	74°41'44.20"	WD	1.62	5400000	1.650	98
140	Kaup	13°13'26.04"	74°46'01.08"	WD	1.58	24000	0.007	8
141	Nadsal	13°06'42.77"	74°46'36.57"	WD	1.55	280000	0.078	12
142	Hejamadi	13°04'31.04"	74°48'22.09"	WD	1.55	3820000	1.068	178
143	NMPT	12°55'37.45"	74°49'40.85"	WD	1.52	1540000	0.414	505
144	Netravati & Gurupur	12°50'43.55"	74°51'49.84"	WD	1.5	18820000	4.929	332
145	Kanwatheertha	12°45'38.70"	74°53'15.69"	WD	1.48	200000	0.051	35

Table A5: Tidal inlets along Kerala coast

Col 1.	Col 2	Col 3	Col 4	Col 5	Col 6	Col 7	Col 8	Col 9
146	Hosabettu	12°42'28.76"	74°55'13.85"	WD	1.47	495418.5	0.125	31
147	Bandiyod	12°37'55.99"	74°55'54.92"	WD	1.45	69281.77	0.017	-
148	Shiriya	12°36'25.02"	74°57'30.22"	WD	1.45	1590949.32	0.389	86
149	Puthur	12°32'28.03"	74°59'15.77"	WD	1.44	563249.45	0.136	36
150	Thalangara	12°28'30.68"	75°00'16.70"	ME	1.43	4608648.3	1.097	81
151	chembirika	12°26'26.99"	75°00'48.79"	WD	1.43	178096.36	0.042	22
152	Thekkekara	12°25'15.06"	75°01'40.95"	ICOLL	1.42	29966.71	0.007	-
153	Tharavadu	12°23'56.69"	75°03'41.29"	ICOLL	1.42	362198.78	0.085	-
154	Kadapuram	12°20'39.37"	75°07'12.98"	WD	1.41	690108.48	0.160	28
155	Kaithakkad	12°11'59.86"	75°13'37.10"	WD	1.4	19961777.86	4.554	260
156	Madayi	12°01'18.30"	75°17'46.82"	WD	1.36	3174978.08	0.684	86
157	Azhikkal	11°56'37.00"	75°24'16.63"	ME	1.36	24752433.18	5.329	366
158	Thottada	11°50'17.81"	75°25'56.01"	WD	1.34	40754	0.009	23
159	Nadal	11°48'30.71"	75°27'18.12"	WD	1.33	23785.16	0.005	25
160	Dharmadom	11°46'42.28"	75°28'17.94"	WD	1.33	1381881.62	0.285	118
161	Koduvalli	11°45'55.98"	75°31'53.97"	WD	1.33	1051898.08	0.217	383
162	Mahe	11°42'13.75"	75°32'36.54"	WD	1.32	1173256.11	0.238	110
163	Olavilam	11°40'46.16"	75°32'51.21"	ICOLL	1.32	2142.46	0.000	14
164	Chombala	11°40'14.70"	75°33'31.73"	WD	1.31	5237.46	0.001	-
165	Madappally	11°38'49.13"	75°35'22.90"	ICOLL	1.31	6057.56	0.001	-
166	iringal	11°34'06.64"	75°37'50.48"	WD	1.3	3429991.15	0.675	146
167	Nandi	11°28'06.82"	75°42'07.03"	WD	1.29	8618	0.002	24
168	Puthiyapurayil	11°25'02.50"	75°44'08.04"	ICOLL	1.28	3214	0.001	8
169	Elathur	11°20'46.21"	75°46'46.46"	WD	1.27	7327762.89	1.376	82
170	Thekepuram	11°13'39.50"	75°48'13.03"	WD	1.25	361373.44	0.066	138
171	Beypore	11°09'42.91"	75°49'32.80"	WD	1.24	9216513.86	1.650	272
172	Kudalundi	11°07'27.70"	75°51'26.16"	WD	1.23	1416752.8	0.249	222
173	Chiramangalam	11°01'11.50"	75°54'42.27"	WD	1.22	670920.74	0.116	82
174	Malappuram	10°47'13.70"	75°56'10.66"	ME	1.19	13374000	2.205	229

175	Veliancode	10°43'56.06"	75°58'48.42"	WD	1.18	1553087.06	0.252	81
176	Nallamkallu 2	10°37'57.94"	75°58'56.33"	ICOLL	1.17	2095	0.000	14
177	Nallamkallu 1	10°37'39.72"	76°02'18.55"	ICOLL	1.17	3019	0.000	26
178	Chettuva	10°30'30.17"	76°04'56.79"	WD	1.16	8353067.68	1.308	330
179	Nattika	10°25'09.77"	76°05'54.13"	ICOLL	1.14	4935	0.001	-
180	Muriyamthodu	10°22'45.08"	76°06'34.72"	WD	1.14	17553.69	0.003	15
181	Palapetty	10°20'59.10"	76°06'44.76"	WD	1.14	10406	0.002	15
182	Chamakala	10°20'34.04"	76°07'24.18"	ICOLL	1.13	13156	0.002	19
183	Vazhiyambalam	10°18'41.40"	76°07'39.62"	ICOLL	1.13	10878	0.002	10
184	Perinjanam	10°17'54.49"	76°08'12.04"	ICOLL	1.13	5667	0.001	25
185	Ambalanada	10°15'47.63"	76°09'51.08"	ICOLL	1.13	2310	0.000	15
186	Munambam	10°10'41.70"	76°14'03.21"	WD	1.13	10757923.38	1.599	196
187	Kochi inlet	9°58'10.93"	76°17'04.09"	WD	1.11	198250871.8	28.433	479
188	Andhakaranazhy	9°44'57.35"	76°17'31.71"	WD	1.05	883068	0.113	44
189	Arthunkal	9°39'45.00"	76°17'35.82"	ICOLL	1.04	13262	0.002	-
190	Kackary	9°39'04.59"	76°17'46.46"	ICOLL	1.04	41593	0.005	-
191	Perunermangalm	9°37'23.30"	76°17'55.12"	WD	1.04	50792	0.006	85
192	Janakshemam	9°36'06.25"	76°18'01.46"	ICOLL	1.03	6767	0.001	-
193	Valavanadu 2	9°35'18.41"	76°18'04.11"	ICOLL	1.03	10777	0.001	-
194	Valavanadu 1	9°34'58.61"	76°18'09.90"	ICOLL	1.03	19463	0.002	-
195	Pollethai	9°34'20.14"	76°18'19.63"	ICOLL	1.03	18582	0.002	14
196	Kattoor	9°33'25.21"	76°18'28.43"	ICOLL	1.03	25100	0.003	10
197	Omanapuzha	9°32'37.53"	76°18'45.79"	WD	1.03	21575	0.003	-
198	Poomkavu	9°31'04.68"	76°18'52.78"	ICOLL	1.03	18282	0.002	-
199	Padinjare	9°30'25.27"	76°19'26.59"	ICOLL	1.03	9216	0.001	13
200	Eravukadu	9°27'51.94"	76°19'34.26"	WD	1.03	22240	0.003	-
201	Punnapra 2	9°27'25.22"	76°19'55.53"	ICOLL	1.03	21293.76	0.003	-
202	Punnapra 1	9°26'06.78"	76°22'59.14"	ICOLL	1.03	18614.65	0.002	13
203	Thottapally lake	9°18'42.42"	76°27'46.41"	WD	1	1353898	0.158	38
204	Azheekkal	9°08'12.89"	76°31'10.27"	WD	0.97	11115438.73	1.217	200
205	Kandathil	9°01'04.13"	76°32'18.94"	ICOLL	0.95	3750113	0.394	-
206	Neendakara	8°56'03.60"	76°38'55.56"	WD	0.94	51392676.41	5.286	225
207	Paravur lake	8°48'44.33"	76°40'33.49"	WD	0.92	7426732.87	0.732	41
208	Kappil	8°46'38.49"	76°47'11.70"	WD	0.92	4345215.89	0.428	19
209	Madanvila	8°38'00.09"	76°53'10.64"	WD	0.91	3748287	0.361	131
210	Veli	8°30'30.05"	76°57'29.16"	WD	0.9	538101	0.051	-
211	Pachalloor	8°25'29.72"	77°01'43.04"	WD	0.89	213146	0.020	15
212	Kochupally	8°20'45.56"	77°04'45.62"	WD	0.88	26521	0.002	23
213	Paruthiyoor	8°18'20.74"	77°09'59.76"	WD	0.88	431858	0.039	26

Table A6: Tidal inlets along Tamil Nadu coast

Col 1.	Col 2	Col 3	Col 4	Col 5	Col 6	Col 7	Col 8	Col 9
214	Erayumanthurai	8°14'26.6"	77°10'03.0"	WD	0.863	545150	0.047	22
215	Sambasivapuram	8°10'14.4"	77°15'09.1"	TD	0.852	8966	0.001	16
216	Kadiyapattanam	8°08'13.7"	77°18'15.5"	WD	0.85	21274	0.002	25
217	Rajakamangalam Thurai	8°06'54.1"	77°22'23.7"	ICOLL	0.849	22584	0.002	8
218	Manakudi	8°04'57.3"	77°30'58.1"	WD	1.149	403410	0.062	8
219	Kovalam	8°09'27.7"	77°38'26.9"	WD	0.848	5117	0.000	14
220	SRNP	8°09'27.19"	77°48'03.67"	ICOLL	0.848	78613	0.007	237
221	Thottavilai	8°14'21.69"	78°03'32.06"	ICOLL	0.845	267240.46	0.022	34
222	Manapad	8°22'48.48"	78°07'22.98"	WD	0.841	692420	0.057	28
223	Govindamal colony	8°30'12.50"	78°07'35.97"	TD	0.842	63100	0.005	9
224	Veerapandianpattinam	8°31'20.70"	78°07'35.12"	ICOLL	0.842	8378	0.001	15
225	Mangaladevi	8°33'07.26"	78°12'22.66"	ICOLL	0.842	44125	0.004	19
226	Punnaikayal	8°38'27.51"	78°07'46.10"	WD	0.841	5539290.43	0.456	72
227	Veppalodai	8°57'17.82"	78°14'42.40"	WD	0.851	222357.31	0.019	32
228	Sippikulam	8°59'19.60"	78°16'04.43"	ICOLL	0.854	6704	0.001	6
229	Vaippar	9°00'14.43"	78°17'57.81"	WD	0.854	495705	0.042	19
230	Velayudhapuram 2	9°01'27.78"	78°18'56.38"	WD	0.861	111256	0.010	14
231	Velayudhapuram 1	9°02'16.25"	78°22'06.31"	ICOLL	0.864	180685	0.016	-
232	Vembar	9°04'47.97"	78°29'08.59"	ICOLL	0.882	501879	0.045	-
233	Mookaiyur	9°07'42.92"	78°38'51.98"	WD	0.908	834904	0.080	24
234	Valinokkam	9°11'03.77"	78°49'58.85"	WD	0.96	210741	0.023	9
235	Sethu karai	9°14'40.49"	78°54'55.95"	WD	1.033	733379.5	0.091	130
236	Muthariyarnagar	9°15'27.09"	78°55'16.55"	ICOLL	1.051	44900	0.006	13
237	Mandapam	9°17'10.54"	79°08'46.08"	WD	1.082	2223410	0.303	217
238	Atrangarai	9°20'42.44"	79°01'34.80"	WD	1.154	2176459	0.337	38
239	Pudhuvalasai	9°23'32.78"	78°57'54.56"	ICOLL	1.194	3000	0.000	9
240	Thiruppalaikudi	9°31'45.98"	78°57'05.81"	ME	1.316	96108	0.019	48
241	Karankadu	9°38'43.48"	78°58'14.97"	WD	1.386	441355	0.099	40
242	Alikkudi	9°39'30.79"	78°58'22.51"	WD	1.407	130146	0.030	32
243	Pudupattinam	9°40'15.22"	78°59'59.52"	ME	1.407	20365	0.005	11
244	Velangudi	9°44'53.87"	79°01'51.35"	WD	1.441	9160	0.002	9
245	Muthuramalingapattinam	9°45'13.72"	79°02'56.41"	WD	1.44	25690	0.006	9
246	odavayal	9°46'08.24"	79°04'40.94"	ME	1.431	83090	0.020	38
247	Kalियanagari	9°48'01.60"	79°05'54.97"	WD	1.416	28825	0.007	14
248	S.P.Pattinam 2	9°50'01.48"	79°06'22.15"	ME	1.402	33920	0.008	12
249	S.P.Pattinam 1	9°50'15.95"	79°07'23.50"	ME	1.402	164615	0.038	80
250	Muthukuda	9°51'38.29"	79°07'45.21"	ME	1.392	305650	0.069	91
251	Arsanagaripattinam	9°53'02.44"	79°07'25.48"	ME	1.395	111707	0.025	73
252	Embakkottai	9°54'40.59"	79°09'05.77"	ME	1.382	176455	0.039	68

253	Gopalapattinam	9°55'04.82"	79°09'43.35"	ME	1.635	77706	0.024	9
254	Sannathi	9°56'16.23"	79°11'51.10"	ME	1.376	16009	0.004	16
255	Kottaippattannam	9°58'16.40"	79°13'34.38"	WD	1.355	26079	0.006	48
256	Tandalai	10°00'25.38"	79°13'40.52"	WD	0.869	6069	0.001	9
257	Manamelkudi 2	10°02'41.10"	79°16'02.79"	ME	0.997	24046	0.003	7
258	Manamelkudi 1	10°03'09.14"	79°15'11.75"	TD	1.279	55572	0.011	50
259	Mumpalai 5	10°03'24.41"	79°15'13.89"	TD	1.43	53517	0.013	15
260	Mumpalai 4	10°03'43.49"	79°15'22.66"	TD	1.267	23356	0.004	20
261	Mumpalai 3	10°04'18.44"	79°14'53.26"	TD	1.337	50008	0.010	12
262	Mumpalai 2	10°04'24.28"	79°14'29.67"	TD	1.386	41276	0.009	14
263	Mumpalai 1	10°04'24.13"	79°14'16.79"	TD	1.489	11239	0.003	24
264	Kandanivayal	10°04'55.45"	79°14'15.08"	TD	1.266	26935	0.005	15
265	Subramanyapuram	10°06'19.94"	79°13'42.31"	ME	1.715	69066	0.024	95
266	Ravuttanvayal	10°06'32.40"	79°13'42.00"	WD	1.363	2130	0.000	13
267	Sembiyan 3	10°07'59.66"	79°13'48.01"	TD	1.403	1375	0.000	10
268	Sembiyan 2	10°08'06.07"	79°13'46.05"	TD	1.74	3587	0.001	23
269	Sembiyan 1	10°08'10.64"	79°13'43.06"	TD	1.487	20150	0.005	8
270	Manthirippattinam 2	10°08'32.32"	79°13'56.48"	ME	1.487	32301	0.008	22
271	Tiruvathevan 3	10°09'14.22"	79°14'23.42"	ME	1.215	8422	0.001	40
272	Tiruvathevan 2	10°09'25.34"	79°14'28.12"	ME	1.624	2582	0.001	21
273	Tiruvathevan 1	10°09'57.20"	79°14'22.27"	TD	1.105	2111	0.000	17
274	Palliya kulam	10°10'12.50"	79°14'19.90"	TD	1.105	8888	0.001	12
275	Manthiripattinam 1	10°10'24.56"	79°14'42.56"	ME	1.105	8744	0.001	16
276	Perumagalur	10°11'12.37"	79°15'10.46"	WD	1.105	23325	0.003	16
277	Adaikkathevan	10°12'14.54"	79°16'32.57"	ME	1.105	139753	0.020	76
278	Villunivayal	10°13'01.99"	79°17'05.02"	WD	1.105	19497	0.003	34
279	Ravuthanvayal	10°13'40.22"	79°16'03.09"	TD	1.105	3711	0.001	28
280	Marakkavalasai	10°14'32.71"	79°16'46.63"	WD	1.105	9299	0.001	17
281	Nayagathivayal	10°15'01.58"	79°17'32.70"	ME	1.105	2505	0.000	15
282	Manora	10°15'29.74"	79°18'25.85"	ME	1.105	97401	0.014	11
283	Sarabendrarajanpattina	10°15'56.66"	79°19'22.36"	WD	1.013	19621	0.002	38
284	Kallivayal	10°16'50.09"	79°22'02.80"	WD	1.109	511646	0.073	52
285	Keezhathottam	10°17'40.96"	79°31'13.21"	WD	1.078	20833832	2.818	235
286	Thuraikkadu	10°18'45.00"	79°44'21.93"	ME	0.868	62692453.8	5.498	42
287	Kodiyakadu	10°16'40.33"	79°45'40.93"	WD	0.984	132571	0.015	171
288	Kodikkarai	10°16'33.46"	79°50'10.80"	WD	0.751	36212	0.002	870
289	Vedaranyam	10°20'04.06"	80°00'44.46"	WD	0.894	15415	0.001	44
290	Madavilagam	10°22'30.40"	79°52'43.26"	WD	0.927	2459958	0.246	35
291	Thopputhurai	10°24'12.20"	79°52'15.25"	WD	0.922	2719439	0.269	42
292	Naluvethapathi	10°29'31.52"	79°52'00.91"	WD	0.861	39556	0.003	51
293	Vanvanmahadevi	10°31'26.87"	79°51'42.19"	WD	0.87	250514	0.022	85

294	Vettaikarairuppu	10°33'27.11"	79°51'37.09"	WD	0.88	228025	0.021	20
295	pudupalli	10°34'35.33"	79°51'27.44"	WD	0.895	14538	0.001	16
296	Vizhunthamavadi	10°35'37.18"	79°51'24.50"	WD	0.929	18720	0.002	34
297	Tirupoondi	10°38'00.67"	79°51'19.66"	ICOLL	0.951	755958	0.080	23
298	Velankanni	10°40'40.76"	79°51'12.59"	WD	0.994	836870	0.096	51
299	Nagapattinam	10°45'51.95"	79°51'06.94"	WD	0.987	1405773	0.159	56
300	Thethinagar	10°49'34.43"	79°51'05.00"	WD	0.973	271065	0.030	58
301	Keezhaiyur 2	10°50'39.23"	79°51'07.36"	WD	0.959	715906.45	0.077	10
302	Keezhaiyur 1	10°53'16.12"	79°51'10.39"	WD	0.87	15446	0.001	50
303	Bharathi nagar	10°54'49.43"	79°51'12.90"	WD	0.868	110315	0.010	108
304	Akkampettai	10°57'45.54"	79°51'12.61"	WD	0.87	860868	0.076	6
305	Chandirapady	10°59'42.07"	79°51'13.56"	ICOLL	0.872	485465	0.043	-
306	Kittiyandiyur	11°01'13.62"	79°51'20.24"	WD	0.881	112545	0.010	31
307	Veepanchery	11°05'19.90"	79°51'26.83"	WD	0.886	170666	0.016	27
308	Vanagiri	11°06'38.56"	79°51'27.05"	WD	0.887	2662857	0.244	21
309	Pompuhar	11°08'08.77"	79°51'29.31"	WD	0.895	162057	0.015	44
310	Thirumullaivasal	11°14'40.63"	79°50'58.76"	WD	0.906	11131937	1.064	39
311	Chinnakottaimedu	11°18'09.29"	79°50'31.36"	ICOLL	0.906	5667055	0.541	15
312	Pazhaiyar	11°21'31.50"	79°49'56.10"	WD	0.906	4648610	0.444	296
313	Chinna vaikaal	11°27'25.78"	79°48'20.90"	WD	0.902	20924	0.002	139
314	Ariyakoshti	11°30'10.19"	79°46'48.83"	WD	0.902	25025	0.002	72
315	Pudukuppam	11°31'49.33"	79°46'34.96"	WD	0.902	3313080	0.314	36
316	Samiyaar	11°32'25.80"	79°45'52.18"	ICOLL	0.902	1822467	0.173	11
317	Cuddalore	11°42'24.08"	79°47'09.08"	WD	0.944	1692434	0.176	213
318	Devanampattinam	11°44'16.26"	79°47'21.48"	WD	0.902	845950	0.080	369
319	Pudukuppam	11°45'16.02"	79°47'36.99"	ICOLL	0.96	2720001	0.292	86
320	Subauppallavadi	11°46'19.96"	79°47'53.21"	WD	0.944	486699	0.050	80
321	Aladimedu	11°49'59.41"	79°49'20.75"	WD	0.944	3950	0.000	14
322	C veerampattinam	11°52'39.54"	79°49'44.04"	WD	0.96	5484487	0.588	34
323	Puducherry	11°54'22.36"	79°49'50.89"	WD	0.974	7567384	0.836	143
324	Muthaialpet	11°57'47.45"	79°50'45.15"	ICOLL	0.995	839480	0.097	6
325	Vembalur	12°15'49.43"	80°02'54.61"	WD	1.043	29927710	3.790	37
326	Odiyur	12°19'23.34"	80°02'57.24"	WD	1.085	564603	0.077	29
327	KPK	12°26'14.78"	80°08'26.14"	WD	1.072	2775697	0.371	60
328	Sudurangapattinam	12°27'57.17"	80°09'15.82"	WD	1.058	3082200	0.402	12
329	Kalpakkam	12°30'33.84"	80°10'14.06"	ICOLL	1.115	1565036	0.226	16
330	Kokkilamedu	12°34'34.00"	80°11'31.23"	WD	1.239	411493	0.074	24
331	Padur	12°48'12.49"	80°14'56.52"	WD	1.239	3513357	0.628	27
332	Srinivasapuram	13°00'49.43"	80°17'21.52"	WD	1.217	348528622	60.086	16
333	Sathya Nagar	13°04'01.42"	80°18'37.21"	WD	1.217	108836	0.019	150
334	Athipatti	13°14'01.72"	80°20'19.79"	WD	1.217	108860252	18.767	50

Table A7: Tidal inlets along Andhra Pradesh coast

Col 1.	Col 2	Col 3	Col 4	Col 5	Col 6	Col 7	Col 8	Col 9
335	Karimanal	13°27'59.83"	80°18'58.11"	WD	1.22	8452	0.001	124
336	Shar	13°45'57.13"	80°15'04.34"	ICOLL	1.22	6440022	1.116	32
337	Chinnathota	13°49'04.26"	80°14'54.28"	WD	1.22	1417396	0.246	95
338	Nalagamula	13°51'35.89"	80°13'44.53"	ICOLL	1.22	1185671	0.205	20
339	Konduru	14°01'45.12"	80°09'15.61"	WD	1.19	10262	0.002	73
340	Swanamukhi River	14°04'29.03"	80°09'02.09"	WD	1.19	11132	0.002	38
341	Kothapatnam	14°07'32.16"	80°07'47.80"	WD	1.19	2544	0.000	20
342	Srinivasa	14°09'11.30"	80°07'37.31"	ICOLL	1.18	4552	0.001	11
343	Gunnampadia 2	14°11'21.95"	80°07'40.83"	ICOLL	1.2	12584041	2.109	13
344	Gunnampadia 1	14°12'18.68"	80°07'45.06"	ICOLL	1.2	331460	0.056	6
345	Gopalapuram 2	14°13'12.14"	80°08'07.21"	ICOLL	1.2	186187	0.031	9
346	Gopalpuram 1	14°14'42.97"	80°08'15.43"	WD	1.2	71745	0.012	1180
347	Nelaturu	14°19'09.88"	80°09'26.20"	WD	1.19	640105	0.106	31
348	Pathapalem	14°22'22.87"	80°10'37.10"	WD	0.8	6427200	0.479	34
349	Koruturu	14°28'26.58"	80°10'59.90"	ICOLL	1.2	80784	0.014	10
350	Ramudupalem	14°31'58.26"	80°11'04.38"	WD	1.2	2678100	0.449	27
351	Utukuru	14°35'24.43"	80°12'51.64"	ME	1.21	1448175	0.247	225
352	Ramathirtham	14°38'37.61"	80°09'43.47"	ICOLL	1.2	194231	0.033	-
353	Isakapalle	14°44'23.28"	80°07'36.58"	WD	1.2	416098	0.070	123
354	Juvvaladinne	14°49'08.44"	80°06'01.91"	WD	1.2	3150112	0.528	92
355	Ramayapatnam 2	15°02'44.09"	80°04'57.49"	ICOLL	1.22	159462	0.028	-
356	Ramayapatnam 1	15°04'11.35"	80°02'56.41"	WD	1.22	1371686	0.238	37
357	Karedu	15°11'19.72"	80°05'11.59"	WD	1.25	823175	0.150	262
358	Pakala	15°16'56.64"	80°05'22.53"	ICOLL	1.26	1635	0.000	-
359	Anantavaram 2	15°18'47.12"	80°06'16.17"	WD	1.27	2087093	0.392	84
360	Anantavaram 1	15°19'23.45"	80°06'46.04"	WD	1.27	1850600	0.347	89
361	Peddapattapalam	15°21'10.58"	80°06'55.49"	ICOLL	1.27	576638	0.108	15
362	Motumala	15°30'05.83"	80°13'27.95"	WD	1.31	221384	0.044	72
363	Chintayigari palem	15°32'41.39"	80°14'20.39"	WD	0.83	3134340	0.251	512
364	Kanuparthi	15°36'09.79"	80°14'30.17"	WD	1.3	12705	0.002	27
365	Peddaganjam	15°38'00.38"	80°15'48.42"	WD	1.31	18746	0.004	16
366	Pallepalem	15°39'22.25"	80°16'37.29"	WD	1.31	11288	0.002	317
367	Pullaripalem 3	15°43'07.86"	80°18'42.28"	ICOLL	1.3	518215	0.102	739
368	Pullaripalem 2	15°43'27.37"	80°19'15.33"	ICOLL	1.3	30257	0.006	19
369	Pullaripalem 1	15°43'43.90"	80°19'51.67"	ICOLL	1.3	270737	0.053	732
370	Katari palem	15°44'42.18"	80°22'58.52"	WD	1.31	2808696	0.561	23
371	Krupa nagar	15°46'35.94"	80°26'00.35"	WD	1.3	1167374	0.230	11
372	Pandurangapuram	15°48'22.46"	80°32'40.18"	WD	1.3	517818	0.102	17
373	East Gollapallem	15°51'13.72"	80°38'19.72"	WD	1.3	1299581	0.256	27

374	Gokarnamatam	15°52'35.29"	80°41'51.21"	WD	1.29	105953098	20.523	27
375	Dindiadavala	15°52'52.03"	80°46'02.41"	WD	1.29	105953098	20.523	449
376	Haripuram	15°51'45.61"	80°49'54.57"	WD	1.29	2119758	0.411	145
377	LVD	15°42'42.08"	80°55'48.36"	ME	1.28	17576	0.003	132
378	Elachetladibba	15°43'24.53"	81°04'00.91"	ME	1.28	145102	0.028	46
379	RKP	15°54'34.96"	81°06'09.92"	WD	1.27	12150450	2.281	94
380	Ramakrishnapuram 2	15°56'47.11"	81°06'13.53"	ICOLL	1.26	75524	0.014	22
381	Ramakrishnapuram 1	15°56'52.91"	81°07'50.47"	ICOLL	1.26	146708	0.027	51
382	Palakayatippa	15°58'25.50"	81°10'24.88"	ME	1.27	2830025	0.531	345
383	Machilipatnam	16°04'46.67"	81°11'10.10"	WD	1.26	107469	0.020	56
384	polatitippa	16°06'13.64"	81°12'05.76"	ME	1.26	280135	0.052	29
385	Chlilikalapudi	16°08'38.65"	81°12'24.18"	WD	1.26	57091	0.011	141
386	Kara agram	16°10'46.49"	81°14'13.68"	ME	1.25	908234	0.165	23
387	Gokavaram	16°14'21.34"	81°14'54.15"	WD	1.26	6753883	1.248	39
388	Tallapalem	16°15'19.48"	81°15'58.00"	WD	1.26	4371220	0.808	41
389	Kanuru	16°16'43.68"	81°23'46.99"	ME	1.26	7845563	1.450	77
390	Kruthivennu	16°20'37.93"	81°29'23.23"	WD	1.26	33056838	6.109	450
391	Peda Gollapalem	16°21'19.62"	81°32'39.44"	WD	1.27	21503823	4.037	363
392	Chinna Gollapalem	16°20'55.90"	81°43'06.80"	WD	1.27	526506	0.099	388
393	Marritippa	16°19'09.08"	81°57'10.98"	WD	1.3	261633	0.051	502
394	Odalaravu	16°24'20.81"	82°02'01.04"	ME	1.32	16836484	3.415	435
395	Komaragiri patanam	16°26'27.49"	82°08'38.60"	ME	1.33	145166679	29.890	81
396	Gachakayala pora	16°29'55.72"	82°16'51.49"	WD	1.35	487501	0.103	165
397	Kothapalem	16°35'42.11"	82°20'22.34"	ME	1.4	69306	0.016	577
398	Gadimoga	16°43'58.91"	82°20'58.07"	WD	1.42	400473	0.094	1510
399	Sasikanth Nagar	16°59'09.56"	82°18'07.94"	ME	1.46	604239	0.150	41
400	Nemam	17°02'17.02"	82°18'49.23"	WD	1.46	444866	0.110	11
401	Mulapeta 2	17°05'21.55"	82°21'44.42"	WD	1.46	702994	0.174	28
402	Mulapeta 1	17°06'04.68"	82°36'02.01"	WD	1.46	96904	0.024	25
403	Pentakota	17°17'28.00"	82°42'11.08"	WD	1.47	151525	0.038	34
404	Rajanagaram	17°17'07.19"	82°36'40.49"	WD	1.47	1913039	0.481	28
405	Boyapadu	17°20'35.05"	82°44'37.68"	ICOLL	1.47	95830	0.024	23
406	Dhandawaka	17°21'47.66"	82°52'12.09"	ICOLL	1.48	21679	0.006	19
407	Bangarammapalem	17°25'05.41"	82°59'37.95"	WD	1.49	15564	0.004	99
408	Pudimadaka	17°28'32.66"	83°00'27.91"	WD	1.51	282695	0.075	42
409	Chippada	17°29'59.42"	83°03'31.61"	ICOLL	1.51	22434	0.006	13
410	Dosuru	17°31'23.52"	83°05'31.40"	ICOLL	1.51	3422777	0.908	19
411	Cheepurupalle	17°32'19.03"	83°10'13.77"	WD	1.52	7529	0.002	54
412	Peddapalem	17°34'05.48"	83°17'33.97"	WD	1.53	3780	0.001	19
413	Vishaka Port	17°41'17.41"	83°20'35.91"	WD	1.56	7415	0.002	165
414	MVP sector	17°44'01.72"	83°21'44.28"	WD	1.57	1437398	0.412	13

415	Musalayyapalem	17°45'47.52"	83°23'20.98"	ME	1.59	7163	0.002	-
416	Pedda Rushikonda	17°47'25.58"	83°27'19.63"	WD	1.59	785717	0.231	7
417	Kummaripalem	17°54'01.94"	83°33'05.72"	WD	1.61	7160	0.002	64
418	Kancheru	17°58'34.36"	83°34'14.44"	WD	1.63	7173	0.002	-
419	Konada	18°00'47.02"	83°36'25.93"	ME	1.64	13825	0.004	58
420	Kollaya valasa 2	18°02'22.63"	83°36'45.31"	ICOLL	1.65	8990	0.003	10
421	Kollaya valasa 1	18°02'35.16"	83°37'33.68"	ICOLL	1.65	331492	0.105	5
422	Pathiwada	18°03'03.17"	83°39'25.24"	WD	1.65	15237	0.005	6
423	Chintapalli	18°04'23.20"	83°40'46.92"	WD	1.67	498835	0.162	11
424	NJR puram	18°05'19.07"	83°42'19.66"	WD	1.67	1576308	0.512	30
425	Tekkai	18°06'16.96"	83°48'24.23"	ICOLL	1.67	352460	0.114	13
426	Kuppili	18°09'17.17"	83°56'45.45"	WD	1.69	140581	0.047	15
427	Bontala koduru	18°12'48.10"	84°00'28.91"	WD	1.72	2316625	0.798	92
428	Vastavalasa	18°14'49.52"	84°05'19.85"	WD	1.74	195178	0.069	7
429	seepanapeta	18°17'21.41"	84°08'11.50"	WD	1.75	4138	0.001	25
430	Kalingapatanam	18°20'41.14"	84°12'59.53"	ME	1.76	2508056	0.904	145
431	Siddibeharakothuru	18°26'22.85"	84°14'12.08"	WD	1.78	2264468	0.835	82
432	Malagam	18°27'30.60"	84°21'22.45"	ICOLL	1.78	4160	0.002	18
433	Devunalthada	18°33'50.33"	84°27'17.06"	WD	1.8	80420	0.030	110
434	Vajrapukothuru	18°41'42.58"	84°30'42.22"	WD	1.82	461171	0.178	79
435	Metturu	18°45'27.65"	84°34'33.78"	ICOLL	1.82	1376420	0.531	7
436	Pithali	18°50'48.19"	84°35'23.30"	ICOLL	1.83	59885	0.023	13
437	Uppalam	18°52'18.52"	84°41'03.22"	ICOLL	1.84	527309	0.208	116
438	Borivenka	18°58'14.70"	84°42'28.98"	ICOLL	0.97	2291877	0.251	88
439	Pukkalapalyam	19°00'03.78"	84°44'42.58"	ICOLL	1.86	78078	0.031	31
440	Donkuru	19°03'02.52"	84°47'16.76"	ICOLL	1.86	916084	0.369	151

Table A8: Tidal inlets along Odisha coast

Col 1.	Col 2	Col 3	Col 4	Col 5	Col 6	Col 7	Col 8	Col 9
441	Sonpur	19°06'59.72"	84°48'14.39"	WD	1.92	10823800	4.644	228
442	Alladpur	19°08'49.02"	84°50'10.08"	WD	1.92	412248	0.177	44
443	Dhepanuapada	19°11'15.61"	84°55'03.26"	WD	1.93	330663	0.143	50
444	Venketaipur	19°15'53.75"	85°04'14.92"	WD	1.95	531728	0.235	27
445	Pallibandha	19°22'23.92"	85°31'23.98"	WD	1.92	3622675	1.554	116
446	Anandapur	19°40'24.92"	85°47'11.82"	WD	1.97	671525619	303.354	637
447	Baliapanda	19°46'56.96"	85°54'58.26"	WD	2.01	433643	0.204	67
448	Bhimapur	19°49'09.48"	86°02'49.31"	WD	2.03	2212640	1.061	161
449	Sahukhanata	19°50'55.03"	86°13'44.43"	WD	2.05	2685650	1.314	148
450	Tandahar	19°54'11.05"	86°22'13.36"	WD	2.06	3241390	1.601	221
451	Dhanuhar Belari	19°57'38.63"	86°25'40.67"	WD	2.07	45608408	22.748	1479
452	Saharabedi	20°02'47.51"	86°33'53.54"	WD	2.05	4661037	2.280	200

453	Nuagan	20°12'29.02"	86°42'30.41"	WD	2.1	15605780	8.011	1440
454	Kaudia	20°17'36.17"	86°43'31.01"	WD	2.16	34767435	18.881	471
455	Baligarh	20°23'40.31"	86°44'24.47"	RD	2.28	6569228	3.975	398
456	Banapada	20°28'14.99"	86°45'22.12"	WD	2.36	686253	0.445	300
457	Joginatha	20°30'25.24"	86°51'13.05"	TD	2.33	5873865	3.712	607
458	Krishnapriyapur	20°35'14.82"	86°57'38.81"	WD	2.41	531458	0.359	207
459	Amarnagar	20°46'43.97"	87°03'38.89"	ME	2.89	47465390	46.145	2120
460	Pirikhi	21°28'29.46"	87°07'19.40"	WD	3.95	6233297	11.321	260
461	Huladigudi	21°30'54.72"	87°12'26.38"	ME	4.05	3546401	6.771	640
462	Jambhirei	21°32'49.38"	87°22'05.64"	TD	3.98	108049	0.199	50
463	Chandrabali	21°33'58.93"	87°32'50.10"	WD	3.8	21150974	35.551	2025

Table A9: Tidal inlets along West Bengal coast

Col 1.	Col 2	Col 3	Col 4	Col 5	Col 6	Col 7	Col 8	Col 9
464	Begundiha	21°38'01.57"	87°38'27.31"	WD	3.41	1242805	1.682	472
465	Tajpur	21°38'55.14"	87°45'32.41"	WD	1.69	889380	0.296	211
466	Serpupalpai	21°41'41.39"	87°53'22.42"	ME	1.78	1279900	0.472	967
467	Nijkashba	21°47'31.88"	88°00'05.27"	WD	1.7	5523177	1.858	410
468	Gagra char	21°54'19.98"	88°01'00.28"	WD	1.73	249623	0.087	80
469	Jadu bari chak	21°56'30.91"	88°03'09.51"	WD	2.36	74050	0.048	49
470	Haldia	22°01'00.95"	88°11'45.07"	WD	2.84	21852069	20.516	840
471	Durgachak	22°02'19.32"	88°11'45.07"	TD	3.3	233583550	296.091	4851

Inclusion of turbine in MIKE21:

The effect of tidal turbines is modelled as sub-grid structures using a simple drag-law to capture the increasing resistance imposed by the turbine blades as the flow speed increases. Turbines are assumed always to have their axis aligned with the flow direction. Depending on the site characteristics, turbine is inserted in the hydrodynamic module by means of providing the geographic coordinates. The turbine is labelled and the properties of the turbine are input. Diameter of the turbine and the drag coefficient are provided. The resistance imposed by the turbine blades can be specified by means of fixed drag coefficient. A fixed drag coefficient of 0.4 is considered for the simulation. When “Fixed drag coefficient” is selected, the turbine is assumed to have the axis aligned with the flow direction. Hence no lift force is calculated. For a constant drag coefficient, a correction factor of 1 is provided.

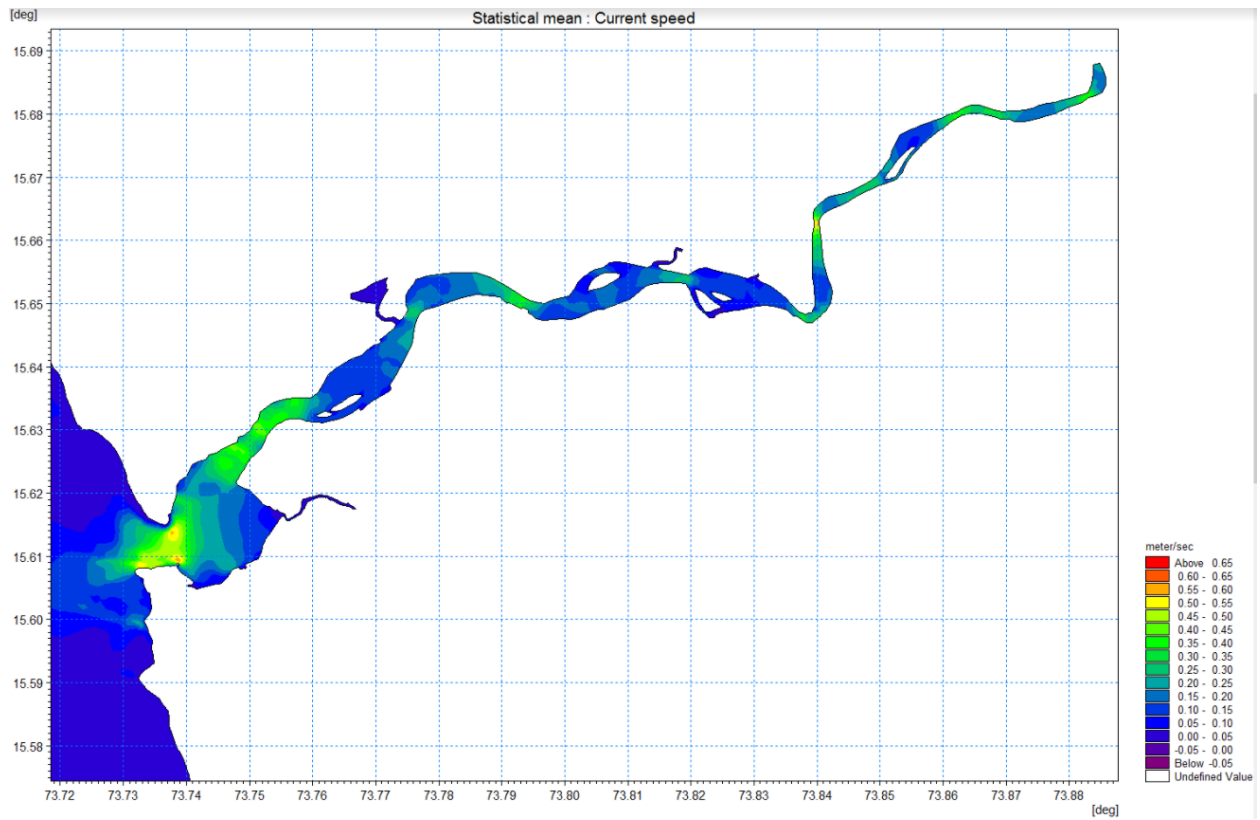


Figure A1: Current speeds (mean) at Chapora

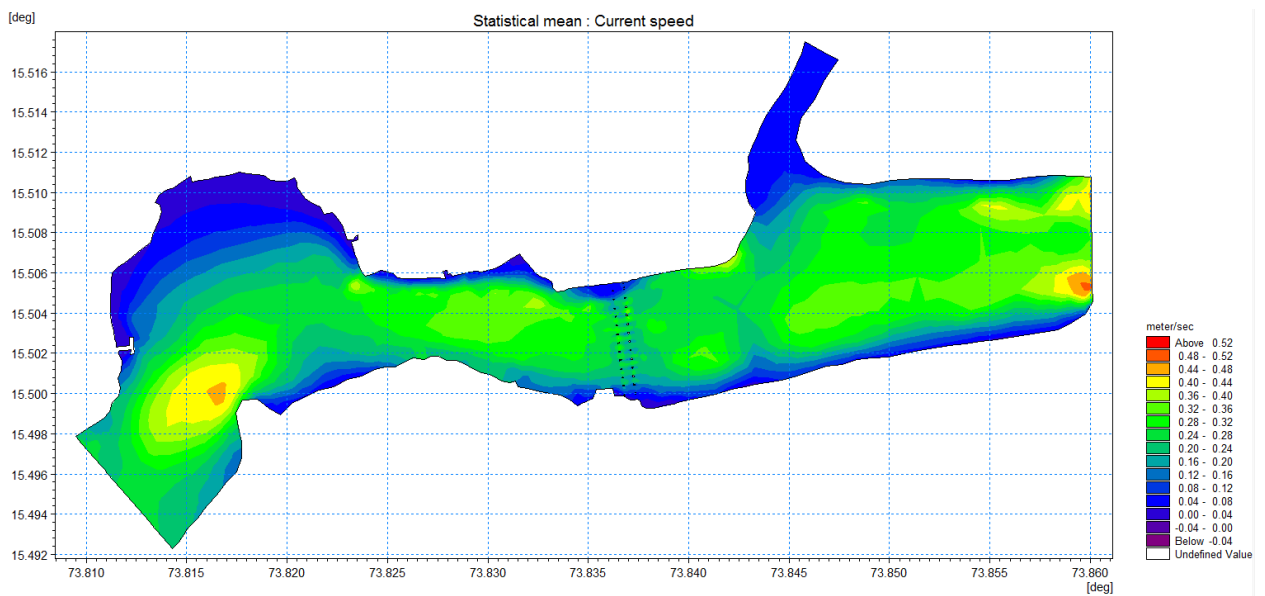


Figure A2: Current speeds (mean) at Mandovi

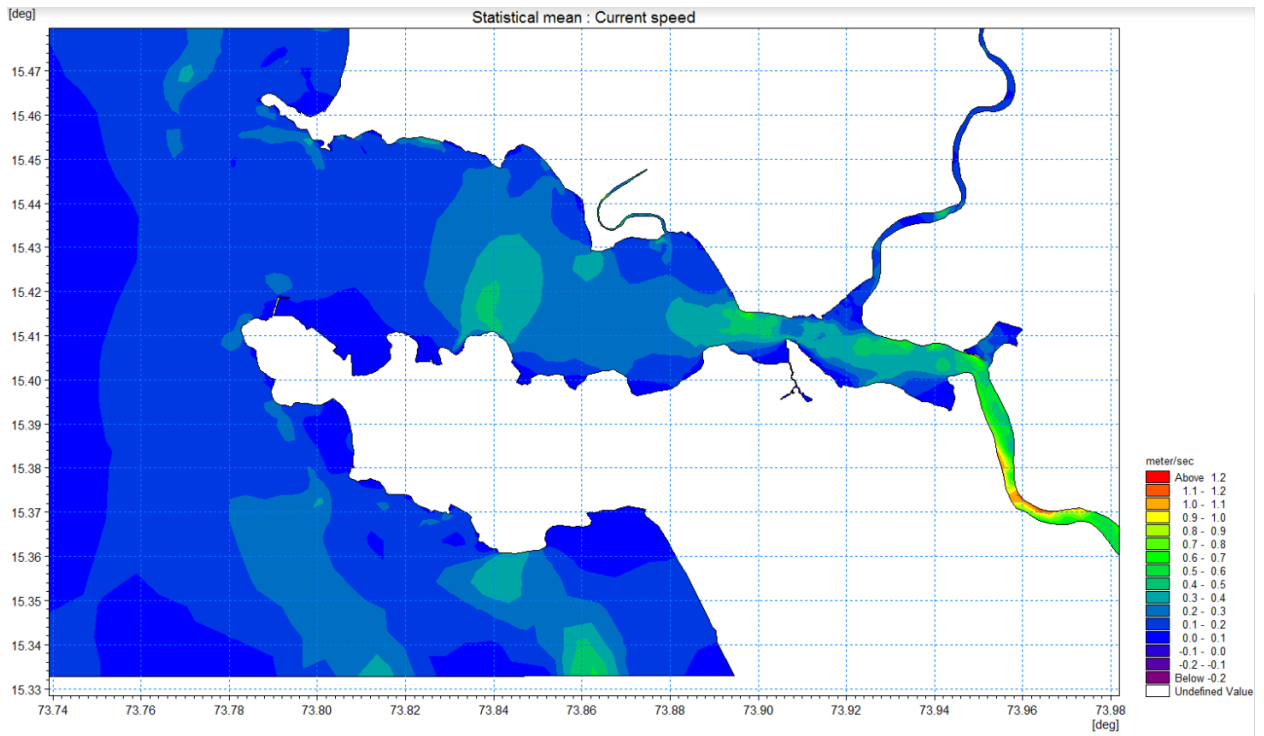


Figure A3: Current speeds (mean) at Zuari

BRIEF BIODATA

Name: Vikas M
Date of Birth: 05-Jan-1992
Address: Department of Civil Engineering
RV College of Engineering®
RV Vidyaniketan post
Mysuru Road, Bengaluru-560059
Mobile: (+91) 7411194545
Email(s): kbl9dad@gmail.com, vikasm@rvce.edu.in
Qualification: B.E. (Civil Engineering)
M.Tech.(Marine Structures)
Publications: International journals: 3
National conferences: 4
International conferences: 15

